Some inverse scattering problems on star-shaped graphs: application to fault detection on electrical transmission line networks

Filippo Visco Comandini

THÈSE

préparée à

L'INSTITUT DE RECHERCHE EN INFORMATIQUE ET EN AUTOMATIQUE, INRIA CENTRE PARIS ROCQUENCOURT

en vue de l'obtention du titre de

DOCTEUR EN SCIENCES

Spécialité

MATHÉMATIQUES APPLIQUÉES

délivrée par

L'UNIVERSITÉ VERSAILLES SAINT QUENTIN EN YVELINES

présentée par

Filippo VISCO COMANDINI

Sujet de la thèse:

Some inverse scattering problems on star-shaped graphs: application to fault detection on electrical transmission line networks

Soutenue le 05/12/2011 devant le jury composé de:

Directeur	**Michel SORINE**	Directeur de recherche INRIA
Co-directeur	**Mazyar MIRRAHIMI**	Chargé de recherche INRIA
Rapporteurs	**Lionel PICHON**	Directeur de recherche CNRS
	Pierre ROUCHON	Professeur École des Mines
Examinateurs	**Fabrice AUZANNEAU**	Chef de laboratoire CEA
	Otared KAVIAN	Professeur UVSQ

Remerciements

Je tiens en premier lieu à remercier Michel Sorine et Mazyar Mirrahimi, qui m'ont encadré pendant la durée de cette thèse. Mazyar et Michel ont toujours su m'indiquer de bonnes directions de recherche quand il le fallait, me laisser chercher seul quand il le fallait, et ont ce talent de savoir expliquer les concepts les plus techniques en des termes très intuitifs. Je pense avoir énormément appris à leur contacts, j'ai sincèrement apprécié de travailler avec eux et je suis reconnaissant pour le temps qu'ils m'ont consacré à trouver les fautes de ma thèse, apparemment dénombrables.

Je suis également très reconnaissant à Giulia Saccá pour m'avoir suggéré de postuler à l'INRIA et de m'avoir transmis sa passion pour la France. Sans elle, je serais dans une autre part du monde et je doute que j'aurais pu avoir une vie aussi heurese.

Par ailleurs je voudrais remercier Martine Verneuille, assistante du projet SISYPHE, pour m'avoir accompagné tous ces années a travers les longues démarches de la douce bureaucratie française. Son aide était fondamentale depuis le début de mon arrivée en France.

Je remercie aussi tous mes collègues du projet SISYPHE Julien Barral, Frédérique Clément, Claire Médigue et Pierre-Alexandre Bliman. Merci aussi aux autres étudiants avec qui j'ai eu l'occasion d'interagir: Xioung et Antoine, colocataires de bureau et Zaki, Leila, Mohamed et Mohamad pour les discussions fructueuses. Mes remerciements vont également à Qinghua Zhang, qui sans être mon directeur de thèse, a grandement contribué à ma formation.

J'ai eu la chance de rencontrer toutes les personnes du bâtiment 16. Je ne me risquerais pas à citer tous mes collègues de l'INRIA parce que je serais certain d'en oublier, mais je n'en pense pas moins, je vous suis sincèrement reconnaissant pour toutes les pauses café (un merci particulier à Marina).

Je remercie toutes les personnes qui sont venues chez moi partager les plaisirs de la cuisine: Emanuele, Yasmine, Ibrahim, Alfonso, Radek et Joaquin. Le quartet Luna,

Nick, Maya et William a un place spéciale dans mon coeur, aussi maintenant avec l'arrivée de Zoe. Paris ne serait pas la même si je ne vous avais pas rencontrés. Un remerciement tout spécial va à mes compagnons des batailles Sneew et Master B.

Un grand merci à Carlo, coloc, collègue et surtout ami. Pendant les années de thèse on a vécu des grandes expériences ensemble: de la recherche d'un appartement à paris, tache pas facile jusqu'aux dernièrs projets culinaires.

Merci à ma famille, notamment à mes parents Tiziana et Vincenzo, ma sœur Federica et mon frère Giacomo dont l'affection m'a rendu la vie vraiment plus agréable, et mes grands-parents, qui ont eu la gentillesse de toujours s'intéresser à ce que je faisais même si l'intérêt de ce que je faisais ne devait a priori pas être flagrant. Merci surtout à ma mère Tiziana qui m'a poussé à étudier à l'étranger un sujet incompréhensible pour elle comme les mathématiques.

Merci enfin à Clara pour être encore avec moi.

Contents

Introduction

Aujourd'hui, le nombre de matériels électroniques croît rapidement dans le domaine des transports: véhicules, avions et autres systèmes critiques.

Les dernières trente années du développement de l'industrie automobile sont emblématiques: la longueur des câbles embarqués sur un automobile a plus que décuplé passant de près de deux cents à plus de quatre milles mètres. Ce phénomène est dû à l'application des technologies "X-by-wire": les systèmes de contrôle mécaniques et hydrauliques sont remplacés par des systèmes électroniques utilisant des câbles électriques. L'application de telle technologie est présente aussi dans l'industrie aéronautique.

La fiabilité des réseaux filaires et des connexions électriques devient toujours plus importante: un système complet peut être mis en panne à cause des anomalies provenant d'un connecteur ou d'une liaison électrique en mauvais état et les conséquences peuvent être catastrophiques.

Pour satisfaire les nouvelles exigences en matière de sécurité et de qualité de service, il est nécessaire de développer des techniques pour la surveillance de ces lignes de transmissions électriques. Pendant les dernières années son importance a suscité l'intérêt de différents groupes de recherche qui tentent d'élaborer des méthodes de surveillance et diagnostic des réseaux électriques.

Il devient très important d'avoir une méthode qui permette de contrôler l'état de santé des réseaux filaires, et de localiser une éventuelle anomalie pendant que le système est en marche. Parmi les efforts de développement des systèmes fiables électriques, la réflectométrie est la méthode diagnostique la plus prometteuse: basée sur l'injection d'un signal électrique à l'une des extrémités du réseau et sur l'analyse des signaux réfléchis, cette méthode nous permet de détecter et localiser des défauts électriques dans la structure des transmissions. La réflectométrie est couramment utilisée pour la détection et la localisation des défauts francs comme les court-circuits ou des circuits

ouverts, mais l'analyse du signal réfléchi nécessite le débranchement du fil électrique influençant le coût du diagnostic et la performance du système électrique. Il serait alors intéressant d'élaborer des techniques qui permettent de surveiller et diagnostiquer le système de façon non invasive.

Utilisant la méthode diagnostique de la réflectométrie, notre motivation au début de cette thèse était d'explorer les propriétés des mesures du réflectomètre pour obtenir des informations utiles à la surveillance et au diagnostic des réseaux électriques. La mesure de l'expérience de la réflectométrie est traduit par la connaissance du coefficient de réflexion défini de façon heuristique comme le rapport entre une onde électrique réfléchie et une onde incidente.

Détection des défauts vu comme problème inverse de scattering

Les comportements des ondes électriques le long de la ligne sont décrits par le modèle des télégraphistes: la transmission électrique est caractérisée par quatre paramètres de la ligne, connus comme la résistance R, l'inductance L, la capacité C et la conductance linéique transversale G. La modélisation des comportements des ondes électriques stationnaires dépendante de la fréquence k et de l'espace z sur une ligne de transmission est donnée, notamment, par les équations des télégraphistes:

$$\begin{cases} \partial_z V(k,z) + ikL(z)I(k,z) + R(z)I(k,z) = 0, \\ \partial_z I(k,z) + ikC(z)V(k,z) + G(z)V(k,z) = 0. \end{cases}$$

où $V(k,z)$ représente la tension de courant et $I(k,z)$ son intensité.
La méthode de la réflectométrie peut être vue comme un problème inverse de scattering: à partir de la connaissance du coefficient de réflexion, on veut retrouver les défauts électriques représentés par des variations des paramètres de la ligne.

Nous nous sommes inspirés dans un article de Jaulent [30] qui montre l'équivalence entre le problème inverse des scattering pour les équations des télégraphistes et le problème inverse de scattering pour les équations de Zakharov-Shabat donné par

$$\begin{cases} \partial_x \nu_1(x,k) = (q_d(x) - ik)\nu_1(x,k) - q_+(x)\nu_2(x,k), \\ \partial_x \nu_2(x,k) = -q_-(x)\nu_1(x,k) - (q_d(x) - ik)\nu_2(x,k), \end{cases} \qquad x \in [0,l]$$

où les variables ν_1 et ν_2 sont des combinaisons linéaires de la tension $V(x,k)$ et de l'intensité $I(x,k)$ des courants, alors que les potentiels $\mathbf{q} = \{q_+, q_-, q_d\}$ dépendent des paramètres de la ligne R, L, C et G.
À partir de la connaissance du coefficient de réflexion, Jaulent arrive à reconstruire la quantité suivante en fonction du temps parcouru x:

$$\tilde{q}_\pm(x) = \left[\frac{1}{4}\frac{d}{dx}\left(\ln\frac{L}{C}\right) \pm \frac{1}{2}\left(\frac{R}{L} - \frac{G}{C}\right)\right] exp\left(\mp\int_{-\infty}^{\infty}\left(\frac{R}{L} + \frac{G}{C}\right)ds\right).$$

L'objet de cette thèse est donc de savoir si, sur des réseaux filaires, les coefficients de réflexion peuvent nous donner des informations utiles à la surveillance et la détection des défauts.
Une première question se pose: la connaissance de ces coefficients est-elle suffisante pour détecter des défauts électriques? Si oui, quels sont les types des défauts?
Le diagnostic sur un réseau électrique nécessite alors une classification des défauts: nous distinguons les défauts francs, comme les court-circuits et des circuits ouverts, des défauts non francs. Les défauts francs sont localisés sur des points spatiaux précis et leur présence implique que le passage de courant est nié. Ainsi, la longueur électrique d'une branche peut être modifiée de la présence d'un défaut franc. Les défauts non francs sont créés par un changement local des paramètres le long de la ligne; ces types de défauts ne sont pas ponctuels, mais se diffusent le long de la ligne.

Dans cette thèse, l'objet géométrique est un réseaux filaire composé par N branches rejointes au noeud central. Le réseaux à étoile est le cas plus simple non trivial d'un graphe planaire.
Notre modèle est donc donné par un système de Zakharov-Shabat défini sur chaque branche

$$\begin{cases} \partial_x \nu_{1j}(x,k) = (q_{j,d}(x) - ik)\nu_{1j}(x,k) - q_{j,+}(x)\nu_{2j}(x,k), \\ \partial_x \nu_{2j}(x,k) = -q_{j,-}(x)\nu_{1j}(x,k) - (q_{j,d}(x) - ik)\nu_{2j}(x,k), \end{cases} \qquad x \in [0, l_j]$$

où l_j représente la longueur électrique de la branche e_j et le point $x = 0$ correspond au noeud central. Toutes les fonctions serons indexées par le nombre j de la branche.
En générale, l'expérience de la réflectométrie est fortement reliée aux entrées disponibles: nous examinerons le cas minimal où on a accès au réseau que pour une seule entrée. La réflectométrie, basée sur une approche "far-field", consiste à brancher un fil uniforme

(avec les paramètres de la ligne constants) au noeud central du réseau. Sur cette branche test, indexée par 0, les équations des télégraphistes se réduisent à un système découplé

$$\begin{cases} \partial_x \nu_{10}(x,k) = -ik\nu_{10}(x,k), \\ \partial_x \nu_{20}(x,k) = +ik\nu_{20}(x,k), \end{cases} \qquad x \in [-l_0, 0]$$

Au noeud central, les conditions du système

$$\begin{cases} \nu_{10}(0,k) + \nu_{20}(0,k) = \nu_{1j}(0,k) + \nu_{2j}(0,k) \quad \forall j \in \{1,\dots,N\} \\ \sum_{j=1}^{N} \nu_{1j}(0,k) - \nu_{2j}(0,k) = \nu_{10}(0,k) - \nu_{20}(0,k). \end{cases}$$

dérivent de les lois de Kirchhoff pour la conservation de l'énergie.
Les conditions générals aux noeuds externes $x = l_j$ sont données par

$$\nu_{1j}(l_,k) - \rho_j(k)\nu_{2j}(l_j,k) = 0,$$

où les coefficients $\rho_j(k)$ caractérisent les différentes configurations à la fin de chaque ligne. Naturellement, les choix des $\rho_j(k)$ déterminent le coefficient de réflexion. À travers une seule entrée, nous pourrons ainsi faire différentes expériences tant que nous pouvons changer les valeurs de ces coefficients ρ_j.

Dans la suite de cette introduction, nous présentons un résumé des résultats obtenus dans la thèse. Ces résultats sont volontairement simplifiés pour n'en garder que le principe. Pour l'énoncé rigoureux des théorèmes, les hypothèses exactes de validité et les démonstrations, le lecteur se rapportera aux chapitres correspondants.

Problèmes inverses de scattering pour l'operateur de Schrödinger

Nous avons d'abord traité le cas particulier d'un réseau électrique sans pertes, i.e. $R_j = G_j = 0$ pour toutes les branches. Le système de Zakharov-Shabat sur Γ est équivalent à l'équation de Schrödinger indépendant du temps sur chaque branche:

$$\frac{d^2}{d^2x} y_j(x,k) - q_j(x) = k^2 y_j(x,k), \qquad \forall j = 0,\dots,N$$

Le potentiel $q_j(x)$ est un agrégé des paramètres linéique $L_j(x)$ and $C_j(x)$

$$q_j(x) = \left[\frac{C_j(x)}{L_j(x)}\right]^{-\frac{1}{4}} \frac{d^2}{dx^2} \left[\frac{C_j(x)}{L_j(x)}\right]^{\frac{1}{4}}.$$

L'avantage de cette formulation est qu'on peut utiliser des techniques provenant de la littérature académique sur les problèmes inverses de scattering pour l'opérateur de Schrödinger. Par exemple, pour une ligne de transmission , il y a différentes méthodes pour reconstruire le potentiel $q(x)$ à partir du coefficient de réflexion [34],[17] [18].
Sur le réseau à étoile, nous sommes obligé de montrer que le problème direct de scattering est bien posé: les potentiels $q_j(x)$ caractérisent le coefficient $r(k)$.
Le premier résultat sur les problèmes inverses concerne l'identification géométrique. La connaissance du $r(k)$ est suffisante pour retrouver les longueurs des branches:

Theorem (Theorem 3 du Chapitre 3)**.** *On considère un réseau à étoile Γ^+ fait de n_j branches de longueur l_j. Alors la connaissance du coefficient $r(k)$ détermine de façon unique les paramètres $(n_j, l_j)_{j=1}^N$.*

Pour la preuve, on a besoin des comportements à hautes fréquences des solutions fondamentales et des propriétés des fonctions quasi-périodiques. Identifier les longueurs se traduit dans l'expérience de la réflectométrie par la localisation des défauts francs, comme les circuits ouverts et fermés.
Les défauts non francs sont représentés par la connaissance des potentiels $q_j(x)$. Détecter la présence de ces défauts, appelés aussi "défauts d'isolement", et les localiser sur le réseau implique l'identifiabilité des potentiels q_j. Pour l'identification des potentiels q_j, une seul expérience n'est pas suffisante. En fait on a le résultat suivant:

Theorem (Theorem 4 du Chapitre 3)**.** *Sur un réseau à étoile Γ^+ vérifiant*

B1 *les longueurs sont toutes différents, i.e. $l_j \neq l_i$ pour chaque $i, j = 1, \dots, N$ tels que $i \neq j$.*

Si deux potentiels $\boldsymbol{q} = \otimes_{j=1}^N q_j(x)$ et $\boldsymbol{q'} = \otimes_{j=1}^N q'_j(x)$ tels que

$$q_j(0) = q_i(0) \qquad j \neq i,$$

nous donnent le même coefficient de réflexion $r(k) = r'(k)$, alors on a

$$\int_0^{l_j} q_j(s)ds = \int_0^{l_j} q'_j(s)ds \qquad j = 1, \dots, N.$$

La conditions sur les potentiels $q_j(0) = q_i(0) \qquad j \neq i$, est équivalent à dire qu'on exclut des défauts électriques au noeud central.

Pour avoir l'identification complète des potentiels il faut deux expériences différentes pour avoir deux coefficients de réflexion. Chaque expérience est associée à des conditions différentes aux noeuds terminaux. Avec deux coefficients et quelques hypothèses techniques, on a l'identifiabilité des potentiels.

Theorem (Theorem 5 du Chapitre 3)**.** *Sur un réseau à étoile* Γ^+*. On suppose*

A2 *Pour chaque* $i, j = 1, \dots, N$ *tel que* $i \neq j$*,* l_j/l_i *est un nombre algébrique irrationnel.*

Si on a deux potentiels $\boldsymbol{q} = \otimes_{j=1}^N q_j(x)$ *et* $\boldsymbol{q}' = \otimes_{j=1}^N q_j'(x)$ *satisfaisant* $|\boldsymbol{q}|_\Gamma, |\boldsymbol{q}'|_\Gamma < \epsilon$*, nous donnent les mêmes coefficients de réflexion*

$$r_{\mathcal{N}}(k) = r'_{\mathcal{N}}(k), \qquad r_{\mathcal{D}}(k) = r'_{\mathcal{D}}(k)$$

associés à deux expériences différentes, alors on a

$$\boldsymbol{q} \equiv \boldsymbol{q}'.$$

Dans ce cas, on parle d'une identification locale autour du potentiel nul que représente la situation parfaite sans défauts. L'hypothèse **A2** limite fortement l'application réel de ce résultat, parce que cette supposition sur le rapport des longueurs n'est par vérifiable dans l'expérience réelle.
Les preuves de ces deux théorèmes passent pour un résultat d'équivalence entre le problème inverse de scattering sur un réseau Γ^+ et des problèmes spectraux inverses sur la partie compacte de Γ: la connaissance du coefficient de réflexion est équivalent à la connaissance des différentes spectra de l'opérateur de Sturm-Liouville défini sur Γ.

Problèmes inverses de scattering pour les équations de Zakharov-Shabat

Les problèmes inverses sur les réseaux des transmission avec pertes forment un autre chapitre de cette thèse. Le problème direct de scattering est aussi bien posé dans cette situation: une fois fixés les potentiels $\mathbf{q} = \otimes_{j=1}^N (q_{j,+}, q_{j,-}, q_{j,d})$ sur le réseau à étoile, le coefficient de réflexion est unique.

Pour la localisation des défauts francs on a le même résultat que dans le cas d'un réseau sans pertes

Theorem (Theorem 6 du Chapitre 4)**.** *Sur un réseau à étoile* Γ *vérifiant la condition* ***B1*** *le coefficient* $r(k)$ *determine les longueurs* l_j*.*

Aussi, dans ce cas, la preuve utilise les comportements à hautes fréquences des solutions fondamentales et des propriétés des fonctions quasi-périodiques.
Les problèmes inverses pour retrouver les potentiels sont, a priori, plus compliqués: sur chaque branche les potentiels sont trois $(q_{j,+}, q_{j,-}, q_{j,d})$. Déjà sur la ligne Jaulent [30] arrive à retrouver que des agrégés de potentiels, le coefficient $r(k)$ permet de calculer la quantité suivante

$$\tilde{q}_{\pm}(x) = q_{\pm}(x) \exp(\mp 2 \int_{-\infty}^{\infty} q_d(s) ds).$$

Le résultat plus important de ce chapitre regarde l'identification de la quantité

$$\int_0^{l_j} q_{j,d}(x) dx = \frac{1}{2} \int_0^{l_j} \frac{R_j}{L_j}(x) + \frac{G_j}{C_j}(x) dx \qquad j = 1, \ldots, N$$

appelée le factuer de dissipation de la ligne.

Theorem (Theorem 7 du Chapitre 4)**.** *On assume que pour un réseau à étoile* Γ^+*, la condition* ***B1*** *est valide. Si on a deux potentiels* $\boldsymbol{q} = \otimes_{j=1}^{N}(q_{j,+}, q_{j,-}, q_{j,d})$ *et* $\boldsymbol{q'} = \otimes_{j=1}^{N}(q'_{j,+}, q'_{j,-}, q'_{j,d})$ *qui nous donnent le même coefficient de réflexion* $r(k) = r'(k)$ *on a nécessairement*

$$\int_0^{l_j} q_{j,d}(x) dx = \int_0^{l_j} q'_{j,d}(x) dx.$$

L'idée de la preuve est similaire à la preuve des Théorèmes 4 et 5. Aussi dans le cas avec pertes, on montre l'équivalence entre le problème inverse de scattering pour le système de Zakharov-Shabat sur Γ^+ et des problèmes spectraux inverses pour l'opérateur de Zakharov-Shabat défini sur la partie compacte Γ.
Le dernier résultat concerne un cas particulier du réseau. Sur un réseau uniforme de transmission où les paramètres de la ligne sont constants, les trois potentiels sont

donne sur chaque branche simplement par

$$\begin{aligned} q_{j,d}(x) : &= \tfrac{1}{2}\left(\tfrac{R_j}{L_j} + \tfrac{G_j}{C_j}\right), \\ q_{j,+}(x) : &= +\tfrac{1}{2}\left(\tfrac{R_j}{L_j} - \tfrac{G_j}{C_j}\right), \\ q_{j,-}(x) : &= -\tfrac{1}{2}\left(\tfrac{R_j}{L_j} - \tfrac{G_j}{C_j}\right). \end{aligned}$$

Dans ce cas, on a le résultat suivant

Theorem (Théorème 8 du Chapitre 4)**.** *Sur un réseau* Γ *vérifiant l'hypothèse* ***B1****. Si on a sur chaque branche*

$$\frac{G_j}{C_j} < \frac{R_j}{L_j}, \qquad \forall j = 1, \dots, N,$$

alors le coefficient de réflexion détermine de façon unique ces deux quantités

$$\frac{G_j}{C_j} \quad et \quad \frac{R_j}{L_j}, \qquad \forall j = 1, \dots, N.$$

Organisation de la thèse

Ce manuscrit de thèse est composé de quatre chapitres:

Chapitre 1 Le premier chapitre est consacré aux problématiques industrielles et à leur modélisations. L'expérience de la réflectométrie est modélisée par les équations des télégraphistes, et la détection des défauts électriques peut être vue comme un problème inverse de scattering: à partir de la mesure du coefficient de réflexion on cherche à avoir des informations sur les paramètres de la ligne qui influencent les comportements des ondes électriques.

Nous nous intéressons d'abord aux réseaux de transmission sans perte: dans ce cas, les équations des télégraphistes peuvent être réduites à l'équation de Schrödinger indépendante du temps. Ensuite, on montre que le cas général avec perte est équivalent au système de Zakharov-Shabat, deux équations couplées de premier ordre.

Le lecteur pourra bénéficier d'un tableau dans l'appendice A qui montre l'équivalence des expériences d'ingénieurs avec les fonctions mathématiques.

Chapitre 2 Dans le deuxième chapitre nous présentons l'état de l'art de la recherche du côté ingénieur et du côté mathématique. Si les ingénieurs ne perdent pas de vue l'aspect d'application de la réflectométrie, la recherche académique sur l'opérateur de Schrödinger et sur le système de Zakharov-Shabat concerne plutôt les aspects délicieusement mathématiques et oublie l'application industrielle.

Chapitre 3 La résolution de quelques problèmes inverses pour l'opérateur de Schrödinger fait l'objet du troisième chapitre. Dans une première partie, nous étudierons le problème direct: une fois choisis les paramètres de la ligne, le coefficient de réflexion est unique. Ensuite nous introduisons les différents problèmes inverses. Plus précisément, on s'intéresse aux problèmes d'identification des paramètres géométriques comme le nombre de branches et leur longueurs, et aux problèmes d'identification partielle ou totale des potentiels, une agrégation des paramètres de la ligne.

Chapitre 4 Dans le chapitre quatre, nous traitons le cas général des réseaux de transmission avec perte. Ce chapitre est la généralisation du précédent: on cherche d'abord à montrer que le problème direct est bien défini et après on passe à l'étude des problèmes inverses. Le coefficient de réflexion nous permet de retrouver les défauts francs et leur position sur le réseau, par la résolution d'un problème d'inversion géométrique. Un deuxième problème est donné par l'identifiabilité des taux d'amortissement le long de la ligne. Dans le cas d'un réseau uniforme, on arrive à identifier deux quantités fondamentales pour les opérations de maintenance des compagnies de trains.

Chapter 1

Fault detection in electric networks as inverse scattering problem

1.1 Examples of Industrial Problems

Electrical cables are widely used for power and signal transmissions in embedded systems, buildings and infrastructures. Wired networks are often considered as well known and reliable, so that research on cables diagnosis in critical systems is still neglected.
We are going to illustrate two examples of industrial problems concerning the cables diagnosis.

The main problem consists in detecting and locating electrical faults along the cables. For a better understanding, it is useful to classify them in two types: **hard** and **soft** faults.

- The first one corresponds to the short and open circuits, external breakdown or abnormal resistance. They cause a discontinuity of the impedance and so they can be localized easily in space.

- Soft faults are also called "isolation faults" and they are not punctual in space, but they are spread over the line. They caused by progressive degradations.

Figure 1.1: Hard faults: (0-DEFECT documentation)

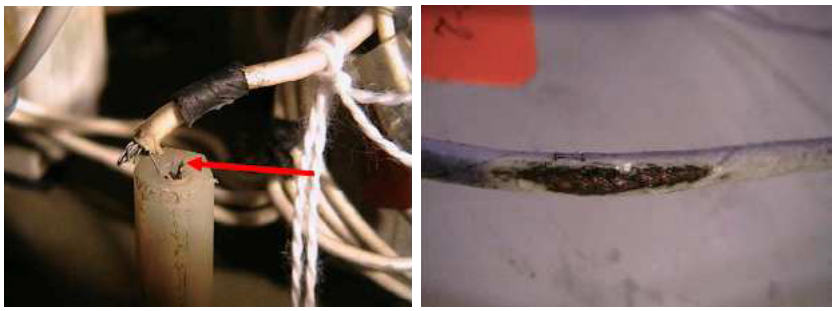

Figure 1.2: Soft faults: conductor's breakdown and sheathing degradation (0-DEFECT documentation)

1.1.1 Embedded Automotive networks

An interesting example of industrial problems comes from the automotive industry.

The number of electronic equipments is increasing rapidly in automotive vehicles, aircrafts, and many other safety critical systems. As well the complexity of wired networks embedded in vehicles is growing up exponentially. For example a modern car can contain up to 4 kilometers electrical wire, while in a civil airplane we can find 400 kilometers of electrical cables. The sensitivity to network's defects evolves as the network complexity increases and various problems can emerge at system level due to the cables. For the automotive industry, a goal is to develop compact and easy to use devices for the diagnosis of electric connection failures in garage or at the end of the production chain. These diagnosis devices will be integrated to the vehicle in order to detect failures under normal working conditions of the vehicle. To find faulty wiring in such networks, it is not always possible to measure end-to-end cable impedances, because the number of available diagnostic port plugs is limited, and furthermore, for

diagnosis purpose, it is not sufficient to detect a high end-to-end impedance as it is also necessary to locate the fault within the cable.

The diagnostic methods affect in a consistent way the security and the economy of the in car industry. In fact, a mechanic can take up to 2 days to find and repair a wiring defect, sometimes after having changed healthy and expensive components. The 70% of the calculators returned to the manufacturer are defect-free. The industrial part proved the feasibility of an external diagnosis system in garage, which preindustrial prototype is identified a commercial product before the end of the project. Automatic fault detection and diagnosis using reflectometry methods is the subject of intense research, both on the technologies of "smart wiring systems" and reflectometers on the foundations of the Time/Frequency Domain reflectometry (TDR/FDR) methods.

0-DEFECT (0-DEFAUT: Outil de Diagnostic Embarqué de Faisceaux AUTomobiles) is project funded by the French National Research Agency (ANR). The goals of this project are to study and to implement new methods more adapted to the problems of embedded diagnosis. Technically, current methods make it possible to obtain about ten centimeters accuracy on the localization of a hard defect, which is already appreciable. On the other hand, it is not completely compatible with certain constraints for embedded systems, in particular because of Electromagnetic compatibility (EMC) and of the interaction of the diagnosis signals with those of the network.

The objects of Chapter 3 and part of Chapter 4 are to improve the hard faults detection methods applied to electrical networks through reflectometry experiments. The reflectometry methods described in Section 1.2 will give us useful informations about the presences of possible electric faults. Looking at the application on the embedded automotive networks, we restrain ourself to a minimal setup of an electrical network where a single plug-in port is available for the reflectometry experiments.

1.1.2 Lossy long lines in railway's systems

In railway systems, the reliability of signal cables is an important aspect for the economy and the security of a train company.
SNCF is France's national state-owned railway company. SNCF operates the country's national rail services, including the TGV, France's high-speed rail network. Its functions include operations of rail services for passengers and freight, and maintenance

and signaling of rail infrastructure owned by Réseau Ferré de France. The french signal cables network is more then 50.000 km long and the subdivision of the french railway company, Infra SNCFm must deal with it. Since the train cables are spread all over the french territory, the maintenance is difficult and expensive.
These maintenance operations are difficult, because there are thousands of kilometers of different signal cables and maintenance teams must travel along the network. Each year more then 10.000 hours are spent in the maintenance operations. Nowadays standard checking procedure is carried out unplugging parts of cable and then detecting and locating electrical defaults. These procedures affect the traffic circulation in a consistent way.
One of the most difficult type of defaults is the "isolation defaults". They are often due to a degradation of the cable its-self. The principal characteristic of these failures is that they are not located in one point of the line, but they are distributed along the cable.

SNCF model cables

Train signal cables are $1500m$ long and they have been used in frequency range $0 - 3$kHz. We are going to model these signals and diagnostic test signals by the telegrapher's equations, presented in Section 1.3. This model is characterized by the inductance L and the linear capacitance C and by some loss terms. The loss terms are represented by a distributed resistance R and a distributed shunt conductance G. The latter one represents the "isolation faults" we like to detect. Even if this conductance has a weak influence on the electrical transmissions (10 nS/km), a small variation becomes unacceptable for train circulation: the accepted limit value is 100 nS/km.
The difficult of this problem comes from the weak influence of the conductance G over the other line parameters R, L and C. The effect of the conductance G is very weak for the dissipation $1/2(R/L+G/C)$ and the dispersion $1/2(R/L-G/C)$, because G/C is very small compared to R/L. Detecting an abnormally high value of G is associated to a carefully observation of both dispersion and dissipation. Modern techniques allow us to see this phenomenon only at low frequencies and that's why the maintenance operations deals with unplugged signal cables.

Another difficulty of this problem comes from the fact that these faults are not located on a single point as for the hard faults leading to breakdowns. Short and open circuits are hard faults and can be located by simple reflectometry. For the isolation

faults preceding breakdowns, we can imagine that aging process or slow degradation involves an entire cable zone. In this way, these faults won't be nor localized in a particular spot or uniform along the line cable: the variation of the conductance G and possibly of C can be uniformly continuous in space.

SNCF Cables parameters

Train signal cables are copper lines, their section is 1 mm^2 and they coupled in a twist way. The transmission line parameters are

- Resistance $R \sim 37$ ohm/km,
- Inductance $L \sim 0.9$ mH/km,
- Capacitance $C \sim 200, 100, 40$ nF/km,

Here the orders of magnitude for R/L and G/C are respectively of 0.025 ms and 1000 s.

The goal of INSCAN project (INfrastructure Safety Cable ANalysis) funded by the French National Research Agency (ANR) is to develop a new method based on the reflectometry experiments to detect abnormal values of G/C without using the low frequency band reserved for the signalization. The new method should contribute to the safety of the railway system, but also improve the ability to deliver on time railway services. In terms of operations, the main challenge consists in the ability to perform the cable diagnosis without train service interruptions while preserving the required safety level for the end-equipments connected by the cables.

In Chapter 4 we study the reflectometry methods applied to an electrical lossy network. Though the reflectometry, we will be able to identify the two quantities R/L and G/C in the particular case of uniform transmission network.

1.2 Fault detection and localization by reflectometry

To improve the reliability of electrical network and facilitate the maintenance operations, the reflectometry is one of the most effective methods.
This method is based on the injection of test signal at one end of the network and on the analysis of reflected signals. Reflectometry provides information on the presence of faults on an electrical network (fault-detection), and also may be used to localize the faults and to reveal their nature (fault-diagnosis).

1.2.1 Some elements of Linear Network Theory

In this section we are going to recall some basic properties of the N-port abstract network that can be found in [66, 11].

In the following, we are going to use some standard notations:

- $L_2^N(\mathbb{R})$ is the set of N-dimensional vectors $(f_1(t), \ldots, f_N(t))$, where each f_j is a real-valued square-integrable function of time t;
- f_T denotes the function $f \times \chi_{[-\infty,T]}$, where χ is the characteristic function on the interval $[-\infty, T]$;
- L_{2e}^N is the set of all f with $f_T \in L_2^N$ for all $T \in \mathbb{R}$.

An N-port network (see figure 1.3), denoted by $\mathcal{N}$, is represented by N pair of external time-dependent variables $(i_j(t), v_j(t))_{j=1}^N$ belonging to L_{2e}^{2N}, here corresponding to the current and voltage at each port. For each network we can consider various representations, each one describing the relationship between these variables, depending on which N of these variables are fixed, while the other N variables are derived.

A pair $(i(t), v(t))$ is called $\mathcal{N}$-**admissible** signal pair in L_{2e}^{2N} which may appear across $\mathcal{N}$.

A network $\mathcal{N}$ admits many possible representations: choosing N variables from the set $\{i(t), v(t)\}$, we can associate the rest of the variables through a particular operator. One may ask when a representation is well-defined.

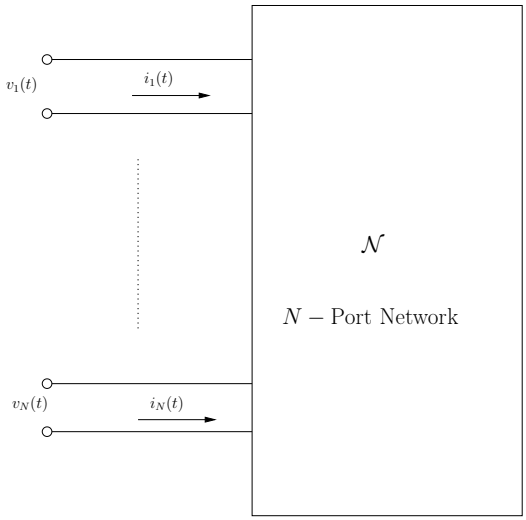

Figure 1.3: schematic N-Port Network

Let us consider the variables ξ and η related to v and i by

$$\begin{bmatrix} v \\ i \end{bmatrix} = \Omega \begin{bmatrix} \xi \\ \eta \end{bmatrix}, \tag{1.1}$$

where Ω is a real invertible $2N \times 2N$ matrix.

Definition 1. We shall say that a network $\mathcal{N}$ has an Ω-representation if, for each $\mathcal{N}$-admissibile $\xi(t)$, there is a unique $\mathcal{N}$-admissible $\eta(t)$, i.e there exists an operator Λ such that

$$\xi = \Lambda\eta.$$

Definition 2. Considering a network $\mathcal{N}$ and a well-defined Ω-representation, we say that the network is *linear time-invariant* if the operator Λ is linear and satisfies

For any $T \in \mathbb{R}$, $\eta \in \mathcal{D}(\Lambda)$ and $\xi = \Lambda\eta \Rightarrow \eta(\cdot\ + T) \in \mathcal{D}(\Lambda)$ and $\xi(\cdot\ + T) = \Lambda\eta(\cdot\ + T)$.

Here $\mathcal{D}(\Lambda)$ denotes the domain of the operator Λ.

Through this section, we will always consider linear time-invariant (LTI) networks and therefore whenever talking of a network we assume implicitly that it is LTI.

Two important examples of an Ω-representation are the *impedance* and the *admittance* representations. Setting $\Omega = Id_{2N}$ (for the case of impedance), and $\Omega =$

$\begin{pmatrix} 0 & Id_N \\ Id_N & 0 \end{pmatrix}$ (for the case of admittance) we may have the following representations

$$v = \mathcal{Z}i, \qquad i = \mathcal{Y}v. \tag{1.2}$$

Here $\mathcal{Z}$ is called the impedance operator, while $\mathcal{Y}$ is called the admittance operator.

Definition 3. $\mathcal{N}$ is *passive* if for any $T > -\infty$ and for all $\mathcal{N}$-admissible port current-voltage pair (i, v)

$$\int_{-\infty}^{T} \overline{v}(t)i(t)dt \geq 0, \tag{1.3}$$

where the symbol $-$ denotes the conjugate transpose. The integral is finite as we assume $v(t)$ and $i(t)$ in L_{2e}^N.

Boyd and Chua [11] introduce the following variables

$$\begin{aligned} a(t) &= \tfrac{1}{2}v(t) + \tfrac{1}{2}i(t), \\ b(t) &= \tfrac{1}{2}v(t) - \tfrac{1}{2}i(t), \end{aligned} \tag{1.4}$$

We can reformulate (1.3) as

$$\forall T \in \mathbb{R} \qquad \int_{-\infty}^{T} (\overline{a}(t)a(t) - \overline{b}(t)b(t))dt \geq 0. \tag{1.5}$$

Definition 4. We say that $\mathcal{N}$ is *solvable* if the set of $\mathcal{N}$-admissible a's includes L_2^N.

For a passive solvable network $\mathcal{N}$, it is a direct consequence of the linearity and the inequality (1.5) that for each $a \in L_2^N$, there is a unique b such that the pair (a, b) is admissible. Furthermore by (1.5), $\|b\|_{L_2^N} \leq \|a\|_{L_2^N}$. Thus we may define a linear bounded operator $\mathcal{S}$ on L_2^N by

$$\mathcal{S}a = b. \tag{1.6}$$

Theorem. *The passivity of the network $\mathcal{N}$ implies that $\mathcal{S}$ is a* causal *operator, i.e.*

$$a(t) = a'(t) \quad \textit{for } t < T \Rightarrow \quad \mathcal{S}a(t) = \mathcal{S}a'(t) \quad \textit{for } t < T.$$

Proof. Since $\mathcal{N}$ is a linear network, it is sufficient to show if $a(t) = 0$ for $t \leq T$, then

$Sa(t) = 0$ for $t \leq T$. For fixed T, the *passivity* property implies

$$\int_{-\infty}^{T} [\overline{a}(t)a(t) - \overline{b}(t)b(t)]dt \geq -\int_{-\infty}^{T} \overline{b}(t)b(t)dt = -\int_{\infty}^{T} |b|^2 dt \geq 0.$$

We can conclude $b(t) = \mathcal{S}a(t) = 0$ for $t \leq T$. □

Here we recall an important criterium to verify the *passive* property of a network.

Theorem ((Youla et al) [66]). *A solvable network $\mathcal{N}$ is* passive *if and only if*

(1) $\mathcal{N}$ has a scattering matrix, i.e. for any ω there exists a matrix $S(i\omega)$ such that for any admissible pair (a, b) satisfying $a \in L_2^N$,

$$\hat{b}(i\omega) = S(i\omega)\hat{a}(i\omega).$$

Note that thanks to (1.5), $a \in L_2^N$ implies $b \in L_2^N$ and therefore both Fourier transforms $\hat{a}(i\omega)$ and $\hat{b}(i\omega)$ are well-defined.

(2) $S(i\omega)$ has the analytic extension $S(z)$ in the open right half plane (RHP) and verifies

$$\overline{S}(z)S(z) \leq I \qquad \forall z \in RHP \tag{1.7}$$

where I denotes the identity matrix.

A proof of this theorem can be found in [11].

Remark 1. The operators verifying (1.7) are called *bounded-real* operators.

Returning now to the impedance (admittance) representation, [11] proposes another passivity criteria:

Theorem (Boyd and Chua [11]). *Assuming that $\mathcal{N}$ is solvable, then $\mathcal{N}$ is* passive *if and only if*

- *The impedance matrix $\boldsymbol{Z}(i\omega)$ satisfying $\hat{v} = \boldsymbol{Z}\hat{i}$ for admissible pairs $(v, i) \in L_2^{2N}$, has an analytic extension in open right half plane (RHP) and $\boldsymbol{Z}(s) + \overline{\boldsymbol{Z}}(s)$ is positive there , i.e.*

$$\forall s \in RHP, \qquad \Re(c^*(\boldsymbol{Z}(s) + \overline{\boldsymbol{Z}}(s))c) \geq 0 \qquad \forall c \in \mathbb{C}^N. \tag{1.8}$$

The same holds for the admittance matrix $\boldsymbol{Y}$.

Remark 2. The impedance matrix $\mathbf{Z}(s)$ and the scattering matrix $S(s)$ are related through an homographic transformation given by

$$\mathbf{Z}(s) = (S(s) + Id_N)(S(s) - Id_N)^{-1}.$$

It can be shown that homographic transformations map bounded-real operators into positive semidefinite operators.

1.2.2 Principles of reflectometry

Here we present the physics behind the reflectometry experiments. For example, the Hewlett Packard notes [28] describes the functioning of the reflectometer using the notion of power waves. Power waves have been introduced by Kurokawa [39] in order to define the reflection coefficient from an energetic point of view. We have chosen this presentation as it is closer to our theoretical approach, used later in this thesis.

Although a network may have any number of ports, we are going to explain network parameters by considering a network with only two ports (fig. 1.4). Since we are

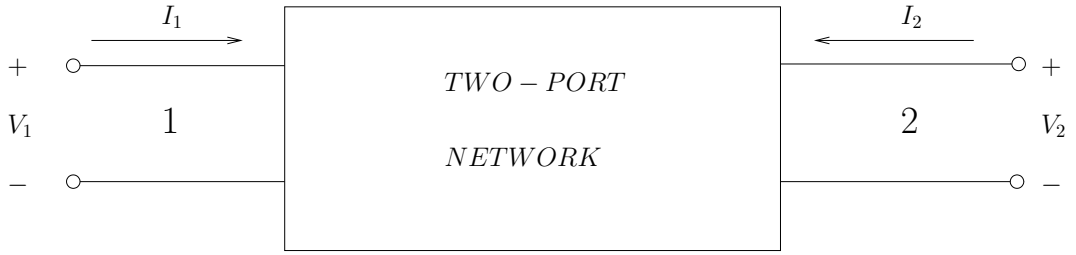

Figure 1.4: 2-Port Network

dealing with reflectometers, it is natural choice to consider the frequency as variable instead of time t. Indeed, voltage $\mathbf{V} = (V_1, V_2)$ and current $\mathbf{I} = (I_1, I_2)$ depend on frequency ω.

We are assuming that the 2-port is a LTI *passive* network an hence the impedance representation is well defined. In this case, following [20] the impedance matrix $\mathbf{Z}(i\omega)$ is defined as

$$\begin{pmatrix} V_1(\omega) \\ V_2(\omega) \end{pmatrix} = \begin{pmatrix} z_{11}(i\omega) & z_{12}(i\omega) \\ z_{21}(i\omega) & z_{22}(i\omega) \end{pmatrix} \begin{pmatrix} I_1(\omega) \\ I_2(\omega) \end{pmatrix} \tag{1.9}$$

where z_{ij} are assumed to be complex variable depending on the frequency ω.

Power waves and S-parameters

Generalized scattering parameters have been defined by Kurokawa [39]. These parameters are based on the concept of traveling power waves associated to the voltage V_i and current I_i flowing into each port i of the network and to a reference impedance Z_i associated to each port. The bar symbol denoting the complex conjugate, we define, following [39]:

$$(\nu_1)_i = \frac{V_i - \overline{Z}_i I_i}{2\sqrt{|\Re Z_i|}}, \qquad (\nu_2)_i = \frac{V_i + Z_i I_i}{2\sqrt{|\Re Z_i|}}. \qquad i = 1, 2. \tag{1.10}$$

where $\Re Z_i$ denotes the real part of Z_i.
These two new variables $(\nu_1, \nu_2)_i$ are called respectively the *reflected* and *incident* power waves associated to the port i (see Fig. 1.5). we can define the S-parameters

Figure 1.5: 2-Port Network with power waves

s_{11}, s_{21}, s_{21} and s_{22} as matrix that relates the incident waves with the reflected ones:

$$\begin{pmatrix} (\nu_1)_1 \\ (\nu_1)_2 \end{pmatrix} = \begin{pmatrix} s_{11} & s_{12} \\ s_{21} & s_{22} \end{pmatrix} \begin{pmatrix} (\nu_2)_1 \\ (\nu_2)_2 \end{pmatrix}. \tag{1.11}$$

The matrix composed by the S-parameters is called S-matrix (see [20]).

Remark 3. A physically realizable scattering matrix $S(\omega)$ is one which represents a LTI *passive* network $\mathcal{N}$.

The parameters, called S-parameters for "scattering" parameters, are important in microwave design because they are easier to measure and work with at high frequencies than other kinds of parameters, like the Z-parameters.

It can be shown the following equivalence between the Z-parameters defined in

(1.9) and the S-parameters defined in (1.11). As soon as the inverse exists,

$$s_{11} = \frac{(z_{11}-\overline{Z}_1)(z_{22}+Z_2)-z_{12}z_{21}}{(z_{11}+Z_1)(z_{22}+Z_2)-z_{12}z_{21}}, \tag{1.12}$$

$$s_{12} = \frac{2z_{12}(\Re Z_1 \Re Z_2)^{1/2}}{(z_{11}+Z_1)(z_{22}+Z_2)-z_{12}z_{21}}, \tag{1.13}$$

$$s_{21} = \frac{2z_{21}(\Re Z_1 \Re Z_2)^{1/2}}{(z_{11}+Z_1)(z_{22}+Z_2)-z_{12}z_{21}}, \tag{1.14}$$

$$s_{22} = \frac{(z_{11}+Z_1)(z_{22}-\overline{Z}_2)-z_{12}z_{21}}{(z_{11}+Z_1)(z_{22}+Z_2)-z_{12}z_{21}}, \tag{1.15}$$

where Z_1 is the source impedance at port 1 and Z_2 the load impedance at port 2 (see Figure 1.7). The impedance Z_1, Z_2 are such that i.e. $\Re Z_1, \Re Z_2 > 0$.

The passivity property of 2-port network is a sufficient condition for the existence of these equations: it is easy to see that if the impedance matrix $\mathbf{Z}$ verifies (1.8), the denominators in (1.12)-(1.15) are different from zero . The transformations (1.12)-(1.15) is is solving a direct scattering problem: from the impedances z_{ij} one gets the scattering parameters s_{ij}.

The inverse transformation is solving an *inverse* scattering problem. From the knowledge of the S-parameters we recover the impedance matrix $\mathbf{Z}$ as follows

$$z_{11} = \frac{(\overline{Z}_1+Z_1 s_{11})(1-s_{22})+Z_1 s_{12}s_{21}}{(1-s_{11})(1-s_{22})-s_{12}s_{21}}, \tag{1.16}$$

$$z_{12} = \frac{2s_{12}(\Re Z_1 \Re Z_2)^{1/2}}{(1-s_{11})(1-s_{22})-s_{12}s_{21}}, \tag{1.17}$$

$$z_{21} = \frac{2s_{21}(\Re Z_1 \Re Z_2)^{1/2}}{(1-s_{11})(1-s_{22})-s_{12}s_{21}}, \tag{1.18}$$

$$z_{22} = \frac{(1-s_{11})(\overline{Z}_2+Z_2 s_{22})+Z_2 s_{12}s_{21}}{(1-s_{11})(1-s_{22})-s_{12}s_{21}}. \tag{1.19}$$

An exemple: T-Network

Image impedance is a concept used in electronic network design and analysis and most especially in filter design. The term image impedance applies to the impedance seen looking in to ports of a network. Formally the image impedance is for a two-port

network is the impedance, $Z_{im,1}$, seen looking in to port 1 when port 2 is terminated with the impedance, $Z_{im,2}$, for port 2.

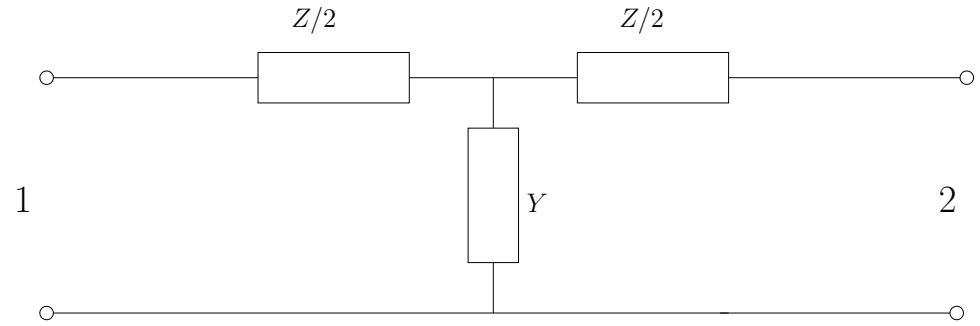

Figure 1.6: A two-port model with 3 terminations

Let us consider the T-network with a series of impedances Z and an admittance Y. This circuit defines naturally an application such that for any branched impedance Z_2 at port 2 it gives an image impedance $Z_{im,1}$ at port 1:

$$Z_2 \mapsto Z_{im,1}.$$

The fixed points Z_c of this application $Z_c \mapsto Z_c$ satisfy

$$Z_c^2 = \frac{1}{4}Z^2 + \frac{Z}{Y}. \tag{1.20}$$

It is natural to take as reference impedance one of the roots (usually the one with $\Re \geq 0$).

Remark 4. We can have a non-symmetric case for the T-model. The choice of $Z/2, Z/2$ is arbitrary and choosing two different impedances, we can have two different references for the left side and the right side. This comes from the fact that the applications $Z_{im,2} \mapsto Z_{im,1}$ and $Z_{im,1} \mapsto Z_{im,2}$ are not the same.

We note that the T-network is passive. It is sufficient to verify the criterium (1.8) for impedance matrix. We compute explicitly the values z_{ij}. Using the Ohm's laws,

we have

$$\begin{aligned} z_{11} &= \frac{1}{Y} + \frac{Z}{2}, \\ z_{12} &= \frac{1}{Y}, \\ z_{21} &= \frac{1}{Y}, \\ z_{22} &= \frac{1}{Y} + \frac{Z}{2}. \end{aligned}$$

The impedance $\mathbf{Z} = (z_{11}, z_{12}, z_{21}, z_{22})$ is definite positive matrix as long as the series impedances verify $Z > 0$,

$$\begin{vmatrix} z_{11} & z_{22} \\ z_{12} & z_{21} \end{vmatrix} = \left(\frac{1}{Y} + \frac{Z}{2}\right)^2 - \frac{1}{Y^2} = \frac{Z}{2}\left(\frac{Z}{2} + \frac{2}{Y}\right) > 0.$$

That is enough to guarantee the passivity of the T-network.

The Z-parameters for the T-network have an important property:

$$z_{12} = z_{21}. \tag{1.21}$$

We say that the impedance matrix $\mathbf{Z}$ is *reciprocal* if it verifies (1.21). A directly consequence of this property can be seen on the S-parameters, from the transformations (1.13) and (1.14) we have

$$s_{12} = s_{21}. \tag{1.22}$$

Moreover if we assume that the loads are the same at both ends $Z_1 = Z_2$, using (1.12) and (1.15) we have

$$s_{11} = s_{22}. \tag{1.23}$$

Symmetric configuration for the T-network implies that the two reflectometry experiences at both ends give the same measurements.

Some properties of power waves

We explain now the physical meaning of the power waves defined in (1.10). Let us consider a two-port network connected to a linear generator at Port 1 and to a load at Port 2, as shown in Figure 1.7. The pair (E_0, Z_1) represents a linear generator: Z_1 is its internal impedance and E_0 is the open circuit voltage of the generator.

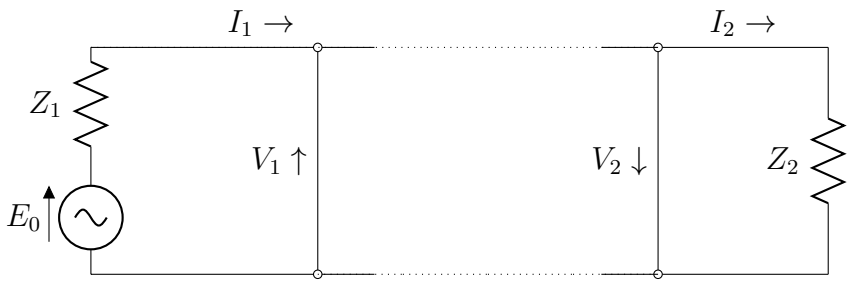

Figure 1.7: A 2-Port network connected to a linear generator (Port 1) and to a load (Port 2)

The power $P_L = \Re(V_1\overline{Z}_1)$ into a load Z_2 is given by

$$P_L = \Re Z_2 |I_1|^2 = \frac{\Re(Z_2)|E_0|^2}{|Z_2 + Z_1|^2} = \frac{|E_0|^2}{4\Re(Z_1) + \frac{(Z_2 - \overline{Z}_1)^2}{\Re(Z_2)}}, \tag{1.24}$$

Note that $\Re(Z_1)$ is positive, because it represents the generator source. It is interesting to know what are the conditions for the terminal impedance Z_2 to maximize the power P_L, i.e.

$$\max_{Z_2} P_L(Z_2).$$

It can found easily we can see that the maximum power P_L is achieved when

$$Z_2 = \overline{Z}_1 \tag{1.25}$$

and its value is

$$P_L^{max} = \frac{|E_0|^2}{4\Re(Z_1)} \qquad (\Re(Z_1) > 0).$$

The maximum power is also called the "available" power of the generator.
The voltage at the generator terminal is given by

$$V_1 = E_0 - Z_1 I_1.$$

Inserting this into (1.10), we have

$$|(\nu_2)_1|^2 = \frac{|E_0|^2}{4|\Re(Z_1)|^2},$$

and we note immediately that

$$P_L^{max} = |(\nu_1)_1|^2. \tag{1.26}$$

Note that if there is no source, i.e. $E_0 = 0$, then $(\nu_2)_1$ becomes also zero.
Now let's look at the difference $|(\nu_2)_1|^2 - |(\nu_1)_1|^2$; direct substitution into (1.10) shows

$$\Re\{V_1 I_1^*\} = |(\nu_2)_1|^2 - |(\nu_1)_1|^2. \tag{1.27}$$

The left-hand side of (1.27) expresses the power which is actually transferred from the generator to the load and this is called the *actual power*. The actual power is equal to $|(\nu_2)_1|^2 - |(\nu_1)_1|^2$: since $-|(\nu_1)_1|^2$ is always negative whether the load contains some source or not, the magnitude of the power of a generator $|(\nu_2)_1|^2$ can be identify as the maximum power that the generator can supply.
The generator is sending the power $|(\nu_2)_1|^2$ toward the load, regardless of the load impedance. However, when the load is not matched, i.e. (1.25) is not satisfied, a part of the incident power is reflected back to the generator. This reflected power is given by $|(\nu_1)_1|^2$ so that the net power absorbed in the load is equal to $|(\nu_2)_1|^2 - |(\nu_1)_1|^2$. Associated with incident and reflected power, there are waves $(\nu_2)_1$ and $(\nu_1)_1$ respectively.

1.2.3 The engineering state of art in reflectometry

Reflectometry experiments consist in sending a signal into a network and analyzing the returning signals, composed by all signals reflected by the heterogeneities of the line. In fact, when a signal comes across an electrical discontinuity, part of its energy is sent back to plug-in port.

The basic reflectometry experiment on 2-port network consists in measuring, for example at port 1, the quantity $(\nu_1)_1$ when $(\nu_2)_2 = 0$ and $(\nu_1)_2 \neq 0$, which is obtained by using a voltage generator.

Being $(\nu_2)_2 = 0$, from (1.11) we can compute the first s-parameter, the reflection coefficient at port 1,

$$s_{11} = \frac{(\nu_2)_1}{(\nu_1)_1}.$$

As well, we are able to able to compute s_{21} measuring the signal $(\nu_1)_2$.

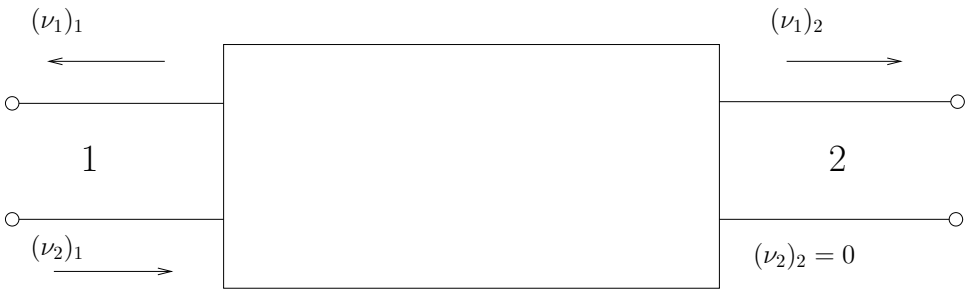

Figure 1.8: Reflectometry on a two-port network

To obtain the other two s-parameters, we need to consider the specular case. Assuming that $(\nu_2)_1 = 0$ and $(\nu_2)_2 \neq 0$ and measuring $(\nu_1)_1$ and $(\nu_1)_2$, we will able to compute s_{12} and s_{22}.

All reflectometry experiments consist in choosing a signal ν_2 of a particular form to inject into network and measuring ν_1: each method has different advantages. In theory all methods are equivalent, but in the real application, there are some constraints that limit the experiments of each kind.

The reflectometry experiments are divided in two main domains: time domain reflectometry (TDR) and frequency domain reflectometry (FDR) presented in this section [21].

Frequency Domain Reflectometry (FRD)

FRD uses a high frequency signal to detect the faults of the network.

In this case the analysis is based on stationary waves. The signal used in the frequency domain reflectometry is an harmonic signal which is stepped over a range of frequencies from ω_1 to ω_2. The transmitted signal is generated by a voltage source of the following form

$$V_1 = V_s \cos(\omega(t)), \tag{1.28}$$

where V_s is voltage source, $\omega(t)$ varies over the range (ω_1, ω_2);

There are three types of FDR can be adapted for the measurements of wires and cables. These are:

(PDFDR) *Phase Detection Frequency Domain Reflectometry* system sends a set of stepped frequency sine wave on cable where at the end there is load. A voltage control oscillator (VCO) injects a sinusoidal signal of the form (1.28). Part of the signal

is sent to a mixer, while the remainder is sent to the cable. The incident signal travels along the cable and it is reflected by the load at the terminal end. Isolated by a directional coupler, the reflected wave is also sent to the mixer: the mixer device "multiplies" the incident and the reflected waves. After filtering the signal, a dc voltage is the output of the mixer used to detect and to determine the length and the load of the cable.
The PDFDR method involves small and inexpensive components and for this reason it has been chosen for "smart wiring system" that can be used to test the integrity of aircraft cables nondestructively on board [21]. The method has been conceived to test the integrity of aircraft cable on board. Thus this system will test all critical wiring system prior to the flight.

(FMCW) *Frequency-Modulated Continuous-Wave* system send, using a VCO, a set of high-frequency sine waves with frequencies that are increased in time [22]. Like the PDFR, this method isolates the reflected wave from the incident. But if PDFDR methods analyze the phase difference, FMCW methods measure the frequency difference. By measuring the difference between the frequency of the reflected wave and the new (ramped up) frequency of the incident wave, the elapsed time and hence the length of the cable can be determined. A necessary condition is the high frequency regime for the reflectometers (typically in the hundreds of megahertz to few gigaherz range).

(SWR) *Standing-Wave Reflectometry* systems systems also sends a high frequency signal into the waveguide [45, 65]. The incident wave is not separated from the reflected wave in this method. The magnitude of the standing wave depends on the location and type of the load on the end of the cable and the frequency of the incident wave. Multiple measurements are required in order to determine the length and the load on the cable. This method can be sensitive to noise and frequency dependent loads, but if frequencies are chosen conveniently, SWR experiments can be reasonably cost effective.

Time Domain Reflectometry (TDR)

The incident and the reflected waves are both seen simultaneously, although their time domain signatures are separated in time because of the travel time delay. The cable impedance, termination, and length give a unique temporal signature that can be used to determine the status of the cable.
Spread Spectrum Time Domain Reflectometry (SSTDR)[60] and Sequence Time Domain Reflectometry (STDR)[31] inject into the cable a recursive linear signal (RLS) of the following form:

$$(\nu_2)_1 = \sum_{n=-\infty}^{\infty} S[n]p(t - nT_s) \tag{1.29}$$

where $S[n]$ is a recursive linear sequence of period K consisting of 1 and -1 and

$$p(t) = \begin{cases} 1, & 0 < t < T_c, \\ 0, & otherwise. \end{cases}$$

The recursive signal has period $T_s = KT_c$, where T_c is the minimum of duration of 1 and -1. SSTDR and STDR have been demonstrated to be effective technologies for locating on intermittent wiring failures such as open circuits and short circuits (hard faults) [60].

Comparison between TDR and FDR

Time domain and frequency domain methods are strongly related. TDR uses short pulses and, in theory, it provides information over an "infinite" range of frequencies. In practice this range is limited by the rise time of the pulse. On the other hand FDR uses stationary wave over a smaller set of frequencies then TDR. In theory, FDR and TDR methods are equivalents: they provide the same kind of informations. In practice, of course, differences in the sensitivities and accuracy of the electronics can cause variation in how the different systems perform. Still, it is useful to know that data received using a TDR can be replicated using an FDR method, and vice versa.

All reflectometry methods rely on a strong reflection on the spots where are the faults on the cable in order to locate them. Open and short circuits provide the largest reflection coefficient, so not surprisingly they are the easiest to detect. Fortunately for detection and localization, many other faults of interest appear as very near open or short circuits at the high frequencies commonly used in reflectometry methods.

1.2.4 Some challenging problems on reflectometry

As we have seen previously, reflectometry methods work well on the hard faults, but there are still some challenging problems on soft-faults detections. Reflectometry experiments shows to be accurate for location of "hard" faults, but the location of "soft" faults such as frays and chafes remains elusive. Griffiths, Parakh, Furse and Baker [26] analyze the impedance of several types of soft faults and their resultant reflectometry returns, which are shown to be smaller than returns from other sources of physical and electrical noise in the system. Through numerical simulations verified by measurement, they show that soft faults are virtually impossible to locate using today's reflectometry methods including TDF, FRD, and SSTDR.

Another interesting class of problem is the application of reflectometry methods directly onto electrical network. When wires contain many singularities, finding electric faults in a network becomes very complex. Furthermore, when complex networks made of several junctions are diagnosed, classical fault detection leads to ambiguities concerning the location. Different methods have been proposed to locate faults on wiring network. In a baseline method, the response of the faulty network is compared to the pre-measured of simulated response of its known healthy condition. Smail-et-al [57, 58] propose a new technique to reconstruct faulty wiring network from TDR responses and genetic algorithms.

In [41], Lelong et al introduce a new method for distributed wire diagnosis by reflectometry; *distributed* diagnosis consists in making reflectometry measurements at several points of a complex network at the same time, thus allowing to isolate ambiguities due to the existence of multiple paths. In fact, when the test points are properly chosen, the association of these multiple measurements allows the exact location of a singularity in the network.

Inspired by these two challenges, this thesis has for goal to study the fault-detection and diagnosis on the electrical network. Using the FDR methods, our purpose is to detect and locate both hard and soft faults along a network through the measurement of one reflection coefficient. Next section will be devoted to the formulation of the mathematical problem about reflectometry methods.

1.3 Telegrapher's Equations and equivalent formulations

In this section we describe the equations that model the transmission of electrical waves through transmission lines [46]. The propagation of electrical signal along a cable is modeled by the "Telegrapher's equations".

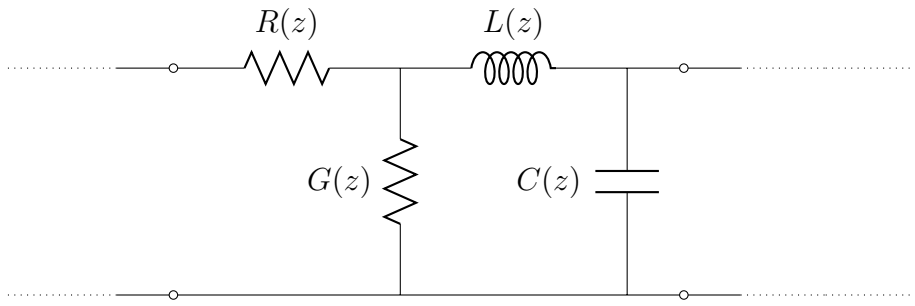

Figure 1.9: Schematic representation of the elementary components of a transmission line

One assumes that cable conductors are composed of an infinite series of two-port elementary components, each representing an infinitesimally short segment of a transmission line:

- The distributed resistance R of the conductors is represented by a series resistor (expressed in ohms per unit length).
- The distributed inductance L (due to the magnetic field around the wires, self-inductance, etc.) is represented by a series inductor (henries per unit length).
- The capacitance C between the two conductors is represented by a shunt capacitor C (farads per unit length).
- The conductance G of the dielectric material separating the two conductors is represented by a shunt resistor between the signal wire and the return wire (siemens per unit length). This resistor in the model has a resistance of 1 / G ohms.

These parameters allow a rather complete and understandable description of transmission lines and they are sufficient to represent the lines in the frequency range used

during reflectometry.

The behavior of electric signal depends upon the intensity of the current $I(t,z)$ and the voltage $V(t,z)$. Both functions are parametrized by a space variable z and the time t.
Eventually the telegrapher's equations for a transmission line write

$$\begin{cases} \frac{\partial}{\partial z}I(t,z) + C(z)\frac{\partial}{\partial t}V(t,z) + G(z)V(t,z) = 0, \\ \frac{\partial}{\partial z}V(t,z) + L(z)\frac{\partial}{\partial t}I(t,z) + R(z)I(t,z) = 0. \end{cases} \tag{1.30}$$

1.3.1 Finite Line Model

Consider a transmission line of finite length ℓ. Assume that the left end and the right end of the line correspond respectively to $z = z_l$ and $z = z_r$, such that $|z_l - z_r| = \ell$.
The generic boundary conditions are:

$$\begin{cases} V(t,z_l) + \mathcal{Z}_l(t) * I(t,z_l) = \mathcal{V}_l(t), \\ V(t,z_r) - \mathcal{Z}_r(t) * I(t,z_r) = \mathcal{V}_r(t), \end{cases} \tag{1.31}$$

where $\mathcal{V}_l$ and $\mathcal{V}_r$ are the voltage sources respectively at $z = z_l$ and $z = z_r$. $\mathcal{Z}_l$ and $\mathcal{Z}_r$ are the transmission line impulse response at $z = z_l$ and $z = z_r$. The symbol $*$ denotes the convolution product.

The linearity of the transmission line model allows to replace any test by an equivalent test in harmonic regime. The harmonic regime of the solutions is imposed by a choice of the source generator of the form:

$$\mathcal{V}_l(t) = V_l(\omega)e^{i\omega t}, \qquad \mathcal{V}_r(t) = V_r(\omega)e^{i\omega t}, \tag{1.32}$$

where ω represents the pulsation of the source generators.
We are looking for the solution $V(t,z)$ and $I(t,z)$ of (1.30) of the form

$$V(t,z) = e^{i\omega t}V(\omega,z) \qquad I(t,z) = e^{i\omega t}I(\omega,z).$$

The variable ω is the time frequency and z is still the position coordinate. $V(\omega,z)$

and $I(\omega, z)$ are solutions of the telegrapher's equation in the harmonic regime.

$$\begin{cases} \frac{\partial}{\partial z}V(\omega,z) + i\omega L(z)I(\omega,z) + R(z)I(\omega,z) = 0, \\ \frac{\partial}{\partial z}I(\omega,z) + i\omega C(z)V(\omega,z) + G(z)V(\omega,z) = 0, \end{cases} \tag{1.33}$$

with boundary conditions

$$\begin{cases} V(\omega,z_l) + Z_l(\omega)I(\omega,z_l) = V_l(\omega), \\ V(\omega,z_r) - Z_r(\omega)I(\omega,z_r) = V_r(\omega). \end{cases} \tag{1.34}$$

where Z_l and Z_r are time-Fourier transformed of $\mathcal{Z}_l$ and $\mathcal{Z}_r$ and $V_l(\omega)$ and $V_r(\omega)$ are defined in (1.32).

Characteristic Impedance

In order to define the characteristic impedance, let us consider the elementary component of a semi-discretization for the space variable z (see Fig. 1.9) and let us suppose that it has the form of a T-network, shown in Fig. 1.6.

Since the T-model represents the elementary component of a $RLGC$ transmission line, the impedances Z and the admittance Y are given by

$$Z = R + i\omega L, \qquad Y = G + i\omega C.$$

Being an infinitesimally short segment z, we have Ydz and Zdz instead of Y and Z. The fixed point of the image application (1.20) becomes, as dz goes to zero,

$$Z_c = \sqrt{Z/Y}.$$

Now we are ready to introduce the following definition.

Definition 5 (Local Characteristic impedance)**.** For the transmission line model based on the telegrapher's equations, the *characteristic impedance* $Z_c(\omega, z)$ is defined by

$$Z_c(\omega,z) = \sqrt{\frac{R(z) + i\omega L(z)}{G(z) + i\omega C(z)}}. \tag{1.35}$$

Note that in the lossless case, i.e. $R = G \equiv 0$, the characteristic impedance Z_c does not depend on frequencies.

Particular boundary conditions

Boundary conditions (1.34) represents all possible electrical configurations for problems described in Section 1.1. In particular we privilege three particular boundary conditions that we will fit to our experiments.

Figure 1.10: One generator source model

On the left end, we connect a source generator $V_s(\omega)$ of frequency ω with an internal impedance $Z_s(\omega)$. On the right terminal, there is no source.

$$\begin{aligned} &V(\omega, z_l) + Z_s(\omega) I(\omega, z_l) = V_s(\omega), \\ &V(\omega, z_r) - Z_r(\omega) I(\omega, z_r) = 0 \qquad . \end{aligned} \tag{1.36}$$

We want to emphasize three possible configurations at right terminal node $z = z_l$

- *Open Circuit*: open-circuit voltage is the difference of electrical potential between two terminals of a device when there is no external load connected, i.e. the circuit is broken or open. Setting $Z_r = \infty$, the boundary condition becomes

$$I(\omega, z_r) = 0.$$

- *Short circuit* : a short circuit is simply a low resistance connection between the two conductors supplying electrical power to any circuit. Short circuits can produce very high temperatures due to the high power dissipation in the circuit. This situation occurs when $Z_r(\omega) = 0$. The condition (1.36) is

$$V(\omega, z_r) = 0.$$

- *Matched Load*: impedance matching is the practice of designing the input impedance of an electrical load or the output impedance of its corresponding signal source in

order to maximize the power transfer and minimize reflections from the load. In this case we need to set the parameter Z_r equal to the characteristic impedance (1.35) at the terminal node, i.e.

$$Z_r(\omega) = Z_c(\omega, z_r).$$

1.3.2 Network model

Graph

A wired network is mathematically represented by a tree Γ. A tree is a simply connected metric graph and it is described by a partially ordered set of nodes $\mathcal{V} = \{v_0, v_1, \dots, v_{n-1}\}$.
We consider a graph Γ with a unique minimal element, named v_0. The set $\mathcal{V}_{ext}$ of maximal elements of $\mathcal{V}$ represents the boundary vertices. The elements which are nor the minimal neither maximals are called *internal* vertices and they form a set denoted by $\mathcal{V}_{int}$.

$$\mathcal{V} = \mathcal{V}_{ext} \cup \mathcal{V}_{int} \cup v_0.$$

When two distinct vertices are comparable, there exists an edge connecting these two vertices. Given two consecutive vertices $v_i < v_{i'}$ the edge e_j connecting these two vertices, is parametrized through the position coordinate z varying from $[z_{l_j}, z_{r_j}]$ where $z = z_{l_j}$ corresponds to the vertex v_i and $z = z_{r_j}$ corresponds to $v_{i'}$.
We say that e_j is *external* if one of its nodes is either minimal or maximal.

Remark 5. This formulation includes also non-compact graphs, where external edges can be also semi-infinite. We note that in this case z_{r_j} can be also assumed to be infinite.

Transmission line equations

Let Γ be the network and let $\mathcal{E} = \{e_0, e_1, \dots e_n\}$ be the set of branches. We define the intensity of the current I and the voltage V on the network Γ as a set of functions $\{I_j\}_{j=1}^n$ and $\{V_j\}_{j=1}^n$, where each intensity I_j and each voltage V_j is defined on the j-th branch.
In general, all functions will be indexed by the edge numbers: for example $R_j(z)$ will denote the resistance R defined on the j-th branch.

On each branch e_j, we define the telegrapher's equation in harmonic regime indexed by the letter j

$$\begin{cases} \frac{\partial}{\partial z}V_j(\omega,z) + i\omega L_j(z)I_j(\omega,z) + R_j(z)I_j(\omega,z) = 0, \\ \frac{\partial}{\partial z}I_j(\omega,z) + i\omega C_j(z)V_j(\omega,z) + G_j(z)V_j(\omega,z) = 0, \end{cases} \quad z \in [z_{l_j}, z_{r_j}]. \tag{1.37}$$

Boundary conditions at the nodes

In order to model the telegrapher's equations on networks, we need to add some boundary conditions at the central nodes $\mathcal{V}_{int}$ and to the external nodes $\mathcal{V}_{ext} \cup v_0$.

Terminal nodes $\mathcal{V}_{ext}$
At the terminal node $v_j \in \mathcal{V}_{ext}$ and on the edge e_j connected to it , i.e. v_j correspond to $z = z_{r_j}$, the generic situation is represented by

$$V_j(\omega, z_{r_j}) - Z_j(\omega)I_j(\omega, z_{r_j}) = V_j(\omega), \tag{1.38}$$

where Z_j is the impulsion response and V_j a possible voltage source generator.

Terminal node v_0
The minimal element v_0 is related to the branch indexed by 0 as its left end $z = z_{l_0}$ and the generic boundary condition for this node is

$$V_0(\omega, z_{l_0}) + Z_0(\omega)I_0(\omega, z_{l_0}) = V_0(\omega). \tag{1.39}$$

Internal node
At any internal node Kirchhoff laws hold:

- we impose the continuity of the voltage,
- the sum of incoming currents must be equal to the sum of the outgoing currents.

Considering v an internal vertex of the network and $\mathcal{E}(v)$ the set of edges joining at v, these matching conditions can be written as

$$\sum_{e \in \mathcal{E}(v)} I_e(\omega, v) = 0 \quad \text{and} \quad V_e(\omega, v) = V_{e'}(\omega, v) \quad \forall e, e' \in \mathcal{E}(v), \tag{1.40}$$

where $I_e(\omega, v)$ and $V_e(\omega, v)$ denote the current and the voltage over the branch e at the vertex v and where the symbol Σ corresponds to an algebraic sum.
The algebraic sum implies that the direction of current is needed to be taken into account

$$\sum_{e \in \mathcal{E}_{out}(v)} I_e(\omega, v) = \sum_{e \in \mathcal{E}_{in}(v)} I_e(\omega, v)$$

where $\mathcal{E}_{in}(v)$ and $\mathcal{E}_{out}(v)$ denotes the set of edges in $\mathcal{E}(v)$ such that the current's direction is respectively inward and outward with respect to v.

Remark 6. The direction of the currents $I_j(\omega, z)$ depends entirely upon the position of the source. The generator source will be placed at the minimal vertex v_0 in a such way that the directions of the current will be oriented as the parametrization of the branches.
In such situation, the outward and inward directions are related to the position of the node v in the parametrization of the edge e_j: given a parametrization $[z_{l_j}, z_{r_j}]$ of the brach e_j, the current will be consider *inward* if the node v corresponds to $z = z_{r_j}$, otherwise if v corresponds to $z = z_{l_j}$ the current will be *outward*.

1.3.3 The Liouville transformation

Reflectometry experiments lead to observing voltages and currents along the time at some position: only the traveling times and amplitudes of waves are accessible by such experiments. A fault can only be localized in terms of the traveling time of the reflected test wave starting from the test point. It becomes natural to work with the traveling time instead of the spatial coordinates. For engineers, the traveling time is also called *electrical distance*.
We introduce the Liouville transformation to change the nature of the position coordinate z into the electrical distance x. For a finite line of length ℓ and parametrized as $[z_l, z_r]$, the Liouville transformation writes

$$x(z) = \int_{z_l}^{z} \sqrt{L(z)C(z)}ds + x_l \quad z \in [z_l, z_r], \tag{1.41}$$

which corresponds to the wave traveling time from the position z_l to the position z. The electrical distance l corresponds to the physical length ℓ . We can say that the

finite line $[z_l, z_r]$ will be parametrized as $[x_l, x_r]$ with $|x_l - x_r| = l$.

The inverse transformation is well defined and we will be able to write $C(x) \equiv C(z(x))$, $L(x) \equiv L(z(x))$, $G(x) \equiv G(z(x))$, $R(x) \equiv R(z(x))$, $V(\omega, x) \equiv V(\omega, z(x))$ and $I(\omega, x) \equiv I(\omega, z(x))$.

The telegrapher's equation (1.33) in the harmonic regime becomes

$$\begin{cases} \frac{\partial}{\partial x} V(\omega, x) = -\frac{i\omega L(x) + R(x)}{\sqrt{L(x)C(x)}} I(\omega, x), \\ \frac{\partial}{\partial x} I(\omega, x) = -\frac{i\omega C(x) + G(x)}{\sqrt{L(x)C(x)}} V(\omega, x). \end{cases} \qquad x \in [x_r, x_l] \tag{1.42}$$

Since we are dealing with reflectometers, it is natural to choose as parameter the frequency ω. On the other side, the mathematical literature rather uses the letter k standing for the wave number.
From now on, we will use $k = \omega$ and this corresponds either to the case where there is no dispersion phenomena, for example in the lossless case or to the case where we are dealing with high frequencies $k \gg 0$. In general, these two parameters k and ω are related through the dispersion relation.
Introducing the quantity $Z_{c0}(x)$ at the point x

$$Z_{c0}(x) = \sqrt{\frac{L(x)}{C(x)}}, \tag{1.43}$$

we have that (1.42) writes

$$\begin{cases} \frac{\partial}{\partial x} V(k, x) = -\left(ik + \frac{R(x)}{L(x)}\right) Z_{c0}(x) I(k, x), \\ \frac{\partial}{\partial x} I(k, x) = -\left(ik + \frac{G(x)}{C(x)}\right) Z_{c0}^{-1}(x) V(k, x). \end{cases} \tag{1.44}$$

1.3.4 Lossy Network: Zakharov-Shabat system

Here we show the equivalence between the telegrapher's equations and a Zakharov-Shabat system, a first order coupled differential equation. This change of variables is particularly interesting since the two new variables will represent backward and foreword waves. The new formalism allows us to see clearly the relations between the reflection coefficient and the potentials, depending on the line parameters.

Let's consider telegrapher's equations (1.44) in the harmonic regime after the Liouville transformation.

Definition 6. Let's set the variables ν_1 and ν_2 as follows

$$\begin{cases} \nu_1(x,k) = \dfrac{1}{\sqrt{2}}\left[Z_{c0}^{-1/2}(x)V(k,x) - Z_{c0}^{1/2}(x)I(k,x)\right], \\ \nu_2(x,k) = \dfrac{1}{\sqrt{2}}\left[Z_{c0}^{-1/2}(x)V(k,x) + Z_{c0}^{1/2}(x)I(k,x)\right]. \end{cases} \tag{1.45}$$

The new variables verify the following coupled equations

$$\begin{cases} \partial_x\nu_1(x,k) + ik\nu_1(x,k) = +q_d(x)\nu_1(x,k) - q_+(x)\nu_2(x,k), \\ \partial_x\nu_2(x,k) - ik\nu_2(x,k) = -q_-(x)\nu_1(x,k) - q_d(x)\nu_2(x,k), \end{cases} \tag{1.46}$$

where

$$q_d(x) = \frac{1}{2}\left(\frac{R(x)}{L(x)} + \frac{G(x)}{C(x)}\right), \tag{1.47}$$

$$q_-(x) = \frac{1}{4}\frac{d}{dx}\left[\log\frac{L(x)}{C(x)}\right] - \frac{1}{2}\left(\frac{R(x)}{L(x)} - \frac{G(x)}{C(x)}\right), \tag{1.48}$$

$$q_+(x) = \frac{1}{4}\frac{d}{dx}\left[\log\frac{L(x)}{C(x)}\right] + \frac{1}{2}\left(\frac{R(x)}{L(x)} - \frac{G(x)}{C(x)}\right). \tag{1.49}$$

The set of equations (1.46) is called the *Zakharov-Shabat* system.

Note that the change of variables (1.45), introduced by Jaulent [30], looks like the Kurokawa power waves (1.10). In these coordinates, ν_1 and ν_2 represent respectively the backward and the foreword wave with respect to the sign of x.

Remark 7. The quantity $Z_{c0}(x)$ defined by (1.43) can be considered as the characteristic impedance defined in (1.35) within high frequency regime ($k \gg 0$) and it coincides with $Z_c(x)$ in the lossless case, when $R = G = 0$.
Instead of the high frequency characteristic impedance Z_{c0}, we could have used the local characteristic impedance Z_c and we would obtain a two potential Zakharov-Shabat system of the following form

$$\begin{cases} \partial_x\nu_1(x,k) + ik\nu_1(x,k) = +q_1(x,k)\nu_1(x,k) - q_2(x,k)\nu_2(x,k), \\ \partial_x\nu_2(x,k) - ik\nu_2(x,k) = -q_2(x,k)\nu_1(x,k) - q_1(x,k)\nu_2(x,k), \end{cases}$$

but the potentials q_1, q_2 would depend also on the frequency k and they are assumed to be complex value functions.

Boundary conditions

Terminal nodes $\mathcal{V}_{ext}$

Let's consider a terminal node $v_j \in \mathcal{V}_{ext}$ and let e_j be the edge connected to this vertex. The change of variables (1.45) implies that (1.38) becomes

$$(Z_{c0,j}(x_{r_j}) + Z_j(k))\nu_{1j}(x_{r_j}, k) + (Z_{c0,j}(x_{r_j}) - Z_j(k))\nu_{2j}(x_{r_j}, k) = \sqrt{2Z_{c0,j}(x_{r_j})}V_j(k).$$

Setting the following variables

$$\begin{aligned}
\rho_j(k) &= \frac{Z_j(k) - Z_{c0,j}(x_{r_j})}{Z_j(k) + Z_{c0,j}(x_{r_j})}, \\
\rho_0(k) &= \frac{Z_0(k) - Z_{c0,0}(x_{l_0})}{Z_0(k) + Z_{c0,0}(x_{l_0})}, \\
\nu_j(k) &= \frac{V_j(k)}{\sqrt{2Z_{c0,j}(x_{r_j})}}, \\
\nu_0(k) &= \frac{V_0(k)}{\sqrt{2Z_{c0,0}(x_{l_0})}},
\end{aligned}$$

the generic boundary conditions at the terminal nodes write

$$\nu_{1j}(x_{r_j}, k) - \rho_j(k)\nu_{2j}(x_{r_j}, k) = (1 - \rho_j(k))\nu_j(k). \tag{1.50}$$

Note that the boundary conditions at the external nodes depends on two parameters $\rho_j(k)$ and $\nu_j(k)$, an aggregates of the terminal impedance $Z_j(k)$, the high frequencies characteristic impedance $Z_{c0,j}$ and a possible generator source $V_j(k)$.

Remark 8. Note that, from its definition, $\rho_j(k)$ can take values

$$|\rho_j(k)| \leq 1 \qquad \forall k \in \mathbb{R}. \tag{1.51}$$

Terminal node v_0

At the left end of the branch e_0, corresponding to the terminal node v_0, the boundary condition (1.39) writes

$$\nu_{20}(x_{l_0}, k) - \rho_0(k)\nu_{10}(x_{l_0}, k) = (1 - \rho_0(k))\nu_0(k). \tag{1.52}$$

Remark 9. We are interested in the case where there is only one source generator at the minimal node v_0.

$$\nu_{20}(x_{l_0}, k) = \nu_S(k)$$

We describe three particular configurations at a generic terminal node v_j without any source, i.e. $V_j(k) = \nu_j(k) = 0$.

- *Open circuit*: The open circuit corresponds to $\rho_j(k) = +1$, the boundary condition (1.50) is

$$\nu_{1j}(x_{r_j}, k) - \nu_{2j}(x_{r_j}, k) = 0.$$

- *Short circuit*: This case is verified when $\rho_j(k) = -1$. In the Zakharov-Shabat coordinates, this is equivalent to

$$\nu_{1j}(x_{r_j}, k) + \nu_{2j}(x_{r_j}, k) = 0.$$

- *Matched Load*: Matching the internal impedance $Z_j(k)$ to the high frequency characteristic impedance $Z_{c0,j}(x_{r_j})$, we obtain the no reflection phenomenon and this is equivalent to setting $\rho_j(k) = 0$.

$$\nu_{1j}(x_{r_j}, k) = 0.$$

Internal nodes.
Let $v \in \mathcal{V}_{int}$ be an internal vertex and let $\mathcal{E}(v)$ be the set of edges connected to v. The Kirchhoff's laws translate to

$$\begin{aligned} Z_{c0,e}^{\frac{1}{2}}(v)[\nu_{1e}(v,k) + \nu_{2e}(v,k)] &= Z_{c0,e'}^{\frac{1}{2}}(v)[\nu_{1e'}(v,k) + \nu_{2e'}(v,k)] \quad \text{for } e, e' \in \mathcal{E}(v) \\ \sum_{e \in \mathcal{E}_{out}(v)} Z_{c0,e}^{-\frac{1}{2}}(v)[\nu_{1e}(v,k) - \nu_{2e}(v,k)] &= \sum_{e \in \mathcal{E}_{in}(v)} Z_{c0,e}^{-\frac{1}{2}}(v)[\nu_{1e}(v,k) - \nu_{2e}(v,k)]. \end{aligned} \tag{1.53}$$

where $\mathcal{E}_{int}$ and $\mathcal{E}_{out}$ represent the set of edges such that the current direction is respectively inward and outward with respect to the node v.

Remark 10. It is interesting to remark that the boundary conditions at the internal nodes depend only upon the quantity $Z_{c0,e}(v)$, i.e. the inductance L_e and the capacitance C_e.

Matrix formulation for the Zakharov-Shabat system

Here we present the matrix formulation for the Zakharov-Shabat system. It is useful when we need to add indices for the branches, but its limit is given by the poor formulation for the boundary conditions.
Let $Y(x,k)$ be the column vector $(\nu_1(x,k),\nu_2(x,k))^{tr}$ and let $Q(x)$ and σ_3 be the matrices defined as

$$Q(x) = \begin{pmatrix} q_d(x) & -q_+(x) \\ -q_-(x) & -q_d(x) \end{pmatrix}, \tag{1.54}$$

$$\sigma_3 = \begin{pmatrix} 1 & 0 \\ 0 & -1 \end{pmatrix}. \tag{1.55}$$

then the harmonic regime (1.46) writes

$$\frac{d}{dx}Y(x,k) + ik\sigma_3 Y(x,k) = Q(x)Y(x,k), \tag{1.56}$$

This notation will be helpful when we are dealing with lossy transmission line network.

Particular cases:

Non uniform lossless network.
A particular case of transmission line network is the non-uniform lossless network.
Let's examine the lossless transmission line model for a segment $x \in [x_l, x_r]$. In this case, the loss terms such as $R(x)$ and $G(x)$ are zero over the whole interval $[x_l, x_r]$, while the distributed parameters L and C vary. This implies that the Zakharov-Shabat potentials are:

$$\begin{aligned} q_d(x) &\equiv 0, \\ q_-(x) &= \frac{1}{4}\frac{d}{dx}\left[\log\frac{L(x)}{C(x)}\right] \\ q_+(x) &= \frac{1}{4}\frac{d}{dx}\left[\log\frac{L(x)}{C(x)}\right]. \end{aligned}$$

The Zakharov-Shabat system involves, hence, only one potential $-q_-(x) = -q_+(x) =$

$Q(x)$ and it writes

$$\frac{d}{dx}Y(x,k)+ik\sigma_3 Y(x,k)=\begin{pmatrix}0 & Q(x)\\ Q(x) & 0\end{pmatrix}Y(x,k). \tag{1.57}$$

Uniform network

Another interesting case to study is the uniform lossy network. Their line parameters R, L, G, C are constant along the branch. Hence there are two potentials

$$\begin{aligned} q_d(x) = \quad q_d \quad &= \frac{1}{2}\left(\frac{R}{L}+\frac{G}{C}\right),\\ q_-(x) = \quad -q_l \quad &= -\frac{1}{2}\left(\frac{R}{L}-\frac{G}{C}\right),\\ q_+(x) = \quad q_l \quad &= +\frac{1}{2}\left(\frac{R}{L}-\frac{G}{C}\right), \end{aligned}$$

The Zakharov-Shabat system writes

$$\frac{d}{dx}Y(x,k)+ik\sigma_3 Y(x,k)=\begin{pmatrix}q_d & q_l\\ -q_l & -q_d\end{pmatrix}Y(x,k). \tag{1.58}$$

1.3.5 Lossless Network: Schrödinger equation

We have shown the equivalence between the transmission line equations and the Zakharov-Shabat system. Now we want to present a particular case of the transmission lines: the lossless network.

Following a result by I.Kay [33], we see the equivalence between the lossless case and the time-independent Schrödinger equation. The necessity of introducing another equation for the transmission line model is due to the fact there exists an enormous literature on the Schrödinger equation.

In the absence of dissipation, the transmission line equations (1.30) write in time domain

$$\begin{cases} \partial_z I(t,z)+C(z)\partial_t V(t,z)=0,\\ \partial_z V(t,z)+L(z)\partial_t I(t,z)=0. \end{cases} \tag{1.59}$$

For a wave frequency k, i.e.

$$I(t,z) = I(k,z)e^{-ikt},$$
$$V(t,z) = V(k,z)e^{-ikt}$$

the telegrapher's equations (1.59) write in the harmonic regime as

$$\frac{d}{dz}\left(\frac{1}{L(z)}\frac{d}{dz}V(k,z)\right) - k^2 C(z)V(k,z) = 0. \tag{1.60}$$

Applying the Liouville transformation (1.41) and setting

$$y(x,k) = [Z_c(x)]^{-\frac{1}{2}}\, V(k,x), \tag{1.61}$$

where $Z_c(x) = \sqrt{L(x)/C(x)}$ denotes the characteristic impedance for a lossless transmission line, the equation (1.60) becomes

$$-\frac{d^2}{dx^2}y(x,k) + q(x)y(x,k) = k^2 y(x,k) \tag{1.62}$$

where the potential $q(x)$ is defined as follows

$$q(x) = \left[\frac{C(x)}{L(x)}\right]^{-\frac{1}{4}} \frac{d^2}{dx^2}\left[\frac{C(x)}{L(x)}\right]^{\frac{1}{4}}. \tag{1.63}$$

Note that in these new terms, the electrical current is given by

$$I(k,x) = \frac{1}{ik}\left(\frac{1}{2}\frac{Z_c'(x)}{Z_c^{3/2}(x)}y(x,k) + \frac{1}{Z_c^{1/2}(x)}\frac{d}{dx}y(x,k)\right)$$

where $Z_c'(x)$ denotes the spatial derivative of the characteristic impedance.

Boundary conditions

Terminal nodes.
Consider the terminal node $v_j \in \mathcal{V}_{ext}$ without a source and let e_j be the associated edge. The boundary conditions are

$$Z_j(k)y_j'(x_{r_j}) = -\left(ikZ_{cj}(x_{r_j}) + \frac{Z_j(k)}{2}\frac{Z_{cj}'(x_{r_j})}{Z_{cj}(x_{r_j})}\right)y_j(x_{r_j}). \tag{1.64}$$

Internal nodes.
In the new formalism, the Kirchhoff rules become for each internal vertex $v \in \mathcal{V}_{int}$

$$\begin{aligned} &A_e^{-1}(v)y_e(k,v) = A_{e'}^{-1}(v)y_{e'}(k,v) \quad \forall e, e' \in \mathcal{E}(v), \\ &\textstyle\sum_{e\in\mathcal{E}(v)} A'_e(v)y_e(k,v) + A_e(v)y'_e(k,v) = 0 \end{aligned} \tag{1.65}$$

where the functions A_e are defined as

$$A_e(x) = \left[\frac{C_e(x)}{L_e(x)}\right]^{\frac{1}{4}}, \qquad \forall e \in \mathcal{E}.$$

By $A'_e(v)$ we denote the derivative with respect to the coordinate x at the point $x = v$.

Between the Zakharov-Shabat system and Schrödinger equation

We have seen that the lossless transmission line equations are equivalent to two different equations: the Schrödinger equation (1.62) and the Zakharov-Shabat system (1.57). Each formulation has its own advantage: if the Zakharov-Shabat system requires less regularity for the line parameters for the definition of the potential (1.48) and (1.49), the Schrödinger equation has been deeply studied by mathematicians and physicists.
It is interesting to note although the two potentials Q and q require different regularities for the R, L, C and G in the two cases, they are related by the following Riccati equation

$$\frac{d}{dx}Q(x) - Q^2(x) + q(x) = 0.$$

1.4 Reflectometry, scattering data and inverse scattering

Reflectometry methods presented in Section 1.2 show how to detect and to locate inhomogeneities in an electric wire. In this section we model the reflectometry experience throughout the Zakharov-Shabat system and we will arrive at the formal definition of the most important object for this thesis: the reflection coefficient. Together with transmission coefficients, reflection coefficients form the scattering matrix, the starting point for the scattering theory.

In this section we will introduce first the reflection coefficient for a finite line, then we extend this definition for an infinite line and for a network. We will also see how the reflectometry experience is translated into an inverse problem.

1.4.1 Reflection and Transmission coefficients for a finite line

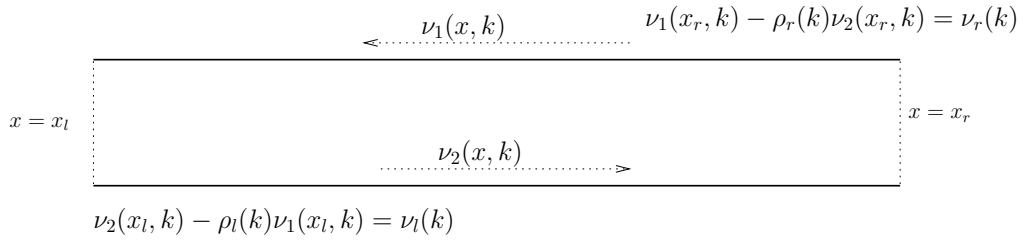

Figure 1.11: Zakharov-Shabat equations model

Let's consider the Zakharov-Shabat system (1.46) on the interval $I=[x_l,x_r]$ with the generic boundary conditions

$$\begin{cases} \nu_1(x_r,k)-\rho_r(k)\nu_2(x_r,k)=(1-\rho_r(k))\nu_r(k), \\ \nu_2(x_l,k)-\rho_l(k)\nu_1(x_l,k)=(1-\rho_l(k))\nu_l(k). \end{cases} \tag{1.66}$$

Using the superposition of solutions for the Zakharov-Shabat system, we can write a solution with the boundary condition (1.66) as a combination of two solutions verifying respectively these two half-homogenous boundary conditions

$$\begin{cases} \nu_1(x_r,k)-\rho_r(k)\nu_2(x_r,k)=0, \\ \nu_2(x_l,k)-\rho_l(k)\nu_1(x_l,k)=(1-\rho_l(k))\nu_l(k). \end{cases} \tag{1.67}$$

and

$$\begin{cases} \nu_1(x_r,k)-\rho_r(k)\nu_2(x_r,k)=(1-\rho_r(k))\nu_r(k), \\ \nu_2(x_l,k)-\rho_l(k)\nu_1(x_l,k)=0. \end{cases} \tag{1.68}$$

The boundary conditions (1.67) and (1.68) being similar, we are going to prove the well-posedness of the problem with boundary conditions (1.67). The condition $\nu_r(k)=0$ represents the absence of the right source generator.

Proposition 1. *Let $|\rho_l(k)|<1$ and let's suppose that $\boldsymbol{q}=(q_+,q_-,q_d)\in L^1([x_l,x_r])$. Then there exists a unique solution for the Zakharov-Shabat system* (1.46) *with the boundary conditions* (1.67).

Remark 11. The hypothesis on the regularity of potentials corresponds to the situation where we are excluding the rupture of the impedance $Z_{c0}(x)$ on the line.

Proof. In order to solve the two-point boundary value problem (1.46),(1.67), we will use the Riccati transformation, a decoupling technique related to the invariant imbedding method [8], [59], [7].
Let us introduce the following Riccati equation

$$\begin{cases} \partial_x r_l(x,k) = q_-(x) r_l^2(x,k) + 2(q_d(x) - ik) r_l(x,k) - q_+(x), \\ r_l(x_r,k) = \rho_r(k). \end{cases} \tag{1.69}$$

This ordinary differential equation has a unique local solution as soon as the functions q_d and $q_\pm$ are regular enough, say integrable.
We will show in Lemma 1 that the solution $r_l(x,k)$ is bounded, so that (1.69) has a unique global solution defined for all $x \leq x_r$.
Now, we will change the variables in (1.46),(1.67), by setting

$$\tilde{\nu}_1(x,k) = \nu_1(x,k) - r_l(x,k)\nu_2(x,k).$$

The new equivalent system is

$$\begin{cases} \partial_x \tilde{\nu}_1(x,k) = (q_d(x) - ik + q_-(x) r_l(x,k))\tilde{\nu}_1(x,k), \\ \partial_x \nu_2(x,k) = -q_-(x)\tilde{\nu}_1(x,k) - (q_d(x) - ik + q_-(x) r_l(x,k))\nu_2(x,k), \\ \tilde{\nu}_1(x_r,k) = 0, \\ (1 - \rho_l(k) r_l(x_l,k))\nu_2(x_l,k) - \rho_l(k)\tilde{\nu}_1(x_l,k) = (1 - \rho_l(k))\nu_l(k). \end{cases} \tag{1.70}$$

The unique solution of the first equation is $\tilde{\nu}_1(x,k) \equiv 0$, so that $\nu_1(x,k) = r_l(x,k)\nu_2(x,k)$ and the second equation becomes

$$\begin{cases} \partial_x \nu_2(x,k) = -(q_d(x) - ik + q_-(x) r_l(x,k))\nu_2(x,k), \\ (1 - \rho_l(k) r_l(x_l,k))\nu_2(x_l,k) = (1 - \rho_l(k))\nu_l(k). \end{cases}$$

We have supposed that $|\rho_l(k)| < 1$ (which is not restrictive because this coefficient is close to 0 in our applications), so that, with Lemma 1 (see below),

$$1 - \rho_l(k) r_l(x_l,k) \neq 0$$

and this equation has also a unique solution. The proof is complete. □

The proof of the proposition is constructive: it gives us a method to obtain the solution of a Zakharov-Shabat system. In particular the Riccati coefficient $r_l(x,k)$ plays an important role for the construction of the solutions.

Lemma 1. *Let $r_l(x,k)$ be the solution of (1.69). If we suppose that $\boldsymbol{q} = (q_+, q_-, q_d) \in L^1([x_l, x_r])$, then for all $\rho_r(k)$ such that $|\rho_r(k)| \leq 1 \qquad \forall k \in \mathbb{R}$, we have*

$$|r_l(x,k)| \leq 1 \qquad \forall x \leq x_r, \quad \forall k \in \mathbb{R}. \tag{1.71}$$

Proof. In order to prove this lemma, we use some properties of the Riccati equation (1.69) by introducing an auxiliary ODE:

$$r_l(x,k) = \frac{\mu_1(x,k)}{\mu_2(x,k)},$$

with

$$\begin{cases} \dfrac{d\mu_1(x,k)}{dx} = (q_d(x) - ik)\mu_1(x,k) - q_+(x)\mu_2(x,k), \\ \dfrac{d\mu_2(x,k)}{dx} = -q_-(x)\mu_1(x,k) - (q_d(x) - ik)\mu_2(x,k), \end{cases} \qquad \begin{cases} \mu_1(x_r,k) = \rho_r(k) \\ \mu_2(x_r,k) = 1. \end{cases} \tag{1.72}$$

We have that

$$\begin{aligned} \partial_x|\mu_1(x,k)|^2 &= +2q_d(x)|\mu_1(x,k)|^2 - 2q_+(x)\Re(\mu_1(x,k)\overline{\mu_2(x,k)}), \\ \partial_x|\mu_2(x,k)|^2 &= -2q_d(x)|\mu_2(x,k)|^2 - 2q_-(x)\Re(\mu_1(x,k)\overline{\mu_2(x,k)}), \end{aligned} \tag{1.73}$$

In order to prove (1.71), we are going to show that

$$|\mu_1(x,k)|^2 - |\mu_2(x,k)|^2 \leq 0 \qquad \forall x \leq x_r. \tag{1.74}$$

For $x = x_r$, (1.74) is valid, then it is sufficient to show

$$\partial_x(|\mu_1(x,k)|^2 - |\mu_2(x,k)|^2) \geq 0, \qquad \forall x < x_r$$

Using (1.73) and the representation of the potentials (q_+, q_-, q_d) in terms of line parameters (1.47),(1.48),(1.49) we have

$$\begin{aligned}\partial_x(|\mu_1|^2 - |\mu_2|^2) &= 2(q_+ - q_-)\Re(\mu_1, \overline{\mu_2)}) + 2q_d(|\mu_1|^2 + |\mu_2|^2) \\ &= 2\left(\frac{R}{L} - \frac{G}{C}\right)(\mu_1\overline{\mu_2} + \overline{\mu_1}\mu_2) + \left(\frac{R}{L} + \frac{G}{C}\right)(\mu_1\overline{\mu_1} + \mu_2\overline{\mu_2}) \\ &= \frac{R(x)}{L(x)}|\mu_1(x,k) + \mu_2(x,k)|^2 + \frac{G(x)}{C(x)}|\mu_1(x,k) - \mu_2(x,k)|^2 \geq 0\end{aligned}$$

Being a sum of two non-negative numbers, $\partial_x(|\mu_1|^2 - |\mu_2|^2) \geq 0$ and therefore (1.74) is valid. This concludes the proof.

□

Remark 12. We have given a simple proof of (1.71) in the previous lemma. This result is a particular case of a more general result concerning the invariance of the Siegel disk for the Riccati equation, i.e.

$$|r_l(x_r)| \leq 1 \Rightarrow |r_l(x)| \leq 1, \qquad \forall x \geq x_r$$

Redheffer has proved the formula for the n-dimensional case in [53] and also in a more general case in [54]. Let r a local solution (i.e. in a neighborhood of x_0) for

$$\frac{d}{dx}r(x) = a(x) + b(x)r(x) + r(x)d(x) + r(x)c(x)r(x),$$

Then the condition

$$\Re(\eta, a(x)\xi + b(x)\eta) + \Re(\xi, d(x)\xi + c(x)\eta) \geq 0, \quad \forall|\eta| = |\xi| \in \mathbb{C}^N, \tag{1.75}$$

is necessary and sufficient for the invariance of the Siegel disk

$$|r(x_0)| \leq 1 \Rightarrow |r(x)| \leq 1, \qquad \forall x \geq x_0.$$

In our situation, another proof of (1.71) consists in verifying that the condition (1.75) holds for any choice of $\mathbf{q} = (q_+, q_-, q_d)$. Since $r(x)$ is scalar, it is enough to consider ξ and η on the unitary disk.

Let $\eta = e^{i\theta_1}$ and $\xi = e^{i\theta_2}$ and for

$$a(x) = -q_+(x), \qquad b(x) = d(x) = q_d(x) - ik, \qquad c(x) = q_-(x),$$

the condition (1.75) becomes

$$\Re(-q_+(x)e^{i(\theta_2-\theta_1)} + 2q_d(x) - 2ik + q_-(x)e^{i(\theta_1-\theta_2)}) \geq 0, \qquad \forall \theta_1, \theta_2.$$

In terms of line parameters, we have

$$-q_+(x)e^{i(\theta_2-\theta_1)} + q_-(x)e^{i(\theta_1-\theta_2)} = -\left(\frac{R}{L} - \frac{G}{C}\right)\cos(\theta_2 - \theta_1) - \frac{i}{2}\frac{d}{dx}\left(\frac{L}{C}\right)\sin(\theta_2 - \theta_1),$$

hence

$$\Re(-q_+(x)e^{i(\theta_2-\theta_1)} + 2q_d(x) - 2ik + q_-(x)e^{i(\theta_1-\theta_2)}) = \frac{R(x)}{L(x)}(1 - \cos(\theta_2 - \theta_1)) + \frac{G(x)}{C(x)}(1 + \cos(\theta_2 - \theta_1)) \geq 0.$$

Remark 13. It is interesting to study the lossless case. When $-q_+ = -q_- = Q$ and $q_d \equiv 0$ the coefficient $r_l(x,k)$ verifies

$$\begin{aligned} |r_l(x,k)| &< 1, \qquad \text{for } |\rho_r(k)| < 1, \\ |r_l(x,k)| &= 1, \qquad \text{for } |\rho_r(k)| = 1. \end{aligned}$$

The coefficient $r_l(x,k)$ can be seen a Mobius transformation for the parameter $\rho_r(k)$. The solution of the auxiliary equation is given by $\begin{pmatrix} \mu_1(x,k) \\ \mu_2(x,k) \end{pmatrix} = \Phi(x,k) \begin{pmatrix} \rho_r(k) \\ 1 \end{pmatrix}$ with $\Phi(x,k) = \begin{pmatrix} \Phi_1(x,k) & \bar{\Phi}_2(x,k) \\ \Phi_2(x,k) & \bar{\Phi}_1(x,k) \end{pmatrix}$, where

$$\begin{cases} \dfrac{d\Phi_1(x,k)}{dx} = e^{-2ikx}Q(x)\Phi_2(x,k), \\ \\ \dfrac{d\Phi_2(x,k)}{dx} = e^{2ikx}Q(x)\Phi_1(x,k), \end{cases} \qquad \begin{cases} \Phi_1(x_r,k) = 1 \\ \\ \Phi_2(x_r,k) = 0. \end{cases}$$

Now we have

$$r_l(x,k) = \frac{\Phi_2(x,k) + \rho_r(k)\bar{\Phi}_1(x,k)}{\Phi_1(x,k) + \rho_r(k)\bar{\Phi}_2(x,k)}$$

Remark now $\det \Phi(x,k) = |\Phi_1(x,k)|^2 - |\Phi_2(x,k)|^2$ is constant along the segment:

$$\frac{d}{dx}(\phi_1(x,k)\bar{\phi_1}(x,k) - \phi_2(x,k)\bar{\phi_2}(x,k)) = 0,$$

hence so that $|\Phi_1(x,k)|^2 - |\Phi_2(x,k)|^2 = |\Phi_1(x_r,k)|^2 - |\Phi_2(x_r,k)|^2 = 1$.

Note $r_0(x,k) = \dfrac{\Phi_2(x,k)}{\Phi_1(x,k)}$ is a solution for (1.69) with $\rho_r(k) = 0$. We have

$$|r_0(x,k)|^2 = \frac{|\Phi_2(x,k)|^2}{1 + |\Phi_2(x,k)|^2}$$

$$r_l(x,k) = \frac{r_0(x,k)\Phi_1(x,k) + \rho_r(k)\bar{\Phi}_1(x,k)}{\Phi_1(\omega,x,\tau) + \rho_r(k)\bar{r}_0(x,k)\bar{\Phi}_1(x,k)}$$

Note $\alpha(x,k) = \dfrac{\Phi_1(x,k)}{\bar{\Phi}_1(x,k)}$. It follows that

$$r_l(x,k) = \bar{\alpha}(x,k)\frac{\rho_r(k) + \alpha(x,k)r_0(x,k)}{1 + \rho_r(k)\bar{\alpha}(x,k)\bar{r}_0(x,k)}. \tag{1.76}$$

As $|\alpha| = 1$ and $|\alpha r_0| < 1$, the mapping

$$\rho_r(k) \quad \longrightarrow \quad \bar{\alpha}\frac{\rho_r(k) + \alpha r_0}{1 + \rho_r(k)\bar{\alpha}\bar{r}_0}$$

is one-to-one from the unit circle (resp. the open unit disk) onto itself.
For $|\rho_r(k)| = 1$, then $|r_l(x,k)| = 1$ for all $x \le x_r$, for $|\rho_r(k)| < 1$ the solution $|r_l(x,k)| < 1$.

Corollary 1. Let $r_l(x,k)$ be the solution of the Riccati equation (1.69). If there exists a subinterval $I_1 \subset [x_l, x_r]$ such that

$$\min_{x \in I_1}\left(\frac{G(x)}{C(x)}, \frac{R(x)}{L(x)}\right) = \mathfrak{c} > 0, \tag{1.77}$$

then, for any choice of $|\rho_r(k)| \le 1$, we have

$$|r_l(x_l,k)| < 1 \qquad \forall k \in \mathbb{R}. \tag{1.78}$$

Proof. Let us write the solution of the Riccati equation as

$$r_l(x,k) = \frac{\mu_1(x,k)}{\mu_2(x,k)},$$

where $\mu_1(x,k)$ and $\mu_2(x,k)$ are the solution of the auxiliary equation (1.72). To prove (1.78) it is sufficient to show

$$|\mu_1(x_l,k)|^2 - |\mu_2(x_l,k)|^2 < 0.$$

Since $|\mu_1(x_r,k)|^2 - |\mu_2(x_l,k)|^2 \leq 0$, following the proof of Lemma 1, it is sufficient to prove that for some x

$$\partial_x(|\mu_1(x)|^2 - |\mu_2(x)|^2) > 0.$$

In the interval I_1 where it is valid (1.77), we have

$$\partial_x(|\mu_1|^2 - |\mu_2|^2) = \frac{R(x)}{L(x)}|\mu_1+\mu_2|^2 + \frac{G(x)}{C(x)}|\mu_1-\mu_2|^2 \geq$$
$$\geq \mathfrak{c}(|\mu_1+\mu_2|^2 + |\mu_1-\mu_2|^2) > 0. \qquad \forall x \in I_1.$$

The quantities $|\mu_1(x,k)+\mu_2(x,k)|^2$ and $|\mu_1(x,k)-\mu_2(x,k)|^2$ can not be zero at the same time, because otherwise it implies $\mu_1(x,k) = \mu_2(x,k) \equiv 0$ contradicting the initial condition at x_r.

□

Left reflection coefficient and right transmission coefficient

Definition 7. Consider a Zakharov-Shabat system (1.46) on the interval $I = [x_l, x_r]$ with the boundary conditions (1.67) one can associated to the solution of this system, the function $r_l(x,k)$ of the Riccati equation (1.69). We define the *left reflection coefficient* $r_l(k)$ as

$$r_l(k) = r_l(x_l,k). \tag{1.79}$$

We have shown that the reflection coefficient $r_l(k)$ represents the ratio between the reflected wave $\nu_1(x_l,k)$ and the incident wave $\nu_2(x_l,k)$. In particular we remark that $\nu_2(x_l,k) \neq 0$ as soon as the same is true for the source term, i.e. $\nu_l(k) \neq 0$.
Heuristically, the reflection coefficient represents how much of a wave is reflected, it is natural to define an equivalent term for the transmitted wave.

Definition 8. Let's consider the Zakharov-Shabat system (1.46)-(1.67) on the interval $[x_l, x_r]$. We define the *right transmission coefficient* $t_l(k)$ the following quantity

$$t_l(k) = \frac{\nu_2(x_r, k)}{\nu_2(x_l, k)}. \tag{1.80}$$

Note that the notation $t_l(k)$ underlines the presence of the source at the left end.

The transmission coefficient represents physically the ratio between the transmitted wave over the incident wave.

Remark 14. In the case of lossless uniform transmission line, the matched load boundary condition is equivalent to choose the parameter $\rho_r(k) = 0$; the solution of Riccati equation (1.69) is the trivial one $r_l(x, k) \equiv 0$. In particular the reflection coefficient $r_l(k)$ is constantly equal to 0 and this situation corresponds to the case where the entire signal is transmitted and nothing is reflected.

Right reflection coefficient and left transmission coefficient

Let's consider the Zakharov-Shabat system (1.46) with the boundary conditions (1.68). In this case, we are injecting a test signal through an external source on the right end $x = x_r$.
The existence and the uniqueness of the solution can be proved with the same arguments of Proposition 1: the invariant imbedding method gives us an algorithm to construct the solution of this system through the following Riccati equation

$$\begin{cases} \partial_x r_r(x, k) = q_+(x) r_r^2(x, k) - 2(q_d(x) - ik) r_r(x, k) - q_-(x), \\ r_r(x_l, k) = \rho_l(k). \end{cases} \tag{1.81}$$

Let $(\nu_1(x, k), \nu_2(x, k))$ be the unique solution of (1.46), (1.68). We are able to define the right reflection coefficient and the left transmission coefficient.

Definition 9. We define the *right reflection coefficient* $r_r(k)$ as

$$r_r(k) = r_r(x_r, k), \tag{1.82}$$

In analogous way, the *left transmission coefficient* $t_r(k)$ is given by

$$t_r(k) = \frac{\nu_1(x_l, k)}{\nu_1(x_r, k)}. \tag{1.83}$$

Again we remark the index r denotes the position of the source at the right end.

In conclusion for the Zakharov-Shabat system defined on $[x_r, x_l]$ we have defined the *scattering matrix* $S(k)$ as

$$S(k) := \begin{pmatrix} s_{11} & s_{12} \\ s_{21} & s_{22} \end{pmatrix} = \begin{pmatrix} r_l(k) & t_r(k) \\ t_l(k) & r_r(k) \end{pmatrix}. \tag{1.84}$$

For each interval $[x_l, x_r]$, we have the solution of (1.46), (1.66). The associated scattering matrix $S(k) = S([x_l, x_r]; k)$ verifies

$$\begin{bmatrix} \nu_1(x_l) \\ \nu_2(x_r) \end{bmatrix} = S([x_r, x_l]; k) \begin{bmatrix} \nu_2(x_l) \\ \nu_1(x_r) \end{bmatrix}$$

Remark 15. The scattering matrix depends on the particular choice of the decomposition of the waves. For example, for the uniform transmission line, there is another approach to decompose V and I into forward and backward waves different from (1.45). We illustrate the decomposition presented in [52]. Let $Z_c(k)$ be the constant characteristic impedance and let γ be the propagation constant defined as

$$\gamma(k) = \sqrt{(R + ikL)(G + ikC)/LC}.$$

The voltage and current can be written as a sum of forward and reflected traveling waves

$$\begin{aligned} V(k, x) &= V_0^+(k) e^{-\gamma(k)x} + V_0^-(k) e^{\gamma(k)x}, \\ I(k, x) &= \frac{I_0^+(k)}{Z_c(k)} e^{-\gamma(k)x} - \frac{I_0^-(k)}{Z_c(k)} e^{\gamma(k)x}, \end{aligned}$$

The total voltage and current are written as

$$\begin{aligned} V(k, x) &= V^+(k, x) + V^-(k, x), \\ I(k, x) &= I^+(k, x) - I^-(k, x). \end{aligned}$$

The normalized voltage wave amplitudes can be written as

$$\begin{cases} V^+(k,x) = \frac{V(x,k)+Z_c(k)I(k,x)}{2\sqrt{\Re Z_c(k)}}, \\ V^-(k,x) = \frac{V(x,k)-Z_c(k)I(k,x)}{2\sqrt{\Re Z_c(k)}}. \end{cases} \tag{1.85}$$

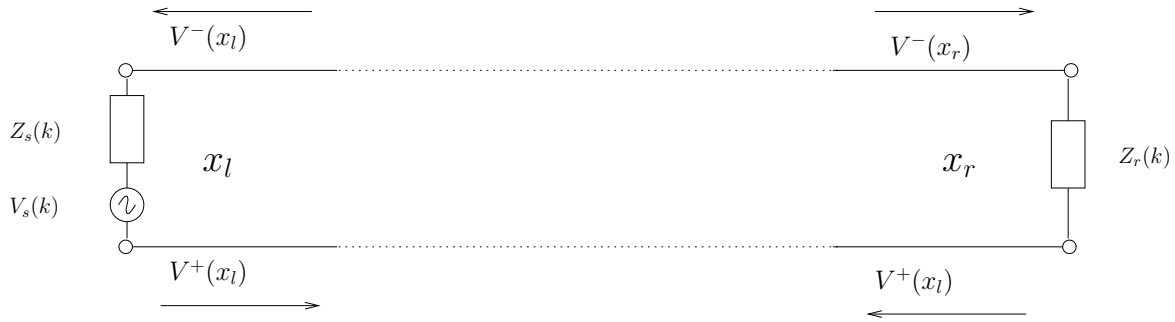

Figure 1.12: 2-port network with a source $V_s(k)$

Associated to this decomposition, we define the $\check{S}(k)$ scattering matrix as following :

$$\begin{bmatrix} V^-(k,x_l) \\ V^-(k,x_r) \end{bmatrix} = \begin{pmatrix} \check{S}_{11}(k) & \check{S}_{12}(k) \\ \check{S}_{21}(k) & \check{S}_{22}(k) \end{pmatrix} \begin{bmatrix} V^+(k,x_l) \\ V^+(k,x_r) \end{bmatrix}.$$

In the standard approach [51], the traveling waves and the associated reflection coefficients and scattering matrices are used. The reflection coefficient is given by

$$\check{R}_l(k) = \check{S}_{11}(k) + \frac{\check{S}_{12}(k)\check{S}_{21}(k)\rho_r(k)}{1-\check{S}_{22}(k)\rho_r(k)}.$$

It is instructive to see the differences in the expression of the power gain for the two approaches. For the traveling waves, the transducer power gain G_T is given by

$$G_T = \frac{|\check{S}_{21}(k)|^2(1-|\rho_l(k)|^2)(1-|\rho_r(k)|^2)}{|1-\rho_l(k)\check{R}_l(k)|^2|1-\check{S}_{22}(k)\rho_r(k)|^2}.$$

For the Zakharov-Shabat approach, the expression of G_T reduces to

$$G_T = |s_{21}|^2.$$

Different wave decompositions yield to different scattering matrices. The scatter-

ing matrices $\check{S}(k)$ are used for representing the properties of microwave components not taking into account the terminal impedances. In general, these scattering matrices are not directly related to power. The characteristic impedance Z_c is used as a normalization factor in (1.85) and the scattering matrices describe the propagation of power if all the transmission lines are terminated with matched loads, i.e. $\rho_l = \rho_r = 0$. The Zakharov-Shabat approach gives a more natural expression, as the scattering matrix element $s_{21}(k)$ (or equivalently $t_l(k)$) is expected to describe the propagation of power from the node x_l to the node x_r.

Remark 16. In Section 1.2, we have seen that the symmetry of T-model implies a symmetry of the s-parameters ((1.22) and (1.23)).
Despite the fact that the T-model is the elementary component for the transmission line model, heterogeneities of the line parameters break the symmetry of the scattering matrix $S(k)$: reflectometry experiments at two ends yield to two different values of the reflection coefficients. In general, the right reflection coefficient differs from the left one, so the two measures give us different information.

1.4.2 Scattering data for an infinite line

In practice setting the matched loads at both extremities is equivalent to emulate the electrical propagation through an infinite line. The mathematical model of electrical propagation is represented by the Zakharov-Shabat system (1.46) defined on the interval $-\infty < x < \infty$ with the potentials q_+, q_- and q_d with compact support $[x_l, x_r]$.

Here we want to extend the definition of the scattering data to the case where the potentials do not have a compact support. It can be shown that this new definition is equivalent to the definition given in the previous subsection. We consider the matrix form of the Zakharov-Shabat system

$$\frac{d}{dx}Y(x,k) + ik \begin{pmatrix} 1 & 0 \\ 0 & -1 \end{pmatrix} Y(x,k) = \begin{pmatrix} +q_d & -q_+ \\ -q_- & -q_d \end{pmatrix} Y(x,k) \qquad x \in \mathbb{R}, \qquad (1.86)$$

and we will assume that the potentials $q_+(x), q_-(x)$ and $q_d(x)$ are absolutely integrable on the interval $(-\infty, \infty)$.

The main problem is to find an equivalent expression for the boundary conditions (1.66) at the infinities $\pm\infty$. As the potentials $\mathbf{q} = (q_+, q_-, q_d)$ decay at the infinities, a solution of (1.86) behaves as a linear combination of exponential functions e^{ikx} and

e^{-ikx}.

In order to understand a scattering solution for (1.86), we need to introduce the Jost solutions for the Zakharov-Shabat system.

Definition 10. Let's assume that the potentials $q_+(x)$,$q_-(x)$ and $q_d(x)$ belong to $L^1(\mathbb{R})$. We define as Jost solutions $F_l(x,k) = (f_{1l}(x,k), f_{2l}(x,k))^{tr}$ and $F_r(x,k) = (f_{1r}(x,k), f_{2r}(x,k))^{tr}$, the solutions of (1.86) verifying the following asymptotic boundary conditions

$$\lim_{x\to+\infty} F_l(x,k)e^{-ikx} = \begin{pmatrix} 0 \\ 1 \end{pmatrix}, \tag{1.87}$$

$$\lim_{x\to+\infty} F_l^J(x,k)e^{+ikx} = \begin{pmatrix} 1 \\ 0 \end{pmatrix}, \tag{1.88}$$

$$\lim_{x\to-\infty} F_r(x,k)e^{+ikx} = \begin{pmatrix} 1 \\ 0 \end{pmatrix}, \tag{1.89}$$

$$\lim_{x\to-\infty} F_r^J(x,k)e^{-ikx} = \begin{pmatrix} 0 \\ -1 \end{pmatrix}. \tag{1.90}$$

Note that $F^J = \begin{pmatrix} 0 & 1 \\ -1 & 0 \end{pmatrix} F := JF$.

The Jost solutions are well-posed and they are the solutions of Volterra type equations. For example, using (1.86) and (1.87), we obtain the Volterra equations for $F_l(x,k)$:

$$\begin{aligned} f_{1l}(x,k) &= -\int_x^\infty e^{-ik(x-s)}[q_d(s)f_{1l}(s,k) - q_+(s)f_{2l}(s,k)]ds, \\ f_{2l}(x,k) &= e^{ikx} + \int_x^\infty e^{ik(x-s)}[q_d(s)f_{2l}(s,k) - q_-(s)f_{1l}(s,k)]ds. \end{aligned} \tag{1.91}$$

Since the potentials belong to $L^1(\mathbb{R})$, for each $k \in \mathbb{R}$ it follows by usual iterative techniques that these Volterra equations are well-posed and hence that the Jost solution $F_l(x,k)$ exists uniquely (see [16], Chapter 1.4). For the other Jost solutions $F_l^J(x,k), F_r(x,k), F_r^J(x,k)$, we apply the same arguments.

Remark 17. The integral formulation (1.91) can be adapted also for the case of the segment $[x_l, x_r]$. The solution of the auxiliary problem (1.72), verifying the boundary

conditions $\mu_1(x_r,k)=0, \mu_2(x_r,k)=1$, can be written for $x\in[x_l,x_r]$ as

$$\begin{aligned}\mu_1(x,k) &= -\int_x^{x_r} e^{-ik(x-s)}[q_d(s)\mu_1(s,k)-q_+(s)\mu_2(s,k)]ds,\\ \mu_2(x,k) &= e^{ik(x-x_r)}+\int_x^{x_r} e^{ik(x-s)}[q_d(s)\mu_2(s,k)-q_-(s)\mu_1(s,k)]ds.\end{aligned}$$

The auxiliary problem (1.72) on the interval $[x_l,x_r]$ can be extended easily to the case of the half line $(\infty,x_r]$. Proposition 1 and Lemma 1 for the half line are still valid: the associated Riccati equation (1.69) defined on $(\infty,x_r]$ has a global solution and moreover it verifies

$$\lim_{x\to-\infty} r_l(x,k)e^{2ikx}=1.$$

It is well-known that the Jost solutions $F_l(x,k), F_l^J(x,k)$ are linearly independent (as well as $F_r(x,k), F_r^J(x,k)$). It is customary to define $a_l(k), a_r(k)$,$b_l(k)$ and $b_r(k)$ as the coefficients relating these two sets of linearly independent solutions:

$$F_r(x,k)=b_l(k)F_l^J(x,k)+a_l(k)F_l(x,k), \tag{1.92}$$

$$F_l(x,k)=b_r(k)F_r^J(x,k)+a_r(k)F_r(x,k). \tag{1.93}$$

It can be shown that the coefficients $a_l(k), a_r(k), b_l(k), b_r(k)$ are given by the Wronskians of the solutions $F_l(x,k), F_l^J(x,k), F_r(x,k), F_r^J(x,k)$.

We are ready to define the scattering data for the Zakharov-Shabat system on the line.

Definition 11. The reflection coefficients to the right and to the left $r_r(k)$ and $r_l(k)$ and the related transmission coefficients $t_r(k)$ and $t_l(k)$ are defined for $k\in\mathbb{R}$ by

$$r_l(k):=\frac{a_l(k)}{b_l(k)},\qquad r_r(k):=\frac{a_r(k)}{b_r(k)},\qquad t_l(k):=\frac{1}{b_l(k)},\qquad t_r(k):=\frac{1}{b_r(k)}. \tag{1.94}$$

Abusing the notation, we use the same symbols for the scattering data defined on the interval and for the scattering data defined on the line.

Lossless case

With the same approach, we can define the scattering data for the Schrödinger equation (1.62). We assume that the potential $q(x)$ is real-valued function belonging to the space

$$L_1^1(\mathbb{R}) = \{q \in L_1(\mathbb{R}) : \int_{\mathbb{R}} (1+|x|)|q(x)|dx < \infty\}, \tag{1.95}$$

then the Jost solutions $f_l(x,k)$ and $f_r(x,k)$ can be seen as the generalized eigen-solutions of operator H defined

$$H := -d^2/dx^2 + q(x), \tag{1.96}$$

associated to the eigenvalues k^2 and behaving

$$\lim_{x\to+\infty} f_l(x,k)e^{-ikx} = 1, \tag{1.97}$$
$$\lim_{x\to-\infty} f_r(x,k)e^{+ikx} = 1. \tag{1.98}$$

It is well known that $f_l(x,k)$ and $f_r(x,k)$ are analytic in k in the open upper complex half plane as well $f_l(x,-k)$ and $f_r(x,-k)$ are analytic in the lower half plane. Moreover for each $k \in \mathbb{R} - \{0\}$ the generalized eigen-solutions $f_l(x,k)$ and , $f_l(x,-k)$ are linearly independent (as well as , $f_r(x,k)$ and $f_r(x,-k)$), the space of the solution to the Schrödinger equation being of dimension two. We can obtain the functions $a_{r,l}(k)$ and $b_{r,l}(k)$ such that for all $x \in \mathbb{R}$

$$f_r(x,k) = a_l(k)f_l(x,k) + b_l(k)f_l(x,-k),$$
$$f_l(x,k) = a_r(k)f_r(x,k) + b_r(k)f_r(x,-k).$$

It can be proved (see [35]) that

$$\overline{(a_l(k))} = a_l(-k), \quad \overline{(a_r(k))} = a_r(-k), \quad b_r(k) = b_l(k), \quad \overline{(b_l(k))} = b_l(-k). \tag{1.99}$$

Using the Jost solutions , we define the scattering solution $y(x,k)$ by the boundary conditions at $\pm\infty$

$$y(x,k) \sim \quad t_l(k)e^{ikx} \qquad\qquad x \to +\infty,$$
$$y(x,k) \sim \quad r_l(k)e^{-ikx} + e^{ikx} \qquad x \to -\infty,$$

The solution $y(x,k)$ describes a plane wave e^{ikx} sent from the left $-\infty$, transmitting

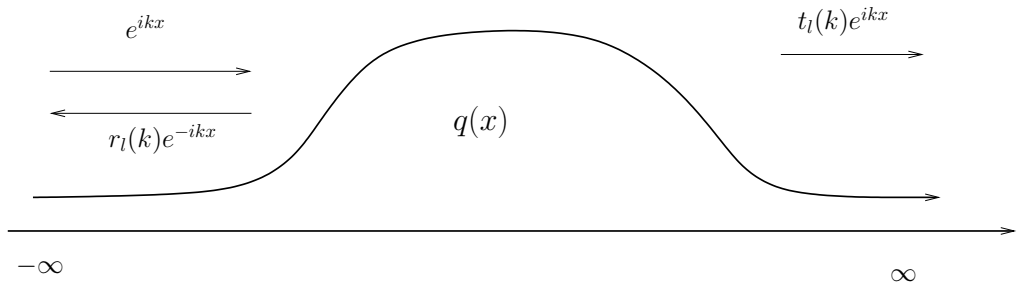

Figure 1.13: Schematic figure for the scattering data

$t_l(k)e^{ikx}$ to $+\infty$ and reflecting $r_l(k)e^{-ikx}$ to $-\infty$.
Using the coefficients $a_l(k), a_r(k), b_l(k)$ and $b_r(k)$. one can define eventually the scattering data for the Schrödinger equation.

Definition 12. The left and right reflection coefficients $r_{l,r}(k)$ and the associated transmission coefficients $t_{r,l}(k)$ are defined as follows

$$t_r(k) = \frac{1}{b_r(k)}, \qquad t_l(k) = \frac{1}{b_l(k)}, \qquad r_r(k) = \frac{a_r(k)}{b_r(k)}, \qquad r_l(k) = \frac{a_l(k)}{b_l(k)}.$$

Definition 13. The matrix

$$S(k) = \begin{pmatrix} r_l(k) & t_r(k) \\ t_l(k) & r_r(k) \end{pmatrix} \qquad \forall k \in \mathbb{R}^* \tag{1.100}$$

is called the *scattering matrix* for the potential q.

The direct problem of scattering theory is to determine the properties of the scattering matrix $S(k)$ from those of a potential q. A classical result is that $S(k)$ is unitary.

Remark 18. As a direct consequences of (1.99), we have that $t_r(k) = t_l(k)$. The transmission coefficients calculated at both ends are equivalent. In the lossless case, the property of reciprocal scattering matrix for an elementary components (1.22) is extended to the whole infinite line.

1.4.3 Scattering data for a network

Here we will give the definitions of scattering data on network.

In order to introduce the scattering data for a network, we need to understand the nature of the network: the first step is to divide the network Γ into the external part Γ_{ext} and the internal part Γ_{int}, also called the *compact* part. The external part Γ_{ext} represents the set of the electric wires where we can inject the test signals. It plays a crucial role for the dimension of the scattering matrix: from j-th eternal edges we can inject the signal that will determine the j-th reflection coefficient and N transmission coefficients, where $N+1$ is the number of the external wires.
We use the formulation described in Section 1.3.2. Let $\mathcal{E}_{ext} = \{e_0, e_1, \dots, e_N\}$ be the set of the external edges with the following parametrization:

- The branch e_0 is parametrized as $[x_{l_0}, x_{r_0}]$, where x_{l_0} corresponds to the minimal element v_0.
- The branch e_j with $j \neq 0$ is parametrized as $[x_{l_j}, x_{r_j}]$, where x_{r_j} corresponds to the external edge.

The Zakharov-Shabat system is defined on each branch of the network as

$$\frac{d}{dx}Y_j(x,k) + ik\sigma_3 Y_j(x,k) = Q_j(x)Y_j(x,k), \qquad \text{on } e_j, \quad \forall e_j \in \mathcal{E}, \tag{1.101}$$

and the boundary conditions for the internal vertices $v \in \mathcal{V}_{int}$ are defined by (1.53).
We will give the definition of the scattering data in the case where the external part Γ_{ext} is made by finite segment and in the case where Γ_{ext} is non-compact, i.e. all external branches are semi-infinite.

Finite external wires

When the network is compact, the Zakharov-Shabat system (1.101)-(1.53) needs also boundary conditions for the external vertices

$$\begin{aligned} \nu_{1j}(x_{r_j},k) - \rho_j(k)\nu_{2j}(x_{r_j},k) &= \quad (1-\rho_j(k))\nu_j(k) \quad \forall j = 1,\dots,N \\ \nu_{20}(x_{l_0},k) - \rho_0(k)\nu_{10}(x_{l_0},k) &= \quad (1-\rho_0(k))\nu_0(k). \qquad\qquad . \end{aligned} \tag{1.102}$$

For the scattering data, we need to look at the solutions of the different scattering problems. In the case of a segment, we are able to define two reflection coefficients associated to two different experiments.

When we are dealing with networks, the number of the reflection coefficients is related to the number of the external wires. Imposing only one source at the time we are able to define the corresponding reflection coefficient. Let us consider the Zakharov-Shabat system on Γ with the boundary conditions (1.53) and

$$\begin{aligned} \nu_{1j}(x_{r_j},k) - \rho_j(k)\nu_{2j}(x_{r_j},k) = &\quad 0, \qquad \forall j = 1,\dots,N \\ \nu_{20}(x_{l_0},k) = &\quad \nu_0(k). \end{aligned} \tag{1.103}$$

then we define the scattering data as follows:

Definition 14. The reflection coefficient $r_{00}(k)$ associated to the experiment (1.103) is defined as

$$r_{00}(k) = \frac{\nu_{10}(x_{l_0},k)}{\nu_{20}(x_{l_0},k)}, \tag{1.104}$$

while the transmission coefficients are given, for $j = 1,\dots,N$, by

$$t_{j0}(k) = \frac{\nu_{2j}(x_{r_j},k)}{\nu_{20}(x_{l_0},k)} \qquad . \tag{1.105}$$

As long as the source generator $\nu_0(k)$ is different from zero, (1.104) and (1.105) are well-defined.

The other reflection coefficients are associated to the experiments where a source $\nu_j(k)$ is placed at the terminal node of the branch e_j with $j \neq 0$.

$$\nu_{1j}(x_{r_j},k) = \nu_j(k), \tag{1.106}$$

$$\nu_{1i}(x_{r_i},k) - \rho_i(k)\nu_{2i}(x_{r_i},k) = 0, \qquad \forall i = 1,\dots,N, \quad i \neq j \tag{1.107}$$

$$\nu_{20}(x_{l_0},k) - \rho_0(k)\nu_{10}(x_{l_0},k) = 0. \tag{1.108}$$

We have the following definitions:

Definition 15. The j-th reflection coefficient $r_{jj}(k)$ associated to the boundary conditions (1.106) is given by

$$r_{jj}(k) = \frac{\nu_{2j}(x_{r_j},k)}{\nu_{1j}(x_{r_j},k)}, \qquad j = 1,\dots,N$$

and the transmission coefficients are

$$t_{ij}(k) = \frac{\nu_{1i}(x_{r_i}, k)}{\nu_{1j}(x_{r_j}, k)} \qquad i \neq j, \qquad i = 1, \dots, N$$

and

$$t_{0j}(k) = \frac{\nu_{10}(x_{l_0}, k)}{\nu_{1j}(x_{r_j}, k)}.$$

We are able to give the definition of the scattering matrix.

Definition 16. Let Γ be a network as above, the matrix $N+1 \times N+1$

$$S(k) := \begin{pmatrix} r_{0\,0}(k) & t_{0\,1}(k) & \dots & t_{0\,N}(k) \\ t_{1\,0}(k) & r_{1\,1}(k) & \dots & t_{1\,N}(k) \\ \dots & \dots & \dots & \dots \\ t_{N\,0}(k) & \dots & t_{N\,N-1}(k) & r_{N\,N}(k) \end{pmatrix}$$

is called the *scattering* matrix.

Remark 19. The definitions of the scattering elements as the reflection and the transmission coefficients are directly related to the existence and the uniqueness of the solution for the Zakharov-Shabat equations (1.101)-(1.102). This will be proved for the general case in Chapter 4.

As for the case of line, the proof will use the invariant imbedding method. A Riccati equation defined on the network Γ will decouple the system (1.101). It will show that the reflection coefficient $r_{jj}(k)$ is the value at the terminal end $x = x_{r_j}$ (for $r_{00}(k)$ the value at $x = x_{l_0}$) of the solution $r(\Gamma, x, k)$ of the Riccati equation defined on network. The chosen parametrization of Γ implies an analogy with the reflection coefficients on the segment: $r_{00}(k)$ is the left reflection coefficient of the object Γ, while the set of $\{r_{jj}(k)\}_{j=1}^{N}$ represents the right reflection coefficients.

Infinite external wires

As for the line, we can define the scattering data on non-compact graphs: the external edges are assumed to be of infinite length. Since the experiments (1.103) and (1.106) require the matched load at the source, it comes natural to consider the external edge e_j as a semi-infinite line.

In particular e_0 is parametrized $(-\infty, x_{r_0}]$, while the rest of the external branches are oriented toward the increasing x, i.e. $[x_{l_j}, \infty)$.

The scattering data are, hence, related to the scattering solutions. There are $N+1$ scattering solutions $\{\mathbf{Y}^j(x,k)\}_{j=0}^N = \{\{Y_l^j(x,k)\}_{l=0}^N\}_{j=0}^N$ of the Zakharov-Shabat system on Γ satisfying (1.101)-(1.53). The asymptotic behaviors for the solutions $\{\mathbf{Y}^j(x,k)\}_{j=1}^N$ are

$$\begin{cases} Y_j^j(x,k) = r_{jj}(k)\begin{pmatrix}0\\1\end{pmatrix}e^{ikx} + \begin{pmatrix}1\\0\end{pmatrix}e^{-ikx}, & \text{as } x\to+\infty \\ Y_l^j(x,k) = t_{jl}(k)\begin{pmatrix}0\\1\end{pmatrix}e^{ikx}, & \text{as } x\to\infty \qquad \text{for } l\neq j, \quad l=1,\dots,N \\ Y_0^j(x,k) = t_{j0}(k)\begin{pmatrix}1\\0\end{pmatrix}e^{-ikx}, & \text{as } x\to-\infty \end{cases} \tag{1.109}$$

while for the scattering solution $\mathbf{Y}^0(x,k)$, we have

$$\begin{cases} Y_0^0(x,k) = r_{00}(k)\begin{pmatrix}1\\0\end{pmatrix}e^{-ikx} + \begin{pmatrix}0\\1\end{pmatrix}e^{ikx}, & \text{as } x\to-\infty \\ Y_j^0(x,k) = t_{0j}(k)\begin{pmatrix}0\\1\end{pmatrix}e^{ikx}, & \text{as } x\to\infty \qquad \text{for } j=1,\dots,N. \end{cases}$$

The existence and uniqueness of the scattering solutions will be proved for the lossless case in the third chapter.

In conclusion we see that the size of the scattering matrix is determined by the number of external channels in the graph. The scattering matrix depends on the structure of the graph, on the boundary conditions and on the potentials appearing in the Zakharov-Shabat system.

1.4.4 Fault detection as inverse scattering problem

In this section, we explain the connection between the reflection coefficient calculated by engineers and the mathematical object presented in the previous section. In the paper [71] and [62], Zhang, Sorine and their students have filled the gap between the inverse scattering transform and its application to electric transmission line fault diagnosis. Their work clarifies and completes the computation of the theoretic scattering data required by the inverse scattering transform from the practically measured engineering scattering data.

We gave two different definitions for the scattering data and now we show their equivalence. We introduced the scattering data for the interval because it represents the engineering scattering data, denoted here by r_{l_e}, r_{r_e} and t_{l_e}. The main discrepancy between the two definitions is related to the fact that the engineering scattering data $\{r_{l_e}, r_{r_e}, t_{l_e}\}$ are defined at the ends of a finite length transmission line whereas the theoretic scattering data r_l, r_r and t are related to the limiting behaviors of Jost solutions.

To solve this problem, Zhang has shown that the finite length transmission line can be extended with arbitrarily long extra line segments in a way such that the voltage and the current remain unchanged in the original part of the transmission line. Let us consider the transmission line equations after the Liouville transformation (1.44) on the interval $[x_l, x_r]$ with the generic boundary conditions (1.34) ($\omega = k$)

$$\begin{cases} V(k, x_l) + Z_s(k) I(k, x_l) = V_s(k), \\ V(k, x_r) - Z_r(k) I(k, x_r) = 0. \end{cases}$$

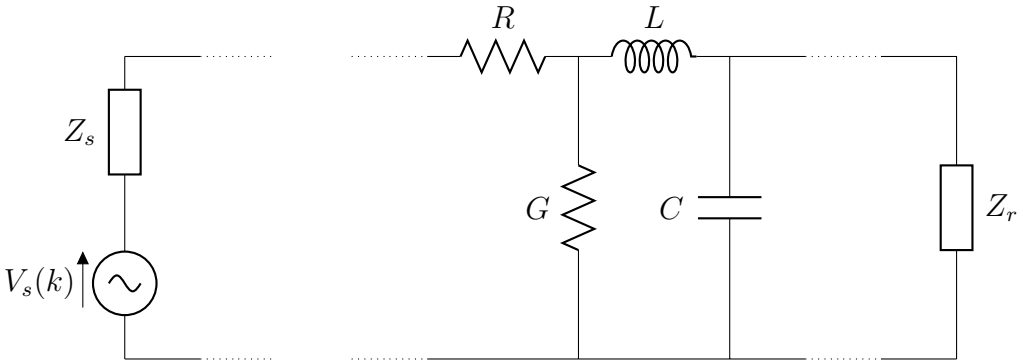

Figure 1.14: Transmission line model with one source generator

Lemma 2. *As shown in the Figure 1.14 , we can extend the circuit as follows:*

- *Insert a uniform lossless transmission line of length a with $R(x) = G(x) = 0$ and the characteristic impedance $Z_0(x_l) = Z_l$ between the source and the left end of the original circuit.*
- *Insert a uniform lossless transmission line of length b with $R(x) = G(x) = 0$ and the characteristic impedance $Z_0(x_r) = Z_r$ between the right end of the original circuit and the load.*

- *Add a phase shift $-ka$ to the source voltage.*

Then for any positive values of a and b, this extended circuits is equivalent to the original one in the sense that they have the same values of $V(k,x)$ and $I(k,x)$ for all $z \in [x_l, x_r]$.

For arbitrary positive values a and b, the quantities $V(k,x)$, $I(k,x)$, and $Z_0(x)$ of the extended circuit are well-defined for all $x \in (-a, l+b)$. The solution of the Zakharov-Shabat equation (1.46) is also valid for $x \in \mathbb{R}$, when a and b tend to $+\infty$. Hence we have the following result:

Proposition 2. *We have the following relationship between the engineering scattering data and theoretic scattering data of the Zakharov-Shabat system:*

$$r_l(k) = r_{l_e}(k), \qquad t(k) = t_e(k)e^{-ikl}, \qquad r_r(k) = r_{r_e}e^{-2ikl}. \tag{1.110}$$

The proofs of Lemma 2 and Proposition 2 can be found in [62].

Remark 20. It is important to remark that the latter results can be obtain directly from the Riccati equation (1.69). For a uniform transmission line (1.69) is reduced to the following equation

$$\partial_x r_l(x,k) = -2ikr_l(x,k).$$

So the reflection coefficients evolve on the uniform transmission line turning only the phase.

This manuscript has for goal to propose fault detection methods based on reflectometry experiments. Hence the problem is to retrieve as much information as possible on an electrical network from the measurements of the scattering data. A natural question arises here: what kind of faults are we able to detect? We have seen that faults are identified as variations of lines parameters and the measurements are equivalent to the knowledge of reflection coefficients.

In the simple case of the line, for example, Furse et al [21] propose a method to retrieve the position of possible hard faults on a uniform transmission line. Using the Phase Detection Frequency Domain Reflectometry (PDFDR) (see Section 1.2.3) on a uniform transmission line where the load is assumed to be either short, open or resistive, the reflectometry experiment yields to the measure of the continuous voltage

at the mixer

$$V_{dc}(k) = |Ae^{ik\ell} + Be^{-ik\ell}|^2 = A + A\left(\frac{B}{A}\right)^2 + 2A\left(\frac{B}{A}\right)\cos(2k\ell)$$

where A is the amplitude of the incident voltage, $\left(\frac{B}{A}\right)$ the reflection coefficient and ℓ is the position of the hard fault. Through the Fourier analysis, the authors are able to calculate ℓ, knowing the function $V_{dc}(k)$.

The inverse scattering problems defined on graphs form a wider class with respect to inverse scattering problems for the single transmission line: the scattering matrix depends also on the structure of the graph and the boundary conditions. Hence the scattering data contains theoretically informations about the geometry and the topology of the network.

Due to the nature of the experiments, we have access only to a part of the scattering data: the transmission coefficients are not taken into account and the knowledge of the reflection coefficients are restrain to a limited number of plug-in ports.

In this thesis, we restrict ourself to the case where there is only one plug-in port for the reflectometry measurements and hence we dispose of one reflection coefficient. We will investigate what information can be retrieved from the measurement of such reflection coefficient.

1.5 Outline of the work

This thesis is devoted to explore the relationship between the reflection coefficients and the parameters of the network.

1.5.1 Inverse Scattering on a star-shaped network for LC transmission line

Having in mind the application of on-board diagnosis and wire fault detection for a lossless network, we consider some inverse scattering problems for Schrödinger operators over star-shaped graphs.

We are interested in locating hard faults and soft faults: the first type is represented by the lengths of the branches, while soft faults are described by the heterogeneities of $q(x)$ (see (1.63)) along the branches. Indeed, in the perfect situation, the

parameters $L(x)$ and $C(x)$ are constant on the network and therefore the potential $q(x) = (L/C)^{1/4}\frac{d}{dx}(C/L)^{1/4}$ is uniformly zero on the whole network.

We consider the case of star-shaped network. This particular choice implies that the set of internal vertices $\mathcal{V}_{int}$ is reduced just to one node. We also assume that there are no failures in the connector at the central node. This is equivalent to assume the continuity of the characteristic impedance $Z_c(x) = \sqrt{L(x)/C(x)}$ at the central node.
We restrict ourselves to the case of minimal experimental setup consisting in measur-

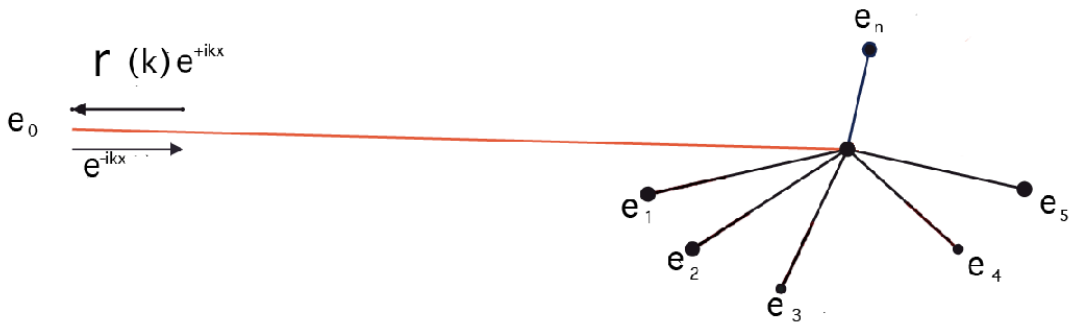

Figure 1.15: Star-shaped network

ing, at most, two reflection coefficients corresponding to two different experiments. We consider the case where the reflectometry experiment is based on a far-field method consisting in adding a uniform infinite wire joined at the central node of the network. The first result concerns the detection and the localization of hard faults on the lossless network. In terms of the Schrödinger operator, we are exploring the identifiability of the geometry of this star-shaped graph: by studying the asymptotic behavior of only one reflection coefficient in the high-frequency limit, we will be able to recover some geometrical information such as the number of edges and their lengths.
Next, we study the potential identification problem by inverse scattering, noting that the potentials represent the inhomogeneities due to the soft faults in the network. The main result states that, under some assumptions on the geometry of the graph, the measurement of two reflection coefficients, associated to two different sets of boundary conditions at the external vertices of the tree, determines uniquely the potentials; it can be seen as a generalization of the theorem of the two boundary spectra on an interval.

1.5.2 Inverse Scattering on a star-shaped network for $RLGC$ transmission line

We generalize some results obtained for the lossless case to the general lossy case on the star-shaped network.

We are interested in the detection and the eventual localization of the hard and soft faults. The hard faults, as for the Schrödinger case, are represented by the lengths of the branches while the soft faults are described as variations of the three potentials $\mathbf{q} = \otimes_{j=1}^{N}(q_{j,+}, q_{j,-}, q_{j,d})$.

As in the lossless case, we are considering the minimal experimental setup for a star-shaped network. Only one source generator is connected to the network and we have access to the measurement of one reflection coefficient. First, we focus on the well-posedness of the direct scattering problem for the Zakharov-Shabat operator on a star-shaped network: the reflection coefficient is uniquely determined by the potentials $\mathbf{q} = \otimes_{j=1}^{N}(q_{j,+}, q_{j,-}, q_{j,d})$.

As a first result, we show the identification of hard faults. We give a constructive algorithm to retrieve the lengths of the branches. As in the lossless case, this result uses the asymptotic behavior of the reflection coefficient.

We investigate some inverse scattering problems concerning the variations of the potentials. The main result states that, the knowledge of one reflection coefficient allows to identify the following quantities:

$$\int_0^{l_j} q_{d,j}(x)dx = \int_0^{l_j} \frac{R_j}{L_j}(x) + \frac{G_j}{C_j}(x)dx.$$

This quantity is called the *loss line factor*.
The last result concerns a particular case of a uniform lossy network. Having in mind a possible application for the train railway's maintenance, we prove, under the assumption of the weak influence of G/C on the electrical transmission, the identifiability of these two quantities

$$\frac{R_j}{L_j} \text{ and } \frac{G_j}{C_j}.$$

from the measurement of a reflection coefficient.

Chapter 2

Elements of the inverse scattering theory for $1-d$ Schrödinger and Zakharov-Shabat equations

This chapter is divided in two sections. In Section 2.1, we illustrate the state of art for the $1-d$ time independent Schrödinger equation, while in Section 2.2 we provide the main results for some inverse scattering problems for the Zakharov-Shabat system.

2.1 Inverse scattering theory for Schrödinger equation

According to Reed and Simon [55], scattering theory is the study of an interacting system on a time and distance scale which is large compared to the scale of the actual interaction. In this section we focus the mathematical aspects of scattering theory for the Schrödinger operator

$$-\frac{d^2}{dx^2}+q(x).$$

We exhibit the main results of the huge literature of the inverse scattering on Schrödinger operator. First we recall an important result by Deift and Trubowitz exploiting the dependence on the potential q of the left and right coefficients. The inverse problem can be divided in three parts: the uniqueness of the potential for a given reflection coefficient, the algorithm to construct the potential q from the scattering data and the characterization of the class of the reflection coefficients.

The last part of this section is devoted to some inverse problems on network. The inverse scattering theory on graphs becomes much more complicated and the number of inverse problems increases. The scattering data contains also informations about the topology and the geometry of the network. As one can imagine, the results on this direction are relatively few and they involve only networks without cycles. Our results concern the simplest network without cycles: the star-shaped graph.

2.1.1 Inverse scattering on a line

Here we present the result by Deift and Trubowizt [17]. We give the solution to the inverse scattering problem for the one-dimensional Schrödinger operator on the line.

Let H be a self-adjoint Schrödinger operator (1.96) with a real potential $q(x)$ in

$$L_2^1 = \{q(x) : \int_{-\infty}^{\infty} |q(x)|(1+x^2)dx < \infty\}. \tag{2.1}$$

H admits an absolutely continuos spectrum $[0, \infty)$ and a finite number of bound states $-\beta_n^2 < \ldots < -\beta_1^2$ below the continuum.
Using the Jost solution for the Schödinger operator (1.97),(1.98), it is possible to define the scattering matrix $S(k)$(see (1.100)). The *inverse scattering problem* is to retrieve the potential q from the knowledge of the scattering matrix $S(k)$. It is a well known result that the knowledge of one reflection coefficient $r_l(k)$ (or $r_r(k)$) and the bound states $-\beta_n^2 < \ldots < -\beta_1^2$ determine uniquely the scattering matrix $S(k)$ (see, for example, the Aktosun's survey in [47]).

The *inverse problem* of scattering theory is to determine the dependence of q on the reflection coefficients $r_r(k)$ and $r_r(k)$. There are three important questions to be answered:

I UNIQUENESS. Do the bound states and a reflection coefficient determine uniquely the potential q?

II RECONSTRUCTION. To find an algorithm for recovering the potential q from the bound states and a reflection coefficient.

III CHARACTERIZATION. Give necessary and sufficient conditions for a matrix

$$\begin{pmatrix} a(k) & b(k) \\ c(k) & d(k) \end{pmatrix}$$

to be the scattering matrix of a potential q in L_2^1.

Remark 21. Note that the scattering matrix $S(k)$ differs from the original notation. Deift and Trubowitz define the scattering matrix as follows

$$S(k) = \begin{pmatrix} t_r(k) & r_l(k) \\ r_r(k) & t_l(k) \end{pmatrix}$$

Uniqueness

The knowledge of one reflection coefficient and the bound states isn't enough to retrieve the potential q. In the simplest case, if two potential q and q' have no *bound* states and give rise to the same reflection coefficients $r(k) = r'(k)$, then they are identical [15]. If the operator H has n bound states $-\beta_n^2 < \ldots < -\beta_1^2$ with associated eigenfunctions $f_1(x, i\beta_1), \ldots, f_n(x, i\beta_n)$, there is an n-dimensional family of potentials with the same bound states and reflection coefficient $r(k)$. In order to ensure the complete identification of the potential, we need to know also the *norming* constants

$$c_j = \left(\int_{-\infty}^{\infty} f^2(x, i\beta_i) dx \right)^{-1}, \qquad j = 1, \ldots, n. \tag{2.2}$$

Eventually a potential is determined by its bound states, norming constants and reflection coefficient [19].

Recontruction

This inverse problem was solved by Faddeev [18]. Let $q(x) \in L_2^1$ and let $r(k)$ be the reflection coefficient. Let consider the following transformation

$$F(y) = \frac{1}{\pi} \int_{-\infty}^{\infty} r(k) e^{2iky} dk \tag{2.3}$$

and let's define the following quantity

$$\Omega(y) = F(y) + 2\sum_{j=1}^{n} c_j e^{-2\beta_j y} \tag{2.4}$$

where c_j are the norming constants defined in (2.2) and $-\beta_j$ the bound states.

Here, we apply the function Ω to define a new auxiliary function $B(x, y)$.

Theorem 1 (Theorem 4.4.2 in [35]). *The integral equation*

$$B(x, y) + \Omega(x + y) + \int_0^\infty \Omega(x + y + t)B(x, t)dt = 0 \qquad \forall y \geq 0 \tag{2.5}$$

admits a unique solution $B(x, \cdot) \in L^2$ for all $x \in \mathbb{R}$. This integral equation is often called Gelfand-Levitan-Marchenko *equation. Moreover, its solution satisfies $q(x) = -\partial_x B(x, 0^+)$.*

Deift and Trubowitz have proved another method to retrieve the potential called the *trace formula.*
For simplicity's sake, we show the algorithm for the case with potential without any bound states.
The first step is to write the *trace formula*

$$q(x) = \frac{2i}{\pi}\int_{-\infty}^{\infty} kr(k)f^2(x, k)dk, \tag{2.6}$$

the potential $q(x)$ is function of $r(k)$ and the unknown variable f.
Now we look at the Schrödinger equation

$$-f'' + qf = k^2 f$$

with two unknown variables f and q. The strategy is to use the trace formula (2.6) to obtain an equation for f alone and solve it. It is convenient to use the auxiliary function $m(x, k)$ defined as

$$m(x, k) = e^{-ikx} f(x, k).$$

The Schrödinger equation becomes

$$\frac{d^2}{dx^2}m(x,k) + 2ik\frac{d}{dx}m(x,k) = q(x)m(x,k), \tag{2.7}$$

where $q(x)$ is expressed in terms of m through the trace formula

$$q(x) = \frac{2i}{\pi}\int_{-\infty}^{\infty} kr(k)e^{2ikx}m^2(x,k)dk.$$

In conclusion, to recover $q(x)$ from the reflection coefficient r, we need to solve (2.7) with initial values at ∞

$$\lim_{x\to\infty} m(x,k) = 1,$$
$$\lim_{x\to\infty} m'(x,k) = 0.$$

Characterization

The problem of the characterization of a scattering matrix $S(k)$ has been solved by Faddeev [18] and completed by Deift and Trubowitz [17].
One starts with the Marchenko equation (2.5) with $r, \{\beta_i\}, \{c_j\}$ and hence Ω given by (2.4). One shows that the equation has a solution $B(x,\cdot)$ for all $x \in \mathbb{R}$ and then setting $q(x) := \partial_x B(x,0)$, one show that $q(x)$ is a potential in certain class with reflection coefficient $r(k)$, bound states $\{-\beta_j^2\}$ and norming constants $\{c_j\}$.
The more general inverse characterization problem is given in terms of scattering data

$$S(k) = \{r_l(k), r_r(k), t_l(k), t_r(k)\}$$

where $r_l(k)$ and $r_r(k)$ represent respectively the reflection coefficients from the right and from the left (the same for the transmission coefficient $t_l(k)$ and $t_r(k)$). It can be shown that one can obtain the scattering data from the reflection coefficient $r(k)$, the bound states and the norming constants remaining in a certain class of potential.
The theorem can be stated as follows:

Theorem 2 (Deift and Trubowizt [17]). *A matrix*

$$\begin{pmatrix} r_l(k) & t_r(k) \\ t_l(k) & r_r(k) \end{pmatrix} \qquad \forall k \in \mathbb{R}$$

is a scattering matrix for a real piecewise absolutely continuous potential $q \in L^1_2$ with its derivative in L^1 and without bound states if and only if

(i) *(Symmetry)* $t_l(k) = t_r(k) = t(k)$.

(ii) *(Unitary)* $|t(k)|^2 + |r_l(k)|^2 = |t(k)|^2 + |r_r(k)|^2 = 1$ *and*

$$r_l(k)\overline{t(k)} + \overline{r_r(k)}t(k) = 0.$$

(iii) *(Analycity)* $t(k)$ *is analytic in the open upper half-plane and continuous down to the axis.*

(iv) *(Asymptotics)*

$$t(k) = 1 + \mathcal{O}\left(\frac{1}{|k|}\right), \qquad \Im k \geq 0,$$
$$r_i(k) = \mathcal{O}\left(\frac{1}{k}\right), \qquad i = l, r \text{ for } k \in \mathbb{R}.$$

(v) *(Rate at* $k = 0$*)*$|t(k) > 0|$, $\Im k \geq 0$, $k \neq 0$ *and either*

(1) $0 < c < |t(k)|$ *for all* $\Im k \geq 0$

(2) $t(k) = \dot{t}(0)k + o(k)$ *with* $\dot{t}(0) \neq 0, \qquad \Im k \geq 0,$
$1 + r_i(k) = \rho_i k + o(k), \quad i = r, l, \qquad k \in \mathbb{R}$ *with* ρ_i *real.*

(vi) *(Reality)* $r_i(k) = \overline{r}_i(-k) \qquad t_i(k) = \overline{t_i}(-k)$ *for* $i = r, l,$

(vii) *The functions* $F_i(y)$ *defined as*

$$F_i(y) = \frac{1}{\pi}\int_{\mathbb{R}} r_i(k)e^{2iky}dk \qquad i = r, l,$$

are absolutely continuous with

$$\int_{-\infty}^{a} |\frac{d}{dt}F_i(t)|(1+t^2)dt \leq a < \infty \qquad i = r, l,$$

for all $a \in \mathbb{R}$.

We have shown how the potential q is related to the scattering data in the case of the line.

2.1.2 Inverse scattering on Network

The scattering problem on branching graphs attracted attention of many scientists and recently it had been becoming more popular since it has different possible applications. The problem can be considered as a generalization of the classical inverse scattering problem for the Schrödinger operator on the line. It appears that this problem is much more complicated than the inverse scattering problem on a simple line. Therefore one can expect that the inverse scattering problem on non compact graphs has several new features compared with the inverse problem on the line.

We have shown the equivalence between the lossless transmission line equations and the Schrödinger equation in the case of a line and a network, but it is useful to know that the equation

$$-\frac{d}{dx}y(x,k) + q(x)y(x,k) = k^2 y(x,k) \qquad x \in [x_l, x_r], \tag{2.8}$$

restrained on a segment with the generic boundary conditions

$$\alpha_1 y(x_r) + \alpha_2 y'(x_r) = 0, \tag{2.9}$$

$$\beta_1 y(x_l) + \beta_2 y'(x_l) = 0, \tag{2.10}$$

with $\alpha_1, \alpha_2, \beta_1, \beta_2 \in \mathbb{R}$, is also called *Sturm-Liouville* equation. Indeed, given a lossless transmission line network, the restriction of the Schrödinger operator to a single branch becomes a "Sturm-Liouville" equation.
Finding the value of k for which there exists a non-trivial solution of (2.8) satisfying the boundary condition (2.9) and (2.10) is part of the "Sturm-Liouville" boundary value problem. The inverse Sturm-Liouville boundary problem consists in retrieving the potential q from the set of k's such that there exists a non-trivial solution of (2.8).

The rather extensive literature concerning the “inverse scattering problem” and the “inverse Sturm-Liouville problem” on graphs have mostly followed separate pathways except for a very few results [25, 24, 2].

The first work for the scattering theory on network has been written by Gerasimenko and Pavlov in [24] and [25] and it contains the first mathematically rigorous definition of the Schrödinger operator on branching graphs. In [25] the direct scattering problem for a Schrödinger operator on a non-compact graph was posed and solved. It shows that the specification of a non-compact graph, the potentials on its rays and the boundary conditions at the vertices makes possible to determine a self-adjoint operator, which Gerasimenko defines as the "Schrödinger operator", together with the scattering data. In [24], Gerasimenko tries to solve the simplest inverse problem: from some set of scattering data for a given non-compact graph, he can find the potentials on its rays. For a non-compact star-shaped graphs, the knowledge of each reflection coefficient $r_j(k)$ associated to the j-th ray and the amplitudes of the eigenfunctions corresponding to the eigenvalues allow to retrieve the potentials $q_j(x)$ on the rays of given graph.
In the case where the non-compact graph has a non-degenerate compact part, the procedure for recovering the potentials from the scattering data decomposes into two steps. The first is the recovery of the potentials on the infinite rays that emanate form the vertices of the graph. The next stage is to recover the potentials on the compact part of the graph (without cycles) and this can be done through the knowledge of the two spectra associated to the Sturm-Liouville boundary problem on each segment for the compact parts.

Inverse scattering problem on non-compact graphs

A first set of results [44] and [43] deals with inverse scattering problems over graphs. Harmer studies the matrix Schrödinger operator with self-adjoint boundary conditions and he presents a solution of the inverse problem using a Marchenko type equation. The motivation for studying the matrix Schrödinger operator is that, in the case of diagonal potentials, it may be identified with the Schrödinger operator on a non-compact star-shaped graph. Although these are really two different operators, for the purposes of the inverse problem they may be identified: each component of the vector on which the matrix Schrödinger operator acts is identified with the value of the function on of the rays of the graph.

The inverse scattering problem investigated in [44] is to recover the potentials on each branch through the knowledge of the reflection coefficients $r_j(k)$ associated to each branch j and the normalization constants. In particular in [43], the author shows that if a self-adjoint boundary condition at central node that preserves the "flux" is

given, then it is possible to recover the potentials with only $N-1$ reflection coefficients and normalization constants, where N is the number of the branches.

The paper [38] copes with the relations between the scattering data and the topology of the graph. The authors show that the knowledge of the scattering matrix is not enough to determine uniquely the topological structure of a generic graph. All counter examples have one common feature: there exists a nontrivial automorphism which preserves the external edges. This condition guarantees the impossibility to identify the topological structure through the scattering data.

In [2], Avdonin and Kurasov consider a star-shaped graph with N finite branches. They prove that the knowledge of a diagonal element of the response operator allows one to reconstruct the graph, i.e. the total number of edges and their lengths. This result is very similar to Theorem 3 of Chapter 3 and can be seen as a time-domain version of Theorem 3 (see the remarks after Theorem 3 for further details). Furthermore, they prove, through the same paper [2], that the knowledge of the diagonal elements of the response operator over all but one external nodes is enough to identify the potentials on the branches. At last they prove an extension of the result to the more generic tree case where they need the whole response operator.

The two more recent papers [4, 3] consider other types of inverse scattering problems on trees. The first paper considers the case of potential-free Schrödinger operators over the branches of a co-planar tree where the matching conditions at the internal nodes of the graph depend explicitly on the angles between the branches. The authors prove, for the case of star graph, that the knowledge of the diagonal elements of the Titchmarsh-Weyl matrix at the external nodes is enough to reconstruct the lengths and the angles between the branches. This result is then extended to the more generic tree case, where further elements of Titchmarsh-Weyl matrix are needed. The second paper [3], based on a previous one [37], considers the inverse problem of characterizing the matching conditions for the internal node of a star graph through the knowledge of a part of the scattering matrix.

Inverse spectral problem for Sturm-Liouville operators on compact graphs

As mentioned above, in parallel to the research on inverse scattering problems, another class of results considers the inverse spectral problem for Sturm-Liouville operators on compact graphs. These results can be seen as extensions of the classical result provided

by Borg [10], on the recovering of the Sturm-Liouville operator from two spectra on a finite interval.

A first set of results has been obtained by Yurko [67, 68, 69]. The article [67] deals with the inverse spectral problem on a tree. It provides a generalization of the Borg's result in the following sense: for a tree with n boundary vertices, it is sufficient to know n spectra, corresponding to n different settings for boundary conditions at the external nodes, to retrieve the potentials on the tree.
In a recent work [69], the same kind of result is proposed for a star-shaped graph including a loop joined to the central node. Finally, [68] provides a generalization of [67] to higher order differential operators on a star-shaped graph.

Pivovarchik and co-workers provide a next set of results in this regard [48, 49, 50, 12]. In particular, in [50], the author proves that under some restrictive assumptions on the spectrum of a Sturm-Liouville operator on a star-shaped graph with some fixed boundary conditions, the knowledge of this spectra can determine uniquely the Sturm-Liouville operator.

A third set of results deal with the problem of identifying the geometry of the graph [27, 64]. In particular, [27] provides a well-posedness result for the identification of the lengths of the branches through the knowledge of the spectrum. This result is to be compared with Theorem 3 of Chapter 3. While [27] considers a more general setting of generic graphs, it assumes the $\mathbb{Q}$-independence of lengths, an assumption that has been removed in Theorem 3 for the simpler case of a star-shaped graph.

Another interesting class of results concern the potential-free Sturm-Liouville operator on graphs. Belishev considers the potential-free case over a tree and proves that the knowledge of the eigenvalues and the normal derivatives of the Dirichlet eigenfunctions at the external node is enough to identify the geometry of the tree up to a spatial isometry [5]. Together with his co-workers, he further provides an identification algorithm and numerical simulations [6]. Carlson considers the potential-free case over a directed graph and provides information on the boundary conditions at the external nodes as well as the lengths through the spectrum of the operator [14]. Finally Kursov and Nowaczyk consider the potential-free case over a finite graph and similarly to [27] treat the problem of identifying the geometry through the spectral data, provided that the branch lengths are rationally independent [36].

2.2 Inverse scattering theory for Zakharov-Shabat system on the line

2.2.1 General theory of inverse scattering problem

In 1972 Zakharov and Shabat introduced their coupled system in order to solve some nonlinear partial differential equations [70]. They applied the inverse problem method discovered by Gardner, Green, Kruskal and Miura [23]: this method is applicable to equations of the type

$$\frac{\partial}{\partial t}u(x,t) = \hat{S}[u] \tag{2.11}$$

where $\hat{S}$ is a nonlinear differential operator. The equation (2.11) can be represented in the form

$$\frac{\partial}{\partial t}\hat{L} = i[\hat{L}, \hat{A}], \tag{2.12}$$

where the bracket [,] denotes the commutator operator (Lax's pair, [40]).
Here $\hat{L}$ and $\hat{A}$ are linear differential operator containing the sought function $u(x,t)$ in the form of a coefficient. If the condition (2.12) is satisfied, then the spectrum of the operator $\hat{L}$ does not depend on the time, and the asymptotic characteristics of its eigenfunctions can easily be calculated at any instant of time form their initial values. The reconstruction of the function $u(x,t)$ at an arbitrarily instant of time is realized by solving the inverse scattering problem for the operator $\hat{L}$.

Studying the solutions of a particular equation, Zakharov and Shabat introduced as operator $\hat{L}$ their particular system on the interval $-\infty < x < \infty$

$$\begin{cases} \partial_x \nu_1(x,k) + i\xi\nu_1(x,k) = q(x)\nu_2(x,k) \\ \partial_x \nu_2(x,k) - i\xi\nu_2(x,k) = -q^*(x)\nu_1(x,k). \end{cases} \tag{2.13}$$

where q^* denote the complex conjugate of the potential q. The authors solved the associated inverse scattering problem.

The scattering problem of this system (2.13) is analogous to the problem of scattering for the one-dimensional Schrödiger equation. Despite this system is not self-adjoint, it has an interesting property: if $v = (v_1, v_2)^{tr}$ is a solution for $\xi = \xi_1$, then

$$v^J = \begin{pmatrix} \overline{v}_2 \\ -\overline{v}_1 \end{pmatrix}$$

is a solution for $\xi = \overline{\xi}_1$.
For $k = \xi \in \mathbb{R}$ the Jost solutions $F_l(x,k)$ and $F_r(x,k)$ for (2.13) behave asymptotically as

$$\begin{aligned}
F_r(x,\xi) &\sim \begin{pmatrix} 1 \\ 0 \end{pmatrix} e^{-i\xi x} \qquad \text{as } x \to -\infty, \\
F_r^J(x,\xi) &\sim \begin{pmatrix} 0 \\ -1 \end{pmatrix} e^{-i\xi x} \qquad \text{as } x \to -\infty, \\
F_l(x,\xi) &\sim \begin{pmatrix} 0 \\ 1 \end{pmatrix} e^{+i\xi x} \qquad \text{as } x \to +\infty, \\
F_l^J(x,\xi) &\sim \begin{pmatrix} 1 \\ 0 \end{pmatrix} e^{+i\xi x} \qquad \text{as } x \to +\infty.
\end{aligned}$$

Since F_l and F_l^J form a basis for the solutions space, the scattering data $a(\xi)$ and $b(\xi)$ are defined as

$$F_r = a(k)F_l^J + b(k)F_l \tag{2.14}$$

The coefficients $a(k)$ and $b(k)$ admit an analytic continuation in the complex plane and the points ξ_j for $j = 1, \ldots, N$ in the upper-complex plane where $a(\xi_j) = 0$, correspond to the eigenvalues of (2.13). Therefore at these points, the Jost solutions are linearly dependent

$$F_r(x,\xi_j) = c_j F_l(x,\xi_j).$$

The set $\{a(k), b(k), \quad k \in \mathbb{R}, \quad c_j \quad j = 1, \ldots, N\}$ forms the scattering data.

Eventually the potential q is reconstructed from the scattering data $a(k)$, $b(k)$ and c_j in two steps [70]: the first step consists in solving a system of $2N + 2$ equations relative to the Jost solutions $F_r(x,k)$ and $F_l(x,k)$.
Let $c(x,\xi) = b(\xi)e^{2i\xi x/a(\xi)}$ and $\tilde{c}_k = c_k/a'(\xi_k)$. Then the system writes

$$F_{r1} - \frac{c(x,\xi)}{2}\left(\overline{F}_{r2} + \frac{1}{\pi i}\int_{-\infty}^{+\infty} \frac{\overline{F}'_{r2}(\zeta)}{\zeta - \xi} d\zeta\right) = -c(x,\xi)\sum_{j=1}^{N} \frac{e^{-i\overline{\xi}_j x}}{\xi - \overline{\xi}_j}\overline{\tilde{c}}_j \overline{F}_{l2}(x,\xi_j)$$

$$\frac{\overline{c}(x,\xi)}{2}\left(F_{r1} - \frac{1}{\pi i}\int_{-\infty}^{+\infty} \frac{F'_{r1}(\zeta)}{\zeta - \xi} d\zeta\right) - \overline{F}_{r2} = \overline{c}(x,\xi) + \overline{c}(x,\xi)\sum_{j=1}^{N} \frac{e^{i\xi_j x}}{\xi - \xi_j}\tilde{c}_j \overline{F}_{l1}(x,\xi_j)$$

and for $j = 1, \ldots, N$

$$F_{l1}(x,\xi_j)e^{-i\xi_j} + \sum_{h=1}^{N} \frac{e^{-i\bar{\xi}_h x}}{\xi_j - \bar{\xi}_h} \bar{\tilde{c}}_h \overline{F}_{l2}(x,\xi_h) = \frac{1}{2\pi i}\int_{-\infty}^{+\infty} \frac{\overline{F}_{r2}(x,\zeta)}{\zeta - \xi_j} d\zeta,$$

$$-\sum_{h=1}^{N} \frac{e^{i\xi_h x}}{\bar{\xi}_j - \xi_h} \tilde{c}_h F_{l1}(x,\xi_h) + \overline{F}_{l2}(x,\xi_j)e^{i\xi_j x} = 1 + \frac{1}{2\pi i}\int_{-\infty}^{+\infty} \frac{F_{r1}(x,\zeta)}{\zeta - \xi_j} d\zeta,$$

The knowledge of the scattering data allows to obtain the Jost solutions. The potential $q(x)$ is recovered by the following formula

$$q(x) = -2i\sum_n \bar{c}_n exp(-i\bar{\xi}_n x)\overline{F}_{l2}(x,\xi_n) - \frac{1}{\pi}\int_{-\infty}^{\infty} \overline{F}_{r2}(x,k)dk$$

$$\int_x^{\infty} |q(s)|^2 ds = -2i\sum_n c_n exp(i\xi_n x)F_{l1}(x,\xi_n) + \frac{1}{\pi}\int_{-\infty}^{\infty} F_{r1}(k)dk.$$

where F_{x1} (resp. F_{x2}) denotes the first (resp. second) component of the vector F_x.

Few years later, Ablowitz, Kaup, Newell and Segur published an article [1] on classes of evolution equations which can be solved by the inverse scattering method. In particular they made a comprehensive study of the direct and inverse scattering problem for two potentials Zakharov-Shabat system on the interval $-\infty < x < \infty$

$$\begin{cases} \partial_x \nu_1(x,\xi) + i\xi\nu_1(x,\xi) = q(x)\nu_2(x,\xi) \\ \partial_x \nu_2(x,\xi) - i\xi\nu_2(x,\xi) = r(x)\nu_1(x,\xi). \end{cases} \tag{2.15}$$

The assumption is that the potentials r and q vanish sufficiently rapidly as $x \to \pm\infty$ so that in these limits, the right hand side in (2.15) can be neglected. The nature of (2.15) is such that we can define four Jost solutions F_l, F_l^J, F_r, F_r^J. For $k \in \mathbb{R}$, these solutions have the asymptotic behavior as (1.87)-(1.90). It is customary to let the scattering data , $a(k), b(k), a^J(k), b^J(k)$ be the coefficients relating these two sets of

linearly independent solutions

$$F_r = aF_l^J + bF_l \to \begin{pmatrix} ae^{-ikx} \\ be^{ikx} \end{pmatrix} \text{ as } x \to +\infty,$$
$$F_r^J = b^J\ F_l^J - a^J F_l^J \to \begin{pmatrix} b^J e^{-ikx} \\ -a^J e^{ikx} \end{pmatrix} \text{ as } x \to +\infty.$$

Not surprisingly, the coefficients $a(k)$ and $a^J(k)$ can be analytically extended respectively in the upper and lower half plane. Indeed the discrete eigenvalues $\{\xi_j\}_{j=1}^N$ in the upper half plane are given by the zeros of $a(\xi)$ at which $F_r(\xi_j) = b_j F_l(\xi_j)$. Similarly the zeros of $a^J(\xi)$ in the lower half plane are also eigenvalues. At these points we have $F_r^J(\overline{\xi}_j) = b_j^J F_l^J(\overline{\xi}_j)$.

Remark 22. It is important to note that the coefficients $a(k), b(k), a^J(k), b^J(k)$ differs from the (1.92) and (1.93). In Section 1.4, the choice of the coefficients $a_l(k), a_r(k), b_l(k)$ and $b_r(k)$ is related to the choice of the two Jost solutions to be determined in (1.92) and (1.93): we favored F_l and F_r representing the two reflectometry experiments at both sides of the line.

The inverse scattering problem for the two potentials Zakharov-shabat system is also solved in two steps: exploiting the integral representations for the four Jost functions and then solving of the associated Marchenko type equations [1].

The integral representation of the Jost solutions

$$\begin{aligned} F_l(\xi, x) &= \begin{pmatrix} 0 \\ 1 \end{pmatrix} e^{+i\xi x} + \int_x^\infty K(x,s) e^{+i\xi s} ds, \\ F_l^J(\xi, x) &= \begin{pmatrix} 1 \\ 0 \end{pmatrix} e^{-i\xi x} + \int_x^\infty K^J(x,s) e^{+i\xi s} ds, \\ F_r(\xi, x) &= \begin{pmatrix} 1 \\ 0 \end{pmatrix} e^{-i\xi x} - \int_{-\infty}^x L(x,s) e^{-i\xi s} ds, \\ F_r^J(\xi, x) &= -\begin{pmatrix} 0 \\ 1 \end{pmatrix} e^{+i\xi x} - \int_{-\infty}^x L^J(x,s) e^{-i\xi s} ds. \end{aligned}$$

defines the kernel vectors K, K^J, L and L^J. Inserting these coefficients in the Zakharov-

Shabat integral representations, we obtain four Marchenko type equations.

$$K^J(x,y) + \begin{pmatrix} 0 \\ 1 \end{pmatrix} F(x+y) + \int_x^\infty K(x,s)F(s+y)ds = 0, \quad (y > x)$$

$$K(x,y) - \begin{pmatrix} 1 \\ 0 \end{pmatrix} F^J(x+y) - \int_x^\infty K^J(x,s)F^J(s+y)ds = 0, \quad (y > x)$$

$$L^J(x,y) + \begin{pmatrix} 1 \\ 0 \end{pmatrix} G(x+y) - \int_{-\infty}^x L(x,s)G(s+y)ds = 0, \quad (y < x)$$

$$L(x,y) + \begin{pmatrix} 0 \\ 1 \end{pmatrix} G^J(x+y) + \int_{-\infty}^x L^J(x,s)G^J(s+y)ds = 0, \quad (y < x)$$

where F, F^J, G and G^J are functions depending on the scattering data.
To be more precisely, the four functions are given by the following formula

$$F(z) \equiv \frac{1}{2\pi}\oint \frac{b(\zeta)}{a(\zeta)} e^{i\zeta z} d\zeta, \quad F^J(z) \equiv \frac{1}{2\pi}\oint_J \frac{b^J(\zeta)}{a^J(\zeta)} e^{-i\zeta z} d\zeta,$$

$$G(z) \equiv \frac{1}{2\pi}\oint \frac{b^J(\zeta)}{a(\zeta)} e^{-i\zeta z} d\zeta, \quad G^J(z) \equiv \frac{1}{2\pi}\oint_J \frac{b(\zeta)}{a^J(\zeta)} e^{i\zeta z} d\zeta.$$

where C is the contour described in the figure 2.2.1. We define C to be the contour

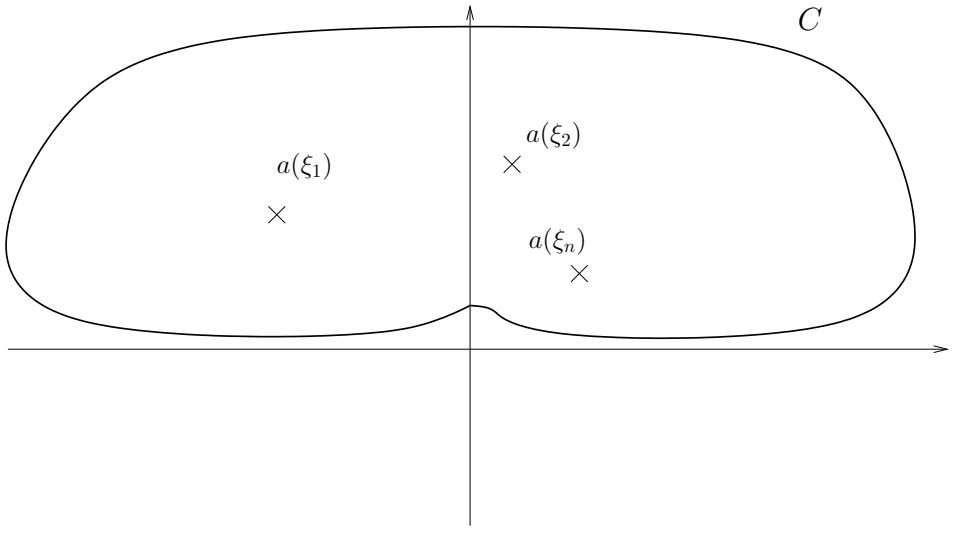

Figure 2.1: Contour C in the complex plane $\mathbb{C}$

in the complex ξ-plane, starting from $\xi = -\infty + i0^+$ passing over all zeros $a(\xi)$ and ending at $\xi = +\infty + i0^+$. Similarly, C^J is the contour starting from $\xi = -\infty + i0^-$ passing over all zeros $a^J(\xi)$ and ending at $\xi = +\infty + i0^-$.

As before, the solutions K, K^J, L and L^J give us the potentials r and q

$$\begin{aligned}
K_1(x,x) &= -L_1^J(x,x) &&= -\frac{1}{2}q(x),\\
K_2(x,x) &= K_1^J(x,x) &&= \frac{1}{2}\int_x^\infty q(s)r(s)ds,\\
L_1(x,x) &= -L_2^J(x,x) &&= \frac{1}{2}\int_{-\infty}^x q(s)r(s)ds,\\
L_2(x,x) &= K_2^J(x,x) &&= \frac{1}{2}r(x).
\end{aligned}$$

In conclusion we have shown how to recover the potentials q and r from the scattering data.

2.2.2 Application to the telegrapher's equations: theoretical and numerical results

In this part we present the results of Jaulent [30]. In particular we show that the inverse scattering problem for $RLGC$ non-uniform transmission lines can be reduced to the inverse scattering problem for the Zakharov-Shabat system.
On the interval $-\infty < z < \infty$ we consider the telegrapher's equations in the harmonic regime (1.33). Applying the Liouville transformation (1.41), and setting the variables as in Section 1.3.4

$$\begin{cases}
\nu_1(x,k) = \dfrac{1}{\sqrt{2}}\left[Z_{c0}^{-1/2}(x)V(k,x) - Z_{c0}^{1/2}(x)I(k,x)\right],\\
\nu_2(x,k) = \dfrac{1}{\sqrt{2}}\left[Z_{c0}^{-1/2}(x)V(k,x) + Z_{c0}^{1/2}(x)I(k,x)\right].
\end{cases} \tag{1.45}$$

the telegrapher's equations become equivalent to the Zakharov-Shabat system (1.46) denoted by $(Z)[q_+, q_-, q_d]$.

Remark 23. Note that $\nu_1(k,x)$ differs by a negative sign from the corresponding notations in [30]. Consequently having the same definition for the three potentials, the matrix Q differs by a negative sign on the anti diagonal elements from the definition (1.54).

The assumptions on the three potentials $q_+(x), q_-(x)$ and $q_d(x)$ are that they are sufficiently regular functions going to 0 fast enough as $|x| \to \infty$. It is convenient to consider both systems $(Z)^{\pm}[q_+, q_-, q_d]$:

$$\frac{d}{dx}Y^{\pm} + ik\sigma_3 Y^{\pm} = \begin{pmatrix} \pm q_d & -q_{\pm} \\ -q_{\mp} & \mp q_d \end{pmatrix} Y^{\pm} \tag{2.16}$$

Note that if $Y^-(k,x)$ is a solution for $(Z)^-$, then $\begin{pmatrix} 0 & 1 \\ 1 & 0 \end{pmatrix} Y^-(-k,x)$ is a solution of $(Z)^+$. This symmetry property allows to reduce the study of two types of Jost Solutions at $-\infty$ to only one.
The right and left Jost solutions of $(Z)^{\pm}$, $F_r^{\pm}(k,x)$ and $F_l^{\pm}(k,x)$ are defined as

$$\begin{aligned} F_r^{\pm}(k,x) &\sim \begin{pmatrix} 0 \\ 1 \end{pmatrix} e^{+ikx} \qquad \text{as } x \to \infty, \\ F_l^{\pm}(k,x) &\sim \begin{pmatrix} 1 \\ 0 \end{pmatrix} e^{-ikx} \qquad \text{as } x \to -\infty, \end{aligned}$$

As usual, one can prove that $F_r^{\pm}(k,x)$ and $F_l^{\pm}(k,x)$ are analytic in k and they form a fundamental system of solutions of $(Z)^{\pm}$ for $k \in \mathbb{R}$.
The reflection coefficients to the right and to the left , $r_r^{\pm}(k)$ and $r_l^{\pm}(k)$ and the transmission coefficients $t^{\pm}(k)$ associated to $(Z)^{\pm}$ are defined for each real value of k by

$$\begin{aligned} F_l^{\pm}(k,x) &= \frac{r_r^{\pm}(k)}{t^{\pm}(k)} F_r^{\pm}(k,x) + \frac{1}{t^{\pm}(k)} \sigma_1 F_r^{\pm}(-k,x), \\ F_r^{\pm}(k,x) &= \frac{r_l^{\pm}(k)}{t^{\pm}(k)} F_l^{\mp}(k,x) + \frac{1}{t^{\pm}(k)} \sigma_1 F_l^{\mp}(-k,x). \end{aligned}$$

The scattering matrix associated to $(Z)^{\pm}$ is defined as

$$S^{\pm}(k) = \begin{pmatrix} r_l^{\pm}(k) & t^{\pm}(k) \\ t^{\pm}(k) & r_r^{\pm}(k) \end{pmatrix}, \qquad k \in \mathbb{R}. \tag{2.17}$$

and their components represent also the scattering data for the transmission line equation. The inverse scattering problem for the line is the construction of quantities connecting L, C, R and G from $S^+(k)$, $L(-\infty)$, $L(\infty)$, $C(\infty)$ and $C(-\infty)$. It can

be proved the existence of solutions

$$\begin{pmatrix} I_l(k,z) \\ V_l(k,z) \end{pmatrix} \qquad \text{and} \qquad \begin{pmatrix} I_r(k,z) \\ V_r(k,z) \end{pmatrix},$$

such that

$$\begin{aligned}
I_l(k,z) &\sim \left[\tfrac{C(-\infty)}{L(-\infty)}\right]^{1/4} t^+(k)e^{-ikx(z)} && z \to -\infty \\
&\sim \left[\tfrac{C(\infty)}{L(\infty)}\right]^{1/4} (r_r^+(k)e^{+ikx(z)} + e^{-ikx(z)}) && z \to +\infty \\
V_l(k,z) &\sim \left[\tfrac{L(-\infty)}{C(-\infty)}\right]^{1/4} t^+(k)e^{-ikx(z)} && z \to -\infty \\
&\sim \left[\tfrac{L(\infty)}{C(\infty)}\right]^{1/4} (-r_r^+(k)e^{+ikx(z)} + e^{-ikx(z)}) && z \to +\infty \\
I_r(k,z) &\sim \left[\tfrac{C(-\infty)}{L(-\infty)}\right]^{1/4} (r_l^+(k)e^{-ikx(z)} + e^{ikx(z)}) && z \to -\infty \\
&\sim \left[\tfrac{C(\infty)}{L(\infty)}\right]^{1/4} t^+(k)e^{+ikx(z)} && z \to +\infty \\
V_r(k,z) &\sim \left[\tfrac{L(-\infty)}{C(-\infty)}\right]^{1/4} (r_l^+(k)e^{-ikx(z)} - e^{ikx(z)}) && z \to -\infty \\
&\sim \left[\tfrac{L(\infty)}{C(\infty)}\right]^{1/4} t^+(k)e^{+ikx(z)} && z \to +\infty.
\end{aligned}$$

Jaulent reduces the inverse scattering problem for three potential Zakharov-Shabat system $(Z)^{\pm}[q_+, q_-, q_d]$ to the more classical two potentials Zakharov-Shabat system (2.15) through the following change of variables

$$\tilde{Y}^{\pm}(k,x) = \begin{pmatrix} exp(\mp i \int_x^\infty q_d(s)ds) & 0 \\ 0 & exp(\pm i \int_x^\infty q_d(s)ds) \end{pmatrix} Y^{\pm}(k,x). \tag{2.18}$$

The new variables $\tilde{Y}^{\pm}(k,x)$ are solutions of the Zakharov-Shabat system $(Z)^{\pm}[\tilde{q}_+, \tilde{q}_-, 0]$

$$\frac{d}{dx}\tilde{Y}^{\pm} + ik\sigma_3\tilde{Y}^{\pm} = \begin{pmatrix} 0 & -\tilde{q}_{\pm} \\ -\tilde{q}_{\mp} & 0 \end{pmatrix} \tilde{Y}^{\pm}, \tag{2.19}$$

with

$$\tilde{q}^{\pm} = q^{\pm} exp(\mp 2i \int_x^\infty q_d(s)ds).$$

It is easy to obtain the connection between the scattering data

$$\begin{cases} \tilde{r}_r^{\pm}(k) & = r_r^{\pm}(k), \\ \tilde{r_l}^{\pm}(k) & = r_l^{\pm}(k) exp(\pm 2i \int_{-\infty}^{\infty} q_d(s) ds), \\ \tilde{t}^{\pm}(k) & = t^{\pm}(k) exp(\pm i \int_{-\infty}^{\infty} q_d(s) ds). \end{cases} \tag{2.20}$$

Using the result of Gardner, Green, Kruskal and Miura [1], Jaulent found that it is possible to reconstruct from the scattering data the potential $q^{\pm}(x)$ as a function of the wave's traveling time x:

$$\tilde{q}^{\pm}(x) = \left[\frac{1}{4} \frac{d}{dx} \left(\ln \frac{L}{C} \right) \pm \frac{1}{2} \left(\frac{R}{L} - \frac{G}{C} \right) \right] exp \left(\mp \int_{-\infty}^{\infty} \left(\frac{R}{L} + \frac{G}{C} \right) ds \right). \tag{2.21}$$

Numerical simulation for the inverse scattering problem for telegrapher's equation

Tang and Zhang have shown some numerical results for the inverse scattering problem for the lossy transmission line [62].

Using the the relationship between the inverse problem for the general lossy electric transmission lines and the inverse scattering problem for the two potential Zakharov-Shabat system established by Jaulent [30], they have studied the soft fault diagnosis for such lines by clarifying and completing the computation for the theoretic scattering data required by the inverse scattering transform (IST) from the practically measured engineering scattering data.

The (IST) computation requires the left reflection coefficient $\tilde{r}_l^+(k)$ for $(Z)^+[\tilde{q}_+, \tilde{q}_-, 0]$ defined by (2.19) and also the left coefficient $\tilde{r}_l^-(k)$ for $(Z)^+[\tilde{q}_-, \tilde{q}_+, 0]$. It is important to remark that, $\tilde{r}_k^-(k)$ is the reflection coefficient for $(Z)^-[\tilde{q}_-, \tilde{q}_+, 0]$, that it does not physically exist. Hence $\tilde{r}_l^-(k)$ cannot be directly measured.

While $\tilde{r}_l^+(k)$ can be easily obtained from the engineering reflection coefficient, $\tilde{r}_l^-(k)$ can be related to the measured engineering scattering data, but it requires the knowledge of transmission line length l and the integral value of dispersion $\int_{\mathbb{R}} q_d(y) dy$.

As we have seen above, the inverse scattering problem for $(Z)^{\pm}[\tilde{q}_+, \tilde{q}_+, 0]$ is solved using two reflection coefficients $\tilde{r}_l^{\pm}(k)$. Unfortunately, the knowledge of the scattering data $\tilde{r}_l^{\pm}(k)$ cannot be retrieved from the reflectometry measurament.

Chapter 3

Inverse scattering for loss-less star-shaped network

We consider a class of inverse scattering problems on star-shaped graphs, having in mind certain applications such as the fault-detection and diagnosis of electrical networks through reflectometry-type experiments. Even though a part of the obtained results, Theorem 3 and 4, can be directly applied to such applications, some of them (see Theorem 5 and assumption **A2**), remain preliminary results and need significant improvement. However, from a theoretical insight all the results are original and provide some new uniqueness results for the solutions of inverse scattering problems on networks.

Note that, similarly to the case of a simple line [17], the existence of a solution to the inverse scattering problem (i.e. classifying the scattering data for which there exists a solution to the inverse scattering problem) remains for itself a complete subject apart and we do not consider here such existence problems. In other words, we assume that the scattering data (and notably the reflection coefficient) are precisely obtained from a real physical system and therefore the existence of the solution to the inverse scattering problem is ensured by the existence of the physical system.

We consider the particular case of star-shaped network, where the reflectometry experiment is based on a far-filed method consisting in adding a uniform infinite wire joined at the central node of the network. Once again, connecting a matched load to the external node of a finite line is sufficient to emulate the electrical propagation through an infinite line.

The results of this chapter has been published as a journal paper in *"Journal of*

Mathematical Analysis and Applications" [63].

3.1 Main hypothesis and physical interpretation

The linearity of the transmission line model allows to replace any test by an equivalent test in harmonic regime. We can therefore start by stating the Telegrapher's equation in the harmonic regime,

$$\begin{aligned} &\frac{\partial}{\partial x}V(k,x) - ikL(x)I(k,x) = 0, \\ &\frac{\partial}{\partial x}I(k,z) - ikC(x)V(k,x) = 0. \end{aligned} \tag{3.1}$$

Through this chapter, we assume that

A1 the distributed parameters $C(x)$ and $L(x)$ are twice continuously differentiable on the transmission lines;

A2 they are strictly positive, $C(x) > 0, L(x) > 0$;

A3 the characteristic impedance $Z_c(x) := \sqrt{L(x)/C(x)}$ is continuous at the central node of the star-shape network;

A4 the transmission lines are uniform in a neighborhood of the extremities of the branches.

The network under test.

Throughout this chapter Γ represents the compact star-shaped network consisting of the branches $(e_j)_{j=1}^N$ joining at the central node and Γ^+ is the extended graph where the test branch e_0 is also added to the graph. We have $N+1$ equations of the form

$$-\frac{d^2y_j}{dx^2} + q_j(x)y_j = k^2 y_j \qquad x \in (0, l_j), \tag{3.2}$$

where l_j is the wave traveling time associated to the branch number j ($l_0 = \infty$ as the added branch e_0 is assumed to be an infinite line). In particular note that, as the infinite branch e_0 is assumed to be a uniform transmission line, we have $q_0(x) = 0, \qquad x \in (0, \infty)$.

Boundary conditions

Boundary condition for the reflectometer.

As explained in the section 1.3, the test branch e_0 is parametrized as $[-\infty, 0]$ where $x = 0$ represent the central node. Our reference forward wave on e_0 is then in the direction of the increasing x. Supposing e_0 of infinite length, the boundary condition for the reflectometer is:

$$y(x,k) \sim r(k)e^{-ikx} + e^{ikx} \qquad \text{as } x \to -\infty \quad \text{on } e_0. \tag{3.3}$$

The two sets of boundary conditions at the network extremities.

In order to recover the potential of the star-shape network, we will need to consider two experimental settings, with open circuit or short circuit boundary conditions at the extremities of the branches. This will lead to a problem similar to solving an inverse spectral problem for the Sturm-Liouville operator when two spectra are known.

The first setting corresponds to open circuit configuration at the extremities of the finite branches $((e_j)_{j=1}^N)$. This, together with the Assumption **A4** on the local uniformity of the lines around l_j's, leads to Neumann type boundary conditions:

$$y_j'(l_j) = 0 \qquad j = 1, \cdots, N. \tag{3.4}$$

The second setting corresponds to the short circuit configuration at the extremities of the finite branches $((e_j)_{j=1}^N)$. This leads to boundary conditions of the form $V_j(\omega, l_j) = 0$, or equivalently, we obtain the setting called, the Dirichlet configuration:

$$y_j(l_j) = 0 \qquad j = 1, \cdots, N. \tag{3.5}$$

Remark 24. In some of the applications that we have in mind, the reflectometry experiment has to take place without perturbing significantly the normal utilization of the transmission network, so that using open or short circuits conditions would be impossible. There is a way to circumvent this problem by computing the results of the open or short circuit experiments from results of two less invasive experiments. The idea is to use nonlinear superposition properties of solutions of Riccati equations as in [61], in order to get a closed-form representation of the reflection coefficient, solution

of (1.69), as a function of a general load impedance (value of Z at the extremity of a branch) and of two particular solutions corresponding to two load impedances more compatible with the network utilization.

The boundary conditions at the central node.

The boundary conditions at the central node write

$$\begin{aligned} y_i(0,k) = y_j(0,k) =: \bar{y}(k) \qquad & i,j = 0,\cdots,N, \\ \sum_{j=1}^{N} y_j'(0,k) - y_0'(0,k) = -\frac{1}{2}\frac{\sum_{j=1}^{N}(Z_c^j)'(0)}{Z_c^0}\bar{y}(k), & \end{aligned}$$

where $y_j'(\omega,0)$ and $(Z_c^j)'(0)$ denote the spatial derivatives at the point $x=0$ and Z_c^j is the characteristic impedance of the branch number j. Note, in particular, that we have applied the continuity of Z_c^j's at the central node (Assumption **A3**): $Z_c^j(0) = Z_c^0$, $\forall j$.

Formulation of the model

In conclusion, in order to study the LC-transmission line equations on the graph Γ^+, we can study the Schrödinger operators

$$\begin{aligned} \mathcal{L}^+_{\mathcal{N},\mathcal{D}} &= \otimes_{j=0}^{N}(-\frac{d^2}{dx^2} + q_j(x)), \\ D(\mathcal{L}^+_{\mathcal{N},\mathcal{D}}) &= \text{closure of } C^\infty_{\mathcal{N},\mathcal{D}} \text{ in } H^2(\Gamma^+), \end{aligned} \tag{3.6}$$

where $C^\infty_{\mathcal{N}}(\Gamma^+)$ (resp. $C^\infty_{\mathcal{D}}(\Gamma^+)$) denotes the space of infinitely differentiable functions $f = \otimes_{j=0}^{N} f_j$ defined on Γ^+ satisfying the boundary conditions at central node

$$\begin{aligned} f_j(0) = f_{j'}(0) \qquad & j,j' = 0,\cdots,N, \\ \sum_{j=1}^{N} f_j'(0) - f_0'(0) = Hf_0(0), \qquad & H = -\tfrac{1}{2}\frac{\left(\sum_{j=1}^{N}(Z_c^j)'(0)\right)}{Z_c^0}, \end{aligned} \tag{3.7}$$

More over we assume for $C^\infty_{\mathcal{N}}(\Gamma^+)$ (resp. for $C^\infty_{\mathcal{D}}(\Gamma^+)$), we assume the Neumann condition (resp. Dirichlet condition) at all boundary vertices:

$$f_j'(l_j) = 0 \quad (f_j(l_j) = 0 \text{ for } C^\infty_{\mathcal{D}}(\Gamma^+)) \tag{3.8}$$

for $j = 1, \cdots, N$.

3.2 Direct scattering problem

Here we show that the direct scattering problem for the Schrödinger operator acting on Γ is well posed. If the reflectometry experiments give us the measurements of the reflection coefficient, we need to define reflection coefficients for the Schrödinger operator and we have to prove their existence and their uniqueness.
The operators $(\mathcal{L}^+_{\mathcal{N},\mathcal{D}}, D(\mathcal{L}^+_{\mathcal{N},\mathcal{D}}))$ are essentially self-adjoint. To prove this fact we observe first that these operators are a compact perturbation of the operators $\otimes_{j=0}^{n}\left(-\frac{d^2}{dx^2}\right)$ with the same boundary conditions. Now, we apply a general result by Carlson [13] on the self-adjointness of differential operators on graphs. Indeed, following Theorem 3.4 of [13], we only need to show that at a node connecting m edges, we have m linearly independent linear boundary conditions. At the terminal nodes of $\{e_j\}_{j=1}^{N}$ this is trivially the case as there is one branch and one boundary condition (Dirichlet or Neumann). At the central node it is not hard to verify that (3.7) define $N+1$ linearly independent boundary conditions as well. This implies that the operators $(\mathcal{L}^+_{\mathcal{N},\mathcal{D}}, D(\mathcal{L}^+_{\mathcal{N},\mathcal{D}}))$ are essentially self-adjoint and therefore that they admit a unique self-adjoint extension on $L^2(\Gamma^+)$.

We are interested in the scattering solution where a signal of frequency k is applied at the infinite extremity of the infinite branch. In such a case, we will be seeking a solution satisfying the asymptotic behavior

$$y_0(x,k) \sim e^{-\imath kx} + r(k)e^{\imath kx}, \qquad \text{for } x \to \infty.$$

The reflection coefficients $r_{\mathcal{N},\mathcal{D}}(k)$ for $\mathcal{L}^+_{\mathcal{N},\mathcal{D}}$ are defined by the following proposition:

Proposition 3. *Under the assumptions **A1** through **A4**, for almost every $k \in \mathbb{R}$, there exists a unique solution*

$$\Psi_{\mathcal{N},\mathcal{D}}(x,k) = \otimes_{j=0}^{N} y^j_{\mathcal{N},\mathcal{D}}(x,k),$$

of the scattering problem and associated to it, a unique reflection coefficient $r_{\mathcal{N},\mathcal{D}}(k)$. This means that for almost every $k \in \mathbb{R}$, there exists a unique function $\otimes_{j=0}^{N} y^j_{\mathcal{N},\mathcal{D}}(x,k)$

and a unique constant $r_{\mathcal{N},\mathcal{D}}(k)$ satisfying

- $-\frac{d^2}{dx^2}y^j_{\mathcal{N},\mathcal{D}}(x,k)+q_j(x)y^j_{\mathcal{N},\mathcal{D}}(x,k)=k^2y^j_{\mathcal{N},\mathcal{D}}(x,k)$ *for* $j=0,\cdots,N$;
- $\left(y^j_{\mathcal{N},\mathcal{D}}(x,k)\right)_{j=0}^{N}$ *satisfy the boundary conditions (3.7) and (3.8) ;*
- $y^0_{\mathcal{N},\mathcal{D}}(x,k)=e^{+ikx}+r_{\mathcal{N},\mathcal{D}}(k)e^{-ikx}$.

Finally, the reflection coefficient $r_{\mathcal{N},\mathcal{D}}(k)$ can be extended by continuity to all $k\in\mathbb{R}$.

Proof. This proof gives us a concrete method for obtaining scattering solutions. Indeed, we will propose a solution and we will show that it is the unique one.
In this aim, we need to use Dirichlet/Neumann fundamental solutions of a Sturm-Liouville boundary problem.

Definition 17. Consider the potentials q_j as before and extend them by 0 on $(-\infty,0)$ so that they are defined on the intervals $(-\infty,l_j]$. The Dirichlet (resp. Neumann) fundamental solution $\varphi^j_{\mathcal{D}}(x,k)$ (resp. $\varphi^j_{\mathcal{N}}(x,k)$), is a solution of the equation,

$$\begin{aligned}-\frac{d^2}{dx^2}\varphi^j_{\mathcal{D},\mathcal{N}}(x,k)+q_j(x)\varphi^j_{\mathcal{D},\mathcal{N}}(x,k)&=k^2\varphi^j_{\mathcal{D},\mathcal{N}}(x,k), \qquad x\in(-\infty,l_j),\\ \varphi^j_{\mathcal{D}}(l_j,k)&=0, \qquad (\varphi^j)'_{\mathcal{D}}(l_j,k)=1,\\ \varphi^j_{\mathcal{N}}(l_j,k)&=1, \qquad (\varphi^j)'_{\mathcal{N}}(l_j,k)=0.\end{aligned}$$

Consider, now, the function

$$\Psi_{\mathcal{D},\mathcal{N}}(x,k)=\otimes_{j=0}^{N}\Psi^j_{\mathcal{D},\mathcal{N}}(x,k),$$

where

$$\begin{aligned}\Psi^0_{\mathcal{D},\mathcal{N}}(x,k) &= e^{+\imath kx}+r_{\mathcal{D},\mathcal{N}}(k)e^{-\imath kx}, && x\in(-\infty,0],\\ \Psi^j_{\mathcal{D},\mathcal{N}}(x,k) &= \alpha^j_{\mathcal{D},\mathcal{N}}(k)\varphi^j_{\mathcal{D},\mathcal{N}}(x,k), && x\in[0,l_j],\quad j=1,\cdots,N.\end{aligned}$$

Here the coefficients $r_{\mathcal{D},\mathcal{N}}$ and $\alpha^j_{\mathcal{D},\mathcal{N}}$ are given by the boundary conditions (3.7) at the central node:

$$r_{\mathcal{D},\mathcal{N}}(k)+1=\alpha^j_{\mathcal{D},\mathcal{N}}(k)\varphi^j_{\mathcal{D},\mathcal{N}}(0,k), \qquad j=1,\cdots,N, \tag{3.9}$$

$$\sum_{j=1}^{N}\alpha^j_{\mathcal{D},\mathcal{N}}(k)(\varphi^j_{\mathcal{D},\mathcal{N}})'(0,k)+\imath k(1-r_{\mathcal{D},\mathcal{N}}(k))=H(r_{\mathcal{D},\mathcal{N}}(k)+1). \tag{3.10}$$

One sees that this $\Psi_{\mathcal{D},\mathcal{N}}$ is in $D(\mathcal{L}^+_{\mathcal{N},\mathcal{D}})$, the domain of the operator, and satisfies the conditions of the proposition. This, trivially, provides the existence of a scattering solution. Here, we show that $\Psi_{\mathcal{D},\mathcal{N}}$ is actually the unique one.
Assume that there exists another $Y_{\mathcal{D},\mathcal{N}} = \otimes_{j=0}^{N} Y^j_{\mathcal{D},\mathcal{N}}(x,k)$ solution of the scattering problem. Since $Y^j_{\mathcal{D},\mathcal{N}}(\cdot,k)$ and $\Psi^j_{\mathcal{D},\mathcal{N}}(\cdot,k)$ are solutions of the same Sturm-Liouville equation over each branch and they (or their derivatives for Neumann case) vanish at l_j, $Y^j_{\mathcal{D},\mathcal{N}}(.,k)$ and $\Psi^j_{\mathcal{D},\mathcal{N}}(.,k)$ are co-linear:

$$Y^j_{\mathcal{D},\mathcal{N}}(x,k) = \beta^j_{\mathcal{D},\mathcal{N}}(k)\varphi^j_{\mathcal{D},\mathcal{N}}(x,k), \qquad x \in [0,l_j], \quad j = 1,\cdots,N.$$

Over the branch e_0, as $Y^0_{\mathcal{D},\mathcal{N}}(.,k)$ satisfies a homogeneous Sturm-Liouville equation ($q_0 = 0$), it necessarily admits the following form

$$Y^0_{\mathcal{D},\mathcal{N}}(x,k) = e^{+\imath kx} + r'_{\mathcal{D},\mathcal{N}}(k)e^{-\imath kx}.$$

We need to show that one necessarily has $r'_{\mathcal{D},\mathcal{N}}(k) \equiv r_{\mathcal{D},\mathcal{N}}(k)$ and similarly $\beta^j_{\mathcal{D},\mathcal{N}}(k) \equiv \alpha^j_{\mathcal{D},\mathcal{N}}(k)$. Indeed, for almost all $k \in \mathbb{R}$, the equations (3.9) and (3.10) provide $N+1$ linear relations for the $N+1$ unknown coefficients $r_{\mathcal{D},\mathcal{N}}$ and $\left(\alpha^j_{\mathcal{D},\mathcal{N}}\right)_{j=1}^N$. Trivially, as soon as, the coefficients $\left(\varphi^j_{\mathcal{D},\mathcal{N}}(0,k)\right)_{j=1}^N$ are non-zero, these linear relations are independent and there exists a unique solution for the unknowns $r_{\mathcal{D},\mathcal{N}}$ and $\left(\alpha^j_{\mathcal{D},\mathcal{N}}\right)_{j=1}^N$. However, the zeros of each one of the coefficients $\left(\varphi^j_{\mathcal{D},\mathcal{N}}(0,k)\right)_{j=1}^N$ correspond to isolated values of k (square-root of the eigenvalues of the operator $-\frac{d^2}{dx^2} + q_j(x)$ with Dirichlet boundary condition at $x = 0$ and Dirichlet or Neumann boundary condition at $x = l_j$).

We can compute explicitly these coefficients for all k except for a set $\mathcal{K}$ of isolated values: dividing (3.10) by $(1 + r_{\mathcal{D},\mathcal{N}}(k))$ and inserting (3.9), we find

$$\frac{1 - r_{\mathcal{D},\mathcal{N}}(k)}{1 + r_{\mathcal{D},\mathcal{N}}(k)} = \frac{H}{\imath k} - \frac{1}{\imath k}\sum_{j=1}^{N} \frac{(\varphi^j_{\mathcal{D},\mathcal{N}})'(0,k)}{\varphi^j_{\mathcal{D},\mathcal{N}}(0,k)} \qquad \forall k \in \mathbb{R}\backslash\mathcal{K}. \tag{3.11}$$

Finally, inserting the value of $r_{\mathcal{D},\mathcal{N}}(k)$ into (3.9), we find

$$\alpha^j_{\mathcal{D},\mathcal{N}}(k) = \frac{r_{\mathcal{D},\mathcal{N}}(k) + 1}{\varphi^j_{\mathcal{D},\mathcal{N}}(0,k)} \qquad \forall k \in \mathbb{R}\backslash\mathcal{K}.$$

What remains to be shown is the extendibility of reflection coefficient $r_{\mathcal{D},\mathcal{N}}(k)$ to

whole real axis. Let $\overline{k} \in \mathcal{K}$ be one of the isolated values where $r_{\mathcal{D},\mathcal{N}}$ is not defined: $\varphi^j_{\mathcal{N},\mathcal{D}}(0,\overline{k}) = 0$ for some j. Then we have to show the continuity of $r_{\mathcal{D},\mathcal{N}}(k)$ at $\overline{k}$, i.e.

$$\lim_{k\to\overline{k}^+} r_{\mathcal{D},\mathcal{N}}(k) = \lim_{k\to\overline{k}^-} r_{\mathcal{D},\mathcal{N}}(k) =: r_{\mathcal{D},\mathcal{N}}(\overline{k}),$$

with $|r_{\mathcal{D},\mathcal{N}}(\overline{k})| < \infty$ (even more $|r_{\mathcal{D},\mathcal{N}}(\overline{k})| = 1$ here).

Indeed, through (3.11), and by the fact that fundamental solutions are analytic with respect to k, the reflection coefficient $r_{\mathcal{D},\mathcal{N}}(k)$ can be written as a fraction of two analytic functions, at least for k's where it is well defined. Furthermore, for these k's we have $|r_{\mathcal{D},\mathcal{N}}(k)| = 1$. These two facts, together, ensure the existence of the limit when $k \to \overline{k}$ and that $|r_{\mathcal{D},\mathcal{N}}(\overline{k})| = 1$. □

3.3 Inverse problems and main results

As a first inverse problem, we consider the inversion of the geometry of the graph. In fact, we will prove the well-posedness of the inverse problem of finding the number of branches N and the lengths $(l_j)_{j=1}^N$ of a star-shaped graph through only one reflection coefficient $r_{\mathcal{N}}(k)$ (the case of Dirichlet reflection coefficient can be treated similarly).

Theorem 3. *Consider a star-shaped network Γ composed of n_j branches of length l_j $(j = 1, \cdots, m)$ all joining at a central node so that the whole number of branches N is given by $\sum_{j=1}^m n_j$. Let assume for the potential q on the network to be $C^0(\Gamma)$ and that it takes the value zero at the central node. Then the knowledge of the Neumann reflection coefficient $r_{\mathcal{N}}(k)$ determines uniquely the parameters $(n_j)_{j=1}^m$ and $(l_j)_{j=1}^m$.*

The problem of identifying the geometry of a graph through the knowledge of the reflection coefficient has been previously considered by many authors: in Section 3.4 we resume the literature about this identification problem and we will give the proof of this theorem.

A second inverse problem can be formulated as the identification of the potentials on the branches. The following theorem provides a global uniqueness result concerning the quantities $\overline{q}_j := \int_0^{l_j} q_j(s)ds$ or in terms of line parameters

$$\int_0^{l_j} \left[\frac{C_j(x)}{L_j(x)}\right]^{-\frac{1}{4}} \frac{d^2}{d^2x} \left[\frac{C_j(x)}{L_j(x)}\right]^{+\frac{1}{4}} dx.$$

The moment $\int_0^{l_j} q_j(s)ds$ can also be written as

$$\int_0^{l_j} q_j(s)ds = \frac{1}{4}\int_0^{l_j} \frac{\left|(Z_c^j)'(s)\right|^2}{\left|Z_c^j(s)\right|^2}ds - \frac{1}{2}\left(\frac{(Z_c^j)'(l_j)}{Z_c^j(l_j)} - \frac{(Z_c^j)'(0)}{Z_c^j(0)}\right), \tag{3.12}$$

where Z_c^j denotes the characteristic impedance over the branch j.

Theorem 4. *Assume for the star-shaped graph Γ that*

B1 *$l_j \neq l_{j'}$ for any $j, j' \in \{1, \cdots, N\}$ such that $j \neq j'$.*

If there exist two potentials $q = \otimes_{j=1}^N q_j$ and $q' = \otimes_{j=1}^N q'_j$ in $H^1(\Gamma)$, satisfying $q_j(0) = q'_j(0) = 0$, and giving rise to the same reflection coefficient, $r_{\mathcal{N}}(k) \equiv r'_{\mathcal{N}}(k)$, one necessarily has

$$\int_0^{l_j} q_j(s)ds = \int_0^{l_j} q'_j(s)ds \qquad j = 1, \cdots, N.$$

This theorem allows us to identify the situations where the soft faults in the network cause a change of the quantities $\overline{q}_j$. In particular, it allows us to identify the branches on which these faults have happened. A next test, by analyzing these branches separately, will then allow the engineer to identify more precisely the faults. A proof of this theorem will be provided in Section 3.6.

Remark 25. In the case where the connectors are assumed to be reliables, the characteristic impedances in the neighborhoods of these connectors can be assumed to be uniform. Therefore

$$(Z_c^j)'(l_j) = (Z_c^j)'(0) = 0 \qquad \forall j.$$

This, together with (3.12) implies that we have identified

$$\int_0^{l_j} \frac{\left|(Z_c^j)'(s)\right|^2}{\left|Z_c^j(s)\right|^2}ds$$

over each branch.

Now, note that in the perfect (no fault) case, the lines are uniform and therefore $(Z_c^j)' \equiv 0$ for all j. Thus by identifying the value $\int_0^{l_j} q_j ds$ and as soon as we observe this to be different from 0, we detect soft faults that appear as hetereogenities of the corresponding branch,

Next, we will consider the situations where the faults in the network, do not affect the quantities $\bar{q}_j$. Keeping in mind the application to the transmission line network, this means that:

A5 $\bar{q}_j = \int_0^{l_j} q_j(s)ds = 0$ for $j = 1, \cdots, N$;

as for the perfect setting, we had assumed uniform transmission lines: L and C constant.

In order to provide a well-posedness result for such situations, we need more restrictive assumptions on the geometry of the graph:

B2 For any $j, j' \in \{1, \cdots, N\}$ such that $j \neq j'$, $l_j/l_{j'}$ is an algebraic irrational number.

Under this assumption, the value

$$M(\Gamma) := \max\left\{ m \in \mathbb{N} \quad \middle| \quad \left|\frac{l_i}{l_j} - \frac{1}{m}\right| < \frac{1}{m^3}, \quad \textit{for some } i \neq j \right\} \tag{3.13}$$

is well defined and is finite. In fact, by Thue-Siegel-Roth Theorem [56], for any irrational algebraic number α, and for any $\delta > 0$, the inequality

$$|\alpha - p/q| < 1/|q|^{2+\delta}, \tag{3.14}$$

has only a finite number of integer solutions p, q $(q \neq 0)$.
Before stating the final theorem, we give a lemma on the asymptotic behavior of the eigenvalues of the Sturm-Liouville operator $-\frac{\partial^2}{\partial x^2} + q(x)$ on the segment $[0, l]$, with Dirichlet boundary condition at 0 and Neumann boundary condition at l (the case of Dirichlet-Dirichlet boundary condition can be treated similarly). This lemma allows us to define a constant $C_0(l)$ which will be used in the statement of the final theorem.

Lemma 3. *Assume for the potential $q(x) \in H^1(0, l)$ that $q(0) = 0$, that $\|q\|_{L^\infty(0,l)} < \frac{\pi^2}{4l^2}$ and that $\int_0^l q(s)ds = 0$. Then, there exists a constant $C_0(l)$ such that λ_n, the n-th eigenvalue of the operator $-\frac{\partial^2}{\partial x^2} + q(x)$ on the segment $[0, l]$, with Dirichlet boundary condition at 0 and Neumann boundary condition at l, satisfies*

$$\left|\lambda_n - \frac{(2n-1)^2\pi^2}{4l^2}\right| \leq C_0(l)\frac{\|q\|_{H^1(0,l)}}{2n-1}.$$

A proof of this lemma, based on the perturbation theory of linear operators [32], will be given in the Appendix B.

In order to state the final theorem, we define the following constants only depending on the geometry of the graph Γ (lengths of branches):

$$C_1(\Gamma) := \min\left\{ \frac{\pi^2}{4l_j^{5/2}} \quad \middle| \quad j = 1, \dots, N \right\}, \tag{3.15}$$

$$C_2(\Gamma) := \min\left\{ \frac{\pi^2}{4l_i l_j (C_0(l_i) + C_0(l_j))} \quad \middle| \quad i \neq j, \quad i, j = 1, \dots, N \right\}, \tag{3.16}$$

$$C_3(\Gamma) := \min\Big\{ \frac{\pi^2}{C_0(l_i) + C_0(l_j)} \cdot \left| \frac{(2n-1)^2}{l_j^2} - \frac{(2n'-1)^2}{l_i^2} \right| \Big| \begin{array}{l} n = 1, 2 \dots, M(\Gamma), \\ n' = 1, 2, \dots, \\ i \neq j \quad i, j = 1, \dots, N \end{array} \Big\}, \tag{3.17}$$

$$C(\Gamma) := \min(C_1(\Gamma), C_2(\Gamma), C_3(\Gamma)). \tag{3.18}$$

Note, in particular that $C_3(\Gamma)$ is strictly positive as the lengths l_i and l_j are two-by-two $\mathbb{Q}$-independent. We have the following theorem:

Theorem 5. *Consider a star-shaped graph Γ satisfying the geometrical assumption **B2**. Take the strictly positive constant $C(\Gamma)$ as defined by (3.18) and consider two potentials q and q' belonging to $H^1(\Gamma)$, satisfying $q_j(0) = q_j'(0) = 0$, the assumption **A5**, and*

$$\|q\|_{H^1(\Gamma)} < C(\Gamma) \quad \text{and} \quad \|q'\|_{H^1(\Gamma)} < C(\Gamma).$$

If they give rise to the same Neumann and Dirichlet reflection coefficients:

$$r_{\mathcal{N}}(k) \equiv r'_{\mathcal{N}}(k) \qquad \text{and} \qquad r_{\mathcal{D}}(k) \equiv r'_{\mathcal{D}}(k),$$

then $q \equiv q'$.

A proof of this theorem will be given in Section 3.7. We end this section by a remark on the assumption **B2**.

Remark 26. The assumption **B2** seems rather restrictive and limits the applicability of Theorem 5 in real settings. In fact, such kind of assumptions have been previously considered in the literature for the exact controllability of the wave equations on net-

works [72]. In general, removing this kind of assumptions, one can ensure approximate controllability results rather than the exact controllability ones. Theorem 5 can be seen in the same vein as providing a first exact identifiability result. However, in order to make it applicable to real settings one needs to consider improvements by relaxing the assumption **B2** and looking instead for approximate identifiability results. This will be considered in future work.

Finally, we note that the only place, where we need the assumption **B2**, is to ensure that there exists at most a finite number of co-prime factors $(p, q) \in \mathbb{N} \times \mathbb{N}$, such that the Diophantine approximation (3.14) holds true. However, this is a classical result of the Borel-Cantelli Lemma that for almost all (with respect to Lebesgue measure) positive real α's this Diophantine approximation has finite number of solutions. Therefore the assumption **B2** can be replaced by the weaker assumption of $l_j/l_{j'}$ belonging to this set of full measure.

3.4 Detection and localization of hard faults

Thanks to Theorem 3, we will be able to detect and to locate hards faults like the open circuits and short circuits. The analysis of the reflection coefficient at high frequencies allows us to locate the positions of hard faults.

This inverse problem can be formulated as the identification of the lengths of the network Γ where the extremities represent the hard faults. The knowledge of one reflection coefficient allows to identify the number of the branches and their lengths,

The problem of identifying the geometry of a graph through the knowledge of the reflection coefficient has been previously considered in [27, 36, 2]. Through the two first papers, the authors consider a more general context of any graph and not only a star-shaped one. However, in order to ensure a well-posedness result, they need to assume a strong assumption on the lengths consisting in their $\mathbb{Q}$-independence. The third result [2] states a very similar result to that of Theorem 3 for time domain reflectometry (see Lemma 2 of [2]). The authors also provide a frequency-domain version of their result (see Lemma 3 of [2]); however their proof is strongly based on the proof of the time-domain result. We believe that the proof provided in this thesis, exploring the high-frequency regime of the reflection coefficient and providing a frequency-based constructive method, can be useful from an engineering point of view, where we are interested in detecting the faults without stopping the normal activity of

the transmission network (we therefore need to apply test frequencies that are much higher than the activity frequencies of the transmission network).

The method is rather constructive and one can think of an algorithm to identify the lengths, at least approximately. The proof is based on an asymptotic analysis in high-frequency regime of the reflection coefficient and some classical results from the theory of almost periodic functions (in Bohr sense).
Before proving Theorem 3, we need the following lemma:

Lemma 4. *Consider a star-shaped network Γ composed of n_j branches of length l_j for $j = 1, \cdots, m$ all joining at a central node so that the whole number of branches N is given by $\sum_{j=1}^{m} n_j$. Assume the potential q on the network to be 0 ($q \equiv 0$). Then the knowledge of the Neumann reflection coefficient $R_{\mathcal{N}}(k)$ determines uniquely the parameters $(n_j)_{j=1}^m$ and $(l_j)_{j=1}^m$.*

Proof. We need to apply the explicit computation of the reflection coefficient provided by (3.11). The fundamental solutions are given, simply, by $\varphi_{\mathcal{N}}^j(x,k) = \cos(k(l_j - x))$. Therefore:

$$\frac{r_{\mathcal{N}}(k) - 1}{r_{\mathcal{N}}(k) + 1} = \frac{1}{\imath k} H - \frac{1}{\imath k} \sum_{j=1}^{m} n_j \frac{k \sin(l_j k)}{\cos(l_j k)}.$$

The knowledge of $r_{\mathcal{N}}(k)$ determines uniquely the signal:

$$f(k) := \sum_{j=1}^{m} n_j \tan(k l_j).$$

Assuming, without loss of generality, that the lengths l_j are ordered increasingly $l_1 < \cdots < l_m$, the first pole of the function $f(k)$ coincides with $\pi/2l_m$ and therefore determines l_m. Furthermore,

$$n_m = \lim_{k \to \pi/2l_m} \cos(k l_m) f(k),$$

and therefore one can also determine n_m. Now, considering the new signal $g(k) = f(k) - n_m \tan(k l_m)$, one removes the branches of length l_m and exactly in the same manner, one can determine l_{m-1} and n_{m-1}. The proof of the lemma follows then by a simple induction. □

Now we are able to prove the main theorem.

Proof of Theorem 3. Assume that, there exist two graph settings $(l_j, q_j)_{j=1}^N$ and $(l'_j, q'_j)_{j=1}^{N'}$ (the lengths l_j are not necessarily different) giving rise to the same Neumann reflection coefficients: $r_{\mathcal{N}}(k) \equiv r'_{\mathcal{N}}(k)$. By the explicit formula (3.11), we have

$$\frac{1}{k}\sum_{j=1}^{N}\frac{\frac{d}{dx}(\varphi^j_{\mathcal{N}})(0,k)}{\varphi^j_{\mathcal{N}}(0,k)} \equiv \frac{1}{k}\sum_{i=1}^{N'}\frac{\frac{d}{dx}(\varphi'^i_{\mathcal{N}})(0,k)}{\varphi'^i_{\mathcal{N}}(0,k)}.$$

This is equivalent to:

$$\prod_{j=1}^{N'}\varphi'^j_{\mathcal{N}}(0,k)\left(\sum_{i=1}^{N}\frac{d}{dx}(\varphi^i_{\mathcal{N}})(0,k)\prod_{l\neq i}\varphi^l_{\mathcal{N}}(0,k)\right) - \prod_{j=1}^{N}\varphi^j_{\mathcal{N}}(0,k)\left(\sum_{i=1}^{N'}\frac{d}{dx}(\varphi'^i_{\mathcal{N}})(0,k)\prod_{l\neq i}\varphi'^l_{\mathcal{N}}(0,k)\right) = 0. \quad (3.19)$$

Now, we use the fact that the high-frequency behavior of the Neumann fundamental solutions $(\varphi^j_{\mathcal{N}})_{j=1}^N$ is given as follows (see [19], page 4):

$$\begin{array}{rcll} \varphi^j_{\mathcal{N}}(0,k) & = & \cos(kl_j) + \mathcal{O}\left(\frac{1}{k}\right), & \text{as } k\to\infty, \\ \frac{d}{dx}(\varphi^j_{\mathcal{N}})(0,k) & = & k\sin(kl_j) + \mathcal{O}(1), & \text{as } k\to\infty, \end{array} \quad (3.20)$$

Defining the function:

$$F(k) := \prod_{j=1}^{N'}\cos(kl'_k)\left(\sum_{i=1}^{N}\sin(kl_i)\prod_{l\neq i}\cos(kl_l)\right) - \prod_{j=1}^{N}\cos(kl_j)\left(\sum_{i=1}^{N'}\sin(kl'_i)\prod_{l\neq i}\cos(kl'_l)\right).$$

The asymptotic formulas (3.20) together with (3.19) imply

$$F(k) = \mathcal{O}(1/k) \qquad \text{as } k\to\infty.$$

However, the function $F(k)$ is a trigonometric polynomial and almost periodic in the Bohr's sense [9]. The function $F^2(k)$ is, also, almost periodic and furthermore, we have

$$\begin{aligned} M(F^2) := \lim_{k\to\infty}\frac{1}{k}\int_0^k F^2(k)dk &= \lim_{k\to\infty}\frac{1}{k}\left(\int_0^1 F^2(k)dk + \int_1^k F^2(k)dk\right) \\ &\leq \lim_{k\to\infty}\frac{1}{k}\left(C_1 + C_2\int_1^k\frac{1}{k^2}dk\right) = 0. \end{aligned}$$

This, trivially, implies that $F = 0$ (one only needs to apply the Parseval's Theorem to the generalized fourier series of the function F). However, the relation $F(k) \equiv 0$ is equivalent to

$$\sum_{j=1}^{N} \tan(kl_j) = \sum_{j=1}^{\hat{N}} \tan(kl'_j),$$

and therefore, by Lemma 4, the two settings are equivalent and the theorem follows. □

3.5 From inverse scattering to inverse spectral problem

Here we present some auxiliary propositions that we will need for the proof of Theorems 4 and 5. The main objective of this subsection is to show the equivalence between the inverse scattering problem on Γ^+ and some inverse spectral problem on Γ.
So, as before, we consider a general star-shaped graph Γ (of N finite branches) and a potential $q = \otimes_{j=1}^{N} q_j$ belonging to $H^1(\Gamma)$. We will see that the knowledge of the reflection coefficient $r_{\mathcal{N}}(k)$ for $\mathcal{L}^+_{\mathcal{N}}$ (resp. $r_{\mathcal{D}}(k)$ for $\mathcal{L}^+_{\mathcal{D}}$) is equivalent to the knowledge of different positive spectra of Sturm-Liouville operators defined on Γ with Neumann (resp. Dirichlet) boundary conditions at terminal nodes and for various boundary conditions at the central node. In fact, defining the function

$$h_{\mathcal{N},\mathcal{D}}(k) = H + \frac{ik(1 - r_{\mathcal{N},\mathcal{D}}(k))}{(1 + r_{\mathcal{N},\mathcal{D}}(k))},$$

where H is given by (3.7), we have the following result

Proposition 4. *Fix $k \in \mathbb{R}$ and define the Schrödinger operators $\mathcal{L}_{\mathcal{N},\mathcal{D}}(k)$ on the compact graph Γ as follows:*

$$\mathcal{L}_{\mathcal{N},\mathcal{D}}(k) = \otimes_{j=1}^{N}(-\frac{d^2}{dx^2} + q_j(x)),$$
$$D(\mathcal{L}_{\mathcal{N},\mathcal{D}}(k)) = \textit{closure of } C^{\infty}_{k;\mathcal{N},\mathcal{D}}(\Gamma) \textit{ in } H^2(\Gamma),$$

where $C^{\infty}_{k;\mathcal{N}}(\Gamma)$ (resp. $C^{\infty}_{k;\mathcal{D}}(\Gamma)$) denotes the space of infinitely differentiable functions

$f = \otimes_{j=1}^{N} f_j$ *defined on* Γ *satisfying the boundary conditions*

$$\begin{aligned} f_j(0) = f_{j'}(0) =: \bar{f} \qquad & j, j' = 1, \cdots, N, \\ \sum_{j=1}^{N} f_j'(0) = h_{\mathcal{N},\mathcal{D}}(k)\bar{f}, & \\ f_j'(l_j) = 0 \quad (f_j(l_j) = 0 \text{ for } C^{\infty}_{k;\mathcal{D}}(\Gamma)), \qquad & j = 1, \cdots, N. \end{aligned}$$

Then we are able to characterize the positive spectrum of $\mathcal{L}_{\mathcal{N},\mathcal{D}}(k)$ *as a level set of the function* $h_{\mathcal{N},\mathcal{D}}(k)$*:*

$$\sigma^+(\mathcal{L}_{\mathcal{N},\mathcal{D}}(k)) = \left\{\xi^2 \mid \xi \in \mathbb{R},\ h_{\mathcal{N},\mathcal{D}}(\xi) = h_{\mathcal{N},\mathcal{D}}(k)\right\}.$$

Remark 27. As it can be seen through the proof, the above proposition holds for the generic case of any compact graph, where a test branch of infinite length is added to an arbitrary node of the graph.

Proof. We prove the proposition for the case of Neumann boundary conditions. The Dirichlet case can be treated exactly in the same manner. We start by proving the inclusion

$$\sigma^+(\mathcal{L}_{\mathcal{N}}(k)) \subseteq \left\{\xi^2 \mid \xi \in \mathbb{R},\ h_{\mathcal{N}}(\xi) = h_{\mathcal{N}}(k)\right\}.$$

Let $\xi^2 \in \sigma^+(\mathcal{L}_{\mathcal{N}}(k))$, then there exists Ψ eigenfunction of the operator $\mathcal{L}_{\mathcal{N}}(k)$ associated to ξ^2. In particular, it satisfies

$$\sum_{j=1}^{N} \Psi_j'(0) = h_{\mathcal{N}}(k)\bar{\Psi},$$

where $\bar{\Psi}$ is the common value of Ψ at the central node.

Now we extend Ψ to the extended graph Γ^+, such that Ψ^+ is a scattering solution for $\mathcal{L}_{\mathcal{N}}^+$ (see Proposition 3). In particular, the function Ψ^+ must satisfy, at the central node,

$$\begin{aligned} \Psi_j^+(0) = \Psi_0^+(0), \qquad & j = 1, \cdots, N, \\ \sum_{j=1}^{N} (\Psi_j^+)'(0) - (\Psi_0^+)'(0) = H\Psi_0^+(0). & \end{aligned}$$

Noting that Ψ is an eigenfunction of $(\mathcal{L}_{\mathcal{N}}(k), D(\mathcal{L}_{\mathcal{N}}(k))$, we have

$$h_{\mathcal{N}}(k)\Psi_0^+(0) - (\Psi_0^+)'(0) = \sum_{j=1}^{N}(\Psi_j^+)'(0) - (\Psi_0^+)'(0) = H\Psi_0^+(0). \tag{3.21}$$

Now, noting that Ψ^+ over the infinite branch admits the following form

$$\Psi_0^+(x) = r_{\mathcal{N}}(\xi)e^{-\imath\xi x} + e^{+\imath\xi x} \qquad x \in (-\infty, 0],$$

the relation (3.21) yields to

$$h_{\mathcal{N}}(k)(r_{\mathcal{N}}(\xi)+1) - \imath\xi(1 - r_{\mathcal{N}}(\xi)) = H(r_{\mathcal{N}}(\xi)+1),$$

or equivalently

$$h_{\mathcal{N}}(k) = H + \frac{\imath\xi(1 - r_{\mathcal{N}}(\xi))}{(r_{\mathcal{N}}(\xi)+1)} = h_{\mathcal{N}}(\xi).$$

This proves the first inclusion. Now, we prove that

$$\sigma^+(\mathcal{L}_{\mathcal{N}}(k)) \supseteq \left\{\xi^2 \mid \xi \in \mathbb{R},\ h_{\mathcal{N}}(\xi) = h_{\mathcal{N}}(k)\right\}.$$

Let $\xi \in \mathbb{R}$ be such that $h_{\mathcal{N}}(\xi) = h_{\mathcal{N}}(k)$. We consider a scattering solution Ψ^+ of the extended operator $\mathcal{L}_{\mathcal{N}}^+$ (defined by (3.6)) associated to the frequency ξ^2. We, then, prove that the restriction of Ψ^+ to the compact graph Γ is an eigenfunction of $\mathcal{L}_{\mathcal{N}}(k)$ associated to the eigenvalue ξ^2. This trivially implies that $\xi^2 \in \sigma^+(\mathcal{L}_{\mathcal{N}}(k))$.

In this aim, we only need to show that this restriction of Ψ^+ to Γ is in the domain $D(\mathcal{L}_{\mathcal{N}}(k))$. Indeed, this is equivalent to proving that the boundary condition:

$$\sum_{j=1}^{N}(\Psi_j^+)'(0) = h(k)\Psi_0^+(0), \tag{3.22}$$

is satisfied. As Ψ^+ is a scattering solution of $\mathcal{L}_{\mathcal{N}}^+$, it satisfies

$$\sum_{j=1}^{N}(\Psi_j^+)'(0) = H\Psi_0^+(0) + (\Psi_0^+)'(0) = \left(H + \frac{(\Psi_0^+)'(0)}{\Psi_0^+(0)}\right)\Psi_0^+(0).$$

Furthermore,

$$\Psi_0^+(0) = r_{\mathcal{N}}(\xi) + 1 \qquad \text{and} \qquad (\Psi_0^+)'(0) = \imath\xi(1 - r_{\mathcal{N}}(\xi)),$$

and so

$$\sum_{j=1}^{N}(\Psi_j^+)'(0) = \left(H + \frac{\imath\xi(1 - r_{\mathcal{N}}(\xi))}{r_{\mathcal{N}}(\xi) + 1}\right)\Psi_0^+(0) = h(\xi)\Psi_0^+(0) = h(k)\Psi_0^+(0).$$

This proves (3.22) and finishes the proof of the proposition. □

The following proposition provides the characteristic equation permitting to identify the eigenvalues of the operator $\mathcal{L}_{\mathcal{N},\mathcal{D}}(k)$:

Proposition 5. *The real $\lambda^2 > 0$ is an eigenvalue of the operator $\mathcal{L}_{\mathcal{N},\mathcal{D}}(k)$ if and only if*

$$\Psi_{\mathcal{N},\mathcal{D}}(\lambda) = h_{\mathcal{N},\mathcal{D}}(k)\Phi_{\mathcal{N},\mathcal{D}}(\lambda),$$

where

$$\Phi_{\mathcal{N},\mathcal{D}}(\lambda) := \prod_{j=1}^{N}\varphi_{\mathcal{N},\mathcal{D}}^j(0,\lambda) \quad \textit{and} \quad \Psi_{\mathcal{N},\mathcal{D}}(\lambda) := \frac{d}{dx}\left(\prod_{j=1}^{N}\varphi_{\mathcal{N},\mathcal{D}}^j(x,\lambda)\right)\Big|_{x=0}, \tag{3.23}$$

$\varphi_{\mathcal{N},\mathcal{D}}^j(x,\lambda)$ being the fundamental solutions on different branches.

Proof. We give the proof for the Neumann boundary conditions, noting that the Dirichlet case can be treated, exactly, in the same manner. Assume λ^2 to be a positive eigenvalue of $\mathcal{L}_{\mathcal{N}}(k)$. The associated eigenfunction, $y_\lambda(x) = \otimes_{j=1}^{N} y_\lambda^j(x)$, has necessarily the following form:

$$y_\lambda^j(x) = \alpha_j\varphi_{\mathcal{N}}^j(x,\lambda),$$

where α_j's are real constants and the vector $(\alpha_1, \cdots, \alpha_N)$ is different from zero. The function y_λ, being in the domain $D(\mathcal{L}_{\mathcal{N}}(k))$, it should satisfy the associated boundary condition at the central node. This implies that the vector $(\alpha_1, \cdots, \alpha_N)$ is in the

kernel of the matrix:

$$M := \begin{pmatrix} \varphi^1_{\mathcal{N}}(0,\lambda) & -\varphi^2_{\mathcal{N}}(0,\lambda) & 0 & \cdots & 0 \\ 0 & \varphi^2_{\mathcal{N}}(0,\lambda) & -\varphi^3_{\mathcal{N}}(0,\lambda) & \cdots & 0 \\ 0 & 0 & \varphi^3_{\mathcal{N}}(0,\lambda) & \cdots & 0 \\ \cdots & \cdots & \cdots & \cdots & \cdots \\ -h_{\mathcal{N}}(k)\varphi^1_{\mathcal{N}}(0,\lambda) + \psi^1_{\mathcal{N}}(0,\lambda) & \psi^2_{\mathcal{N}}(0,\lambda) & \psi^3_{\mathcal{N}}(0,\lambda) & \dots & \psi^N_{\mathcal{N}}(0,\lambda) \end{pmatrix}$$

where $\psi^j_{\mathcal{N}}(0,\lambda)$ denotes $\frac{d}{dx}\varphi^j_{\mathcal{N}}(x,\lambda)|_{x=0}$. This means that the determinant $\det(M)$ is necessarily 0. Developing this determinant we find:

$$\Psi_{\mathcal{N}}(\lambda) = h_{\mathcal{N}}(k)\Phi_{\mathcal{N}}(\lambda).$$

□

Corollary 2. Consider two potentials $q = \otimes_{j=1}^N q_j$ and $q' = \otimes_{j=1}^N q'_j$ and denote by $\mathcal{L}^+_{\mathcal{N}}$ and $(\mathcal{L}')^+_{\mathcal{N}}$, the associated Neumann Schrödinger operators defined on the extended graph Γ^+. Assuming that the reflection coefficients $r_{\mathcal{N}}(k)$ and $r'_{\mathcal{N}}(k)$ are equivalent $r_{\mathcal{N}}(k) \equiv r'_{\mathcal{N}}(k)$, we have

$$\Phi_{\mathcal{N}}(k)\Psi'_{\mathcal{N}}(k) = \Phi'_{\mathcal{N}}(k)\Psi_{\mathcal{N}}(k), \qquad \forall k \in \mathbb{R}, \tag{3.24}$$

where $\Phi_{\mathcal{N}}$, $\Psi_{\mathcal{N}}$, $\Phi'_{\mathcal{N}}$ and $\Psi'_{\mathcal{N}}$ are defined through 3.23 for the potentials q and q'.

Proof. By Proposition 4, k^2 is an eigenvalue of the operators $\mathcal{L}_{\mathcal{N}}(k)$ and $\mathcal{L}'_{\mathcal{N}}(k)$. Applying the Proposition 5, this means that

$$\Psi_{\mathcal{N}}(k) = h_{\mathcal{N}}(k)\Phi_{\mathcal{N}}(k) \qquad \text{and} \qquad \Psi'_{\mathcal{N}}(k) = h'_{\mathcal{N}}(k)\Phi'_{\mathcal{N}}(k).$$

As $r_{\mathcal{N}}(k) \equiv r'_{\mathcal{N}}(k)$, we have $h_{\mathcal{N}}(k) \equiv h'_{\mathcal{N}}(k)$ and thus the above equation yields to (3.24). □

The above corollary is also valid when we replace the Neumann by Dirichlet boundary conditions. Finally, this corollary yields to the following proposition on the difference between the two potentials q and q'.

Proposition 6. *Consider two potentials $q = \otimes_{j=1}^N q_j$ and $q' = \otimes_{j=1}^N q'_j$ and denote by $\mathcal{L}^+_{\mathcal{N}}$ and $(\mathcal{L}')^+_{\mathcal{N}}$, the associated Neumann Schrödinger operators defined on the extended*

graph Γ^+. *Assuming that the reflection coefficients* $r_{\mathcal{N}}(k)$ *and* $r'_{\mathcal{N}}(k)$ *are equivalent* $r_{\mathcal{N}}(k) \equiv r'_{\mathcal{N}}(k)$, *we have*

$$\sum_{j=1}^{N} \prod_{i \neq j} \varphi^i_{\mathcal{N}}(0,k) \varphi'^i_{\mathcal{N}}(0,k) \int_0^{l_j} \tilde{q}_j(x) \varphi^j_{\mathcal{N}}(x,k) \varphi'^j_{\mathcal{N}}(x,k) dx = 0, \qquad \forall k \in \mathbb{R}, \tag{3.25}$$

where $\tilde{q}_j = q'_j - q_j$.

Proof. For $j = 1, \cdots, N$, we have:

$$\begin{aligned} \int_0^{l_j} q'_j(x) \quad & \varphi'^j_{\mathcal{N}}(x,k) \varphi^j_{\mathcal{N}}(x,k) dx - \textstyle\int_0^{l_j} q_j(x) \varphi^j_{\mathcal{N}}(x,k) \varphi'^j_{\mathcal{N}}(x,k) dx = \\ & = \varphi^j_{\mathcal{N}}(x,k) \tfrac{d}{dx} \varphi'^j_{\mathcal{N}}(x,k)\big|_{x=0}^{x=l_j} - \tfrac{d}{dx} \varphi^j_{\mathcal{N}}(x,k) \varphi'^j_{\mathcal{N}}(x,k)\big|_{x=0}^{x=l_j} \\ & = \psi^j_{\mathcal{N}}(0,k) \varphi'^j_{\mathcal{N}}(0,k) - \varphi^j_{\mathcal{N}}(0,k) \psi'^j_{\mathcal{N}}(0,k). \end{aligned} \tag{3.26}$$

Here the second line has been obtained from the first one, replacing $q_j(x)\varphi^j_{\mathcal{N}}(x,k)$ by $\frac{d^2}{dx^2}\varphi^j_{\mathcal{N}}(x,k) + k^2 \varphi^j_{\mathcal{N}}(x,k)$ and integrating by parts. Using (3.24) and the above equation, we have:

$$\begin{aligned} \sum_{j=1}^{N} \prod_{i \neq j} \varphi^i_{\mathcal{N}}(0,k) \varphi'^i_{\mathcal{N}}(0,k) \int_0^{l_j} \tilde{q}_j(x) \varphi^j_{\mathcal{N}}(x,k) \varphi'^j_{\mathcal{N}}(x,k) dx = \\ = \Psi_{\mathcal{N}}(k) \Phi'_{\mathcal{N}}(k) - \Phi_{\mathcal{N}}(k) \Psi'_{\mathcal{N}}(k) = 0. \end{aligned}$$

□

Before finishing this subsection, note that, once more, the above proposition is also valid for the case of Dirichlet boundary conditions and $r_{\mathcal{D}}(k) \equiv r'_{\mathcal{D}}(k)$ implies:

$$\sum_{j=1}^{N} \prod_{i \neq j} \varphi^i_{\mathcal{D}}(0,k) \varphi'^i_{\mathcal{D}}(0,k) \int_0^{l_j} \tilde{q}_j(x) \varphi^j_{\mathcal{D}}(x,k) \varphi'^j_{\mathcal{D}}(x,k) dx = 0, \qquad \forall k \in \mathbb{R}. \tag{3.27}$$

We are now ready to prove Theorems 4 and 5.

3.6 Proof of Theorem 4

In this section we prove Theorem 4 applying the characteristic equation (3.25) and high-frequency behavior of $\varphi^j_{\mathcal{N},\mathcal{D}}(x,k)$. Again, for simplicity's sake, we give the proof

only for the case of Neumann boundary conditions, noting that the Dirichlet case can be done similarly.

We know the asymptotic behavior of fundamental solutions $\varphi^j_{\mathcal{N}}(x,k)$

$$\varphi^j_{\mathcal{N}}(x,k) = \cos(k(l_j - x)) + \mathcal{O}\left(\frac{1}{k}\right).$$

In particular the product writes

$$\varphi^j_{\mathcal{N}}(x,k)\varphi'^j_{\mathcal{N}}(x,k) = \cos^2(k(l_j - x)) + \mathcal{O}\left(\frac{1}{k}\right).$$

Applying the characteristic equation (3.25) and developing the products $\varphi^j_{\mathcal{N}}(x,k)$ $\varphi'^j_{\mathcal{N}}(x,k)$, we have:

$$\begin{aligned}
\sum_{j=1}^{N}\left(\prod_{i\neq j}\cos^2(kl_i)\right)\int_0^{l_j}\tilde{q}_j(s)\cos^2(k(l_j-s))ds &= \mathcal{O}\left(\frac{1}{k}\right),\\
\sum_{j=1}^{N}\left(\prod_{i\neq j}\cos^2(kl_i)\right)\int_0^{l_j}\tilde{q}_j(s)\left(\frac{1+\cos 2(k(l_j-s))}{2}\right)ds &= \mathcal{O}\left(\frac{1}{k}\right),\\
\sum_{j=1}^{N}\left(\prod_{i\neq j}\cos^2(kl_i)\right)\frac{1}{2}\int_0^{l_j}\tilde{q}_j(s)ds &= \mathcal{O}\left(\frac{1}{k}\right). \qquad (3.28)
\end{aligned}$$

In the last passage, we applied the fact that $\int_0^{l_j}\tilde{q}_j(s)\cos 2(k(l_j-s))ds = \mathcal{O}(1/k)$, since $\tilde{q}$ is in $H^1(\Gamma)$.
The left side of (3.28) is an almost periodic function with respect to k, in the Bohr's sense. Following the same arguments as those of Theorem 3 we obtain

$$\sum_{j=1}^{N}\left(\prod_{i\neq j}\cos^2(kl_i)\right)\frac{1}{2}\int_0^{l_j}\tilde{q}_j(s)ds = 0 \qquad \forall k\in\mathbb{R}.$$

Assume, without loss of generality, that the lengths are ordered increasingly $l_1 < \ldots < l_N$ and choose $k_N = \pi/2l_N$:

$$\cos(k_N l_j) \neq 0 \qquad \text{for } j \neq N.$$

Indeed, we have

$$\prod_{i\neq N}\cos^2(k_N l_i)\int_0^{l_N}\tilde{q}_N(s)ds=0\Rightarrow\int_0^{l_N}\tilde{q}_N(s)ds=0.$$

Then, the characteristic equation can be rewritten

$$\cos^2(kl_N)\sum_{j=1}^{N-1}\left(\prod_{i\neq j}\cos^2(kl_i)\right)\frac{1}{2}\int_0^{l_j}\tilde{q}_j(s)ds=0,$$

and, since it is a product of two analytic functions w.r.t k, we have

$$\sum_{j=1}^{N-1}\left(\prod_{i\neq j}\cos^2(kl_i)\right)\frac{1}{2}\int_0^{l_j}\tilde{q}_j(s)ds=0\qquad\forall k\in\mathbb{R},$$

and we finish the proof of Theorem 4, repeating the same argument $N-1$ times.

3.7 Proof of Theorem 5

In this section, we consider two potentials $q=\otimes_{j=1}^N q_j$ and $q'=\otimes_{j=1}^N q'_j$, satisfying the assumptions of Theorem 5. Assuming that they give rise to the same Neumann and Dirichlet reflection coefficients, $R_{\mathcal{N}}(k)\equiv r'_{\mathcal{N}}(k)$ and $R_{\mathcal{D}}(k)\equiv r'_{\mathcal{D}}(k)$, we have the characteristic equations (3.25) and (3.27).

Let us define the operators $\mathcal{L}^j_{\mathcal{N},\mathcal{D}}$ to be the operator $-\frac{d^2}{dx^2}+q_j(x)$ over $[0,l_j]$ with the domain

$$D(\mathcal{L}^j_{\mathcal{N},\mathcal{D}})=\text{closure of } C^\infty_{\mathcal{N},\mathcal{D}}(0,l_j) \text{ in } H^2(0,l_j),$$

where $C^\infty_{\mathcal{N}}(0,l_j)$ (resp. $C^\infty_{\mathcal{D}}(0,l_j)$) denotes the space of infinitely differentiable functions f defined on $[0,l_j]$ satisfying Dirichlet boundary condition at 0 and Neumann (resp. Dirichlet) boundary condition at l_j.
Noting that, we have assumed for the potential $q_j(x)$ to satisfy $\|q_j\|_{H^1(0,l_j)}<C(\Gamma)\leq C_1(\Gamma):=\min_{j=1,\dots,N}\frac{\pi^2}{4l_j^{5/2}}$ and that $q_j(0)=0$, we have $\|q_j\|_{L^\infty(0,l_j)}<\frac{\pi^2}{4l_j^2}$ (one has the Sobolev injection $\|q_j\|_{L^\infty(0,l_j)}\leq\sqrt{l_j}\|q_j\|_{H^1(0,l_j)}$). This implies that the eigenvalues of $\mathcal{L}^j_{\mathcal{N}}$ remain positive. In fact, $\frac{\pi^2}{4l_j^2}$ is the minimum eigenvalue of the potential-less Schrödinger operator (with Neumann boundary conditions) and therefore by adding a potential whose L^∞-norm is smaller than this eigenvalue, the eigenvalues of $\mathcal{L}^j_{\mathcal{N}}$ remain

positive.

Considering $((\lambda_n^j)^2)_{n=1}^{\infty}$ ($\lambda_n^j > 0$) the sequence of eigenvalues of $\mathcal{L}_{\mathcal{N}}^j$, (3.25) implies for each $j = 1, \cdots, N$,

$$\prod_{i \neq j} \varphi_{\mathcal{N}}^i(0, \lambda_n^j) \varphi'^i_{\mathcal{N}}(0, \lambda_n^j) \int_0^{l_j} \tilde{q}_j(x) \varphi_{\mathcal{N}}^j(x, \lambda_n^j) \varphi'^j_{\mathcal{N}}(x, \lambda_n^j) dx = 0, \quad \forall n = 1, 2, \cdots \tag{3.29}$$

where we have applied the fact that $\varphi_{\mathcal{N}}^j(0, \lambda_n^j) = 0$.

At this point, we will use the assumption **B2** on the lengths l_j to obtain a lemma on the non-overlapping of the eigenvalues for different branches:

Lemma 5. *Under the assumptions of Theorem 5, for all $j = 1, \cdots, N$,*

$$\prod_{i \neq j} \varphi_{\mathcal{N}}^i(0, \lambda_n^j) \varphi'^i_{\mathcal{N}}(0, \lambda_n^j) \neq 0 \qquad \forall n \in \mathbb{N}.$$

Proof. In order to prove this lemma, we only need to show that $(\lambda_n^j)^2$ is not an eigenvalue of $\mathcal{L}_{\mathcal{N}}^i$ nor $\mathcal{L}'^i_{\mathcal{N}}$ for $i \neq j$.

In this aim, we first show that, if $\|q\|_{H^1}, \|q'\|_{H^1} < C_2(\Gamma)$ and assumption **B2** holds, then there are at most a finite number of overlapping eigenvalues for different branches. Indeed, for $M(\Gamma)$ defined by (3.13), we show that taking $n_1, n_2 > M(\Gamma)$, $\lambda_{n_1}^i$ is different from $\lambda_{n_2}^j$ and $\lambda'^j_{n_2}$ the eigenvalues of $\mathcal{L}_{\mathcal{N}}^j$ and $(\mathcal{L}')_{\mathcal{N}}^j$ ($j \neq i$). Assume, contrarily, that there exist $n_1, n_2 > M(\Gamma)$ and $i \neq j$, such that

$$\lambda_{n_1}^i = \lambda_{n_2}^j \qquad \text{or} \qquad \lambda_{n_1}^i = (\lambda')_{n_2}^j. \tag{3.30}$$

Without loss of generality, we consider the first case. Applying Lemma 3, we have

$$\begin{aligned} \left| \lambda_{n_1}^i - \frac{(2n_1 - 1)^2 \pi^2}{4 l_i^2} \right| &< \frac{C_0(l_i) C_2(\Gamma)}{2n_1 - 1}, \\ \left| \lambda_{n_2}^j - \frac{(2n_2 - 1)^2 \pi^2}{4 l_j^2} \right| &< \frac{C_0(l_j) C_2(\Gamma)}{2n_2 - 1}. \end{aligned} \tag{3.31}$$

Therefore, the relation (3.30) implies that,

$$\left| \frac{(2n_1 - 1)^2 \pi^2}{4 l_i^2} - \frac{(2n_2 - 1)^2 \pi^2}{4 l_j^2} \right| < C_2(\Gamma) \left(\frac{C_0(l_i)}{2n_1 - 1} + \frac{C_0(l_j)}{2n_2 - 1} \right).$$

Taking (without loss of generality) $n_1 \leq n_2$, and dividing the above inequality by

$(2n_1-1)^2\pi^2/4l_j^2$, we have

$$\left|\frac{l_j^2}{l_i^2}-\frac{(2n_2-1)^2}{(2n_1-1)^2}\right|<C_2(\Gamma)\frac{4l_j^2(C_0(l_i)+C_0(l_j))}{\pi^2}\frac{1}{(2n_1+1)^3}.$$

Applying the trivial inequality

$$\left|\frac{l_j^2}{l_i^2}-\frac{(2n_2-1)^2}{(2n_1-1)^2}\right|=\left|\frac{l_j}{l_i}+\frac{2n_2-1}{2n_1-1}\right|\left|\frac{l_j}{l_i}-\frac{2n_2-1}{2n_1-1}\right|>\frac{l_j}{l_i}\left|\frac{l_j}{l_i}-\frac{2n_2-1}{2n_1-1}\right|,$$

we have

$$\left|\frac{l_j}{l_i}-\frac{2n_2-1}{2n_1-1}\right|<C_2(\Gamma)\frac{4l_il_j(C_0(l_i)+C_0(l_j))}{\pi^2}\frac{1}{(2n_1+1)^3}\leq\frac{1}{(2n_1+1)^3},$$

where we have applied the definition of $C_2(\Gamma)$. This leads to a contradiction with the definition of $M(\Gamma)$.

Now assume that, there exist $n_1\in\{1,\cdots,M(\Gamma)\}$ and $n_2\in\mathbb{N}$ such that for some $i\neq j$, $\lambda_{n_1}^i=\lambda_{n_2}^j$ and we will find a contradiction with the fact that $\|q\|_{H^1}<C_3(\Gamma)$ (the case of $\lambda_{n_1}^i=\lambda'^j_{n_2}$ can be treated exactly in the same manner). In this aim, we apply once again Lemma 3. If $\lambda_{n_1}^i=\lambda_{n_2}^j$, we have

$$\left|\frac{(2n_1-1)^2\pi^2}{4l_i^2}-\frac{(2n_2-1)^2\pi^2}{4l_j^2}\right|<C_3(\Gamma)\left(\frac{C_0(l_i)}{2n_1-1}+\frac{C_0(l_j)}{2n_2-1}\right)\leq$$
$$\leq C_3(\Gamma)(C_0(l_i)+C_0(l_j)).$$

This, trivially, is in contradiction with the definition of $C_3(\Gamma)$. □

Applying Lemma 5 to the (3.29), we have:

$$\int_0^{l_j}\tilde{q}_j(x)\varphi_{\mathcal{N}}^j(x,\lambda_n^j)\varphi'^j_{\mathcal{N}}(x,\lambda_n^j)dx=0,\qquad\forall j=1,\cdots,N,\quad\forall n\in\mathbb{N}$$

From Equation (3.26) we have

$$\int_0^{l_j}\tilde{q}_j(x)\varphi'^j_{\mathcal{N}}(x,\lambda_n^j)\varphi_{\mathcal{N}}^j(x,\lambda_n^j)dx=\psi_{\mathcal{N}}^j(0,\lambda_n^j)\varphi'^j_{\mathcal{N}}(0,\lambda_n^j)-\varphi_{\mathcal{N}}^j(0,\lambda_n^j)\psi'^j_{\mathcal{N}}(0,\lambda_n^j)=0.$$

This leads to $\psi_{\mathcal{N}}^j(0,\lambda_n^j)\varphi'^j_{\mathcal{N}}(0,\lambda_n^j)=0$, since $(\lambda_n^j)^2$ is an eigenvalue of $\mathcal{L}_{\mathcal{N}}^j$. Further-

more, The value $\psi^j_{\mathcal{N}}(0,\lambda^j_n)$ is different from 0, because otherwise we would have a non-zero fundamental solution $\varphi^j_{\mathcal{N}}(x,\lambda^j_n)$ with three zero boundary conditions. Thus $\varphi'^j_{\mathcal{N}}(0,\lambda^j_n)=0$ which implies that $(\lambda^j_n)^2$ is also an eigenvalue of $\mathcal{L}'^j_{\mathcal{N}}$. Therefore, the eigenvalues of $\mathcal{L}^j_{\mathcal{N}}$ and $\mathcal{L}'^j_{\mathcal{N}}$ coincide. In the same manner, we can show that the eigenvalues of $\mathcal{L}^j_{\mathcal{D}}$ and $(\mathcal{L}')^j_{\mathcal{D}}$ coincide as well.
It is well-known result [10, 29] that the specification of two spectra of Sturm-Liouville boundary value problem uniquely determines the potential on the segment e_j, i.e.

$$\tilde{q}_j(x)\equiv 0 \quad \forall x\in[0,l_j] \qquad j=1,\dots,N.$$

This completes the proof of Theorem 5.

3.8 Summary and further directions

In this chapter we have shown some results about the fault-detection and fault-localization on a electric star-shaped network.
A first result is the localization of open and short circuits on the network.

Theorem (Theorem 3)**.** *Consider a star-shaped network Γ composed of n_j branches of length l_j $(j=1,\cdots,m)$ all joining at a central node so that the whole number of branches N is given by $\sum_{j=1}^m n_j$. Let assume for the potential q on the network to be $C^0(\Gamma)$ and that it takes the value zero at the central node. Then the knowledge of the Neumann reflection coefficient $r_{\mathcal{N}}(k)$ determines uniquely the parameters $(n_j)_{j=1}^m$ and $(l_j)_{j=1}^m$.*

Through the analysis of the reflection coefficient $r(k)$, we are able to retrieve geometrical informations such as the number of the branches and their lengths. The knowledge of the lengths is equivalent to localize the hard faults on the branches of the electric network.
A second class of results is toward the identification of the heterogeneities. The first type is a heterogeneities test based on the comparison of reflection coefficients. The measured reflection coefficient is compared with nominal one and this will let us to discover any eventual soft faults.

Theorem (Theorem 4)**.** *Assume for the star-shaped graph Γ that*

B1 *$l_j\neq l_{j'}$ for any $j,j'\in\{1,\cdots,N\}$ such that $j\neq j'$.*

If there exist two potentials $q = \otimes_{j=1}^{N} q_j$ *and* $q' = \otimes_{j=1}^{N} q'_j$ *in* $H^1(\Gamma)$*, satisfying* $q_j(0) = q'_j(0) = 0$*, and giving rise to the same reflection coefficient,* $r_{\mathcal{N}}(k) \equiv r'_{\mathcal{N}}(k)$*, one necessarily has*

$$\int_0^{l_j} q_j(s)ds = \int_0^{l_j} q'_j(s)ds \qquad j = 1, \cdots, N.$$

This result allows to identify the quantities

$$\frac{1}{4}\int_0^{l_j} \frac{\left|\frac{d}{ds}(Z_c^j)(s)\right|^2}{\left|Z_c^j(s)\right|^2} ds - \frac{1}{2}\left(\frac{\frac{d}{dx}(Z_c^j)(l_j)}{Z_c^j(l_j)} - \frac{\frac{d}{dx}(Z_c^j)(0)}{Z_c^j(0)}\right),$$

on each branch. Supposing the reliability of the connectors at the central node and at the terminal nodes, i.e. $\frac{d}{dx}(Z_c^j)'(l_j) = \frac{d}{dx}(Z_c^j)(0) = 0$, the measurement of a reflection coefficient allows to identify all soft faults causing line parameters variations. This test classify all soft faults with respect the quantity $\int_0^{l_j} q(s)ds$.
To have a complete identification of the heterogeneities we have to go further: the last result concerns the identifiability of the potentials.

Theorem (Theorem 5)**.** *Consider a star-shaped graph* Γ *satisfying the geometrical assumption*

B2 *For any* $j, j' \in \{1, \cdots, N\}$ *such that* $j \neq j'$*,* $l_j/l_{j'}$ *is an algebraic irrational number.*

Take the strictly positive constant $C(\Gamma)$ *as defined by (3.18) and consider two potentials* q *and* q' *belonging to* $H^1(\Gamma)$*, satisfying* $q_j(0) = q'_j(0) = 0$*, the assumption*

A5 $\bar{q}_j = \int_0^{l_j} q_j(s)ds = 0$ *for* $j = 1, \cdots, N$*;*

and

$$\|q\|_{H^1(\Gamma)} < C(\Gamma) \quad \text{and} \quad \|q'\|_{H^1(\Gamma)} < C(\Gamma).$$

If they give rise to the same Neumann and Dirichlet reflection coefficients:

$$r_{\mathcal{N}}(k) \equiv r'_{\mathcal{N}}(k) \qquad \text{and} \qquad r_{\mathcal{D}}(k) \equiv r'_{\mathcal{D}}(k),$$

then $q \equiv q'$*.*

The result is only at a theoretical stage, because the assumptions **B2** limit the applicability in the real settings.
Indeed, the assumption of having the ratios between the electrical lengths that are

irrational algebraic numbers is not verifiable in a real setting. This hypothesis has been previously considered in control literature to ensure the exact controllability of wave equations over networks. In such problems, removing such assumption one can still hope to prove the approximate controllability.
Following the same idea, we may look for a similar approximate identifiability result, when such assumption is relaxed.

Chapter 4

Inverse scattering for lossy star-shaped network

In this chapter we consider a class of inverse scattering problems on the star-shaped graphs for the Zakharov-Shabat system, having in mind the reflectometry experiments on a lossy electrical network.

Theorem 6 and Theorem 7 can directly applied to the fault-detection and diagnosis of such networks, while Theorem 8 is a preliminary results towards the detection of isolation faults for the train transmission line.

4.1 Main hypothesis and physical interpretation

After the Liouville transformation, the lossy transmission lines equations write

$$\begin{cases} \frac{\partial}{\partial x}V(k,x) = -\left(ik + \frac{R(x)}{L(x)}\right) Z_{c0}(x) I(k,x), \\ \frac{\partial}{\partial x}I(k,x) = -\left(ik + \frac{G(x)}{C(x)}\right) Z_{c0}^{-1}(x) V(k,x). \end{cases} \tag{1.44}$$

Through this chapter, we assume that

C1 The distributed parameters $C(x)$ and $L(x)$ are continuously differentiable on the transmission line, while the loss terms $R(x)$ and $G(x)$ are continuos;

C2 The line parameters are strictly positive

$$L(x) > 0, \quad C(x) > 0, \quad R(x) > 0, \quad G(x) > 0;$$

C3 The high-frequency characteristic impedance $Z_{c0}(x) = \sqrt{L(x)/C(x)}$ is continuous at the central node of the star-shaped network;

The assumption **C1** is needed for the definitions of the three potentials

$$q_d(x) = \frac{1}{2}\left(\frac{R(x)}{L(x)} + \frac{G(x)}{C(x)}\right), \tag{1.47}$$

$$q_-(x) = \frac{1}{4}\frac{d}{dx}\left[\log\frac{L(x)}{C(x)}\right] - \frac{1}{2}\left(\frac{R(x)}{L(x)} - \frac{G(x)}{C(x)}\right), \tag{1.48}$$

$$q_+(x) = \frac{1}{4}\frac{d}{dx}\left[\log\frac{L(x)}{C(x)}\right] + \frac{1}{2}\left(\frac{R(x)}{L(x)} - \frac{G(x)}{C(x)}\right). \tag{1.49}$$

Network under test

As in Chapter 3, we consider a star-shaped graph Γ with N edges. Each edge e_j connects the extremity l_j to the central node (see Figure 4.1).
Let Γ_{l_0} be the star shaped graph Γ where a branch $e_0 = [-l_0, 0]$ is added to the central node. On each branch $e_j \in \Gamma$, the variables

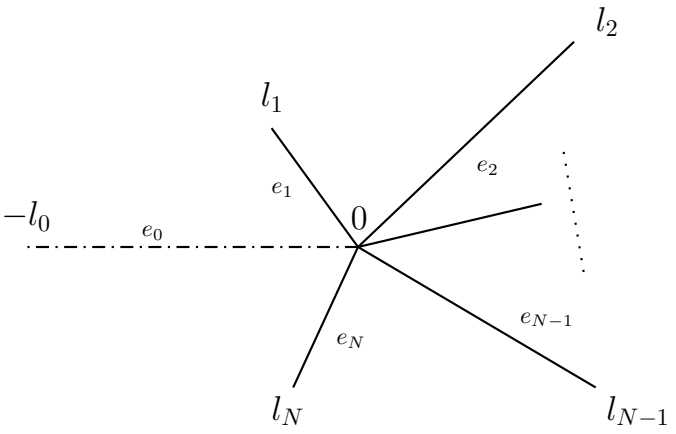

Figure 4.1: The graph Γ_{l_0}

$$\begin{cases} \nu_{1j}(x,k) = \frac{1}{\sqrt{2}}\left[Z_{c0,j}^{-1/2}(x)V_j(k,x) - Z_{c0,j}^{1/2}(x)I_j(k,x)\right], \\ \\ \nu_{2j}(x,k) = +\frac{1}{\sqrt{2}}\left[Z_{c0,j}^{-1/2}(x)V_j(k,x) + Z_{c0,j}^{1/2}(x)I_j(k,x)\right], \end{cases} \tag{1.45}$$

solve the Zakharov-Shabat system

$$\frac{d}{dx}Y_j(x,k) + ik\sigma_3 Y_j(x,k) = Q_j(x)Y_j(x,k), \qquad x \in [0, l_j] \tag{1.101}$$

where l_j is the length of each interval. As before, the branch e_0 represents a matched load uniform lossless wire: the three potentials $\{q_{0,+}, q_{0,-}, q_{0,d}\}$ are zero. We have a linear decoupled first-order system for $x \in [-l_0, 0]$

$$\begin{cases} \partial_x \nu_{10}(x,k) = -ik\nu_{10}(x,k), \\ \partial_x \nu_{20}(x,k) = +ik\nu_{20}(x,k). \end{cases} \tag{4.1}$$

Central node

The continuity of the characteristic impedance Z_{c0} at the central node (assumption **C3**) excludes certain type of faults that can happen at the level of the connector. Here we are only interested in detecting the faults on wires.
Indeed, the continuity of the high-frequency characteristic impedance $Z_{c0,j}(x)$ at central node simplify the central boundary conditions (1.53) for Zakharov-Shabat formulation

$$\begin{cases} \nu_{10}(0,k) + \nu_{20}(0,k) = \nu_{1j}(0,k) + \nu_{2j}(0,k) \quad \forall j \in \{1,\dots,N\} \\ \sum_{j=1}^{N} \nu_{1j}(0,k) - \nu_{2j}(0,k) = \nu_{10}(0,k) - \nu_{20}(0,k). \end{cases}$$

Boundary conditions at the network extremities.

In order to develop diagnostic techniques for electric networks, we need to consider an experimental setting with open circuits boundary conditions.
On each terminal node l_j we are imposing $I_j(l_j,k) = 0$ and this is equivalent to choosing $\rho_j(k) = 1$ for the boundary conditions (1.50) at all terminal nodes:

$$\nu_{1j}(l_j,k) - \nu_{2j}(l_j,k) = 0 \qquad \forall j \in \{1,\dots,N\}.$$

Boundary condition at the source node l_0

At the minimal node l_0, we connect a source generator $\nu_S(k)$

$$\nu_{20}(-l_0,k) = \nu_S(k).$$

We will show in the next section how to relate the source generator to the reflection coefficient.

Formulation of the model.

In order to study the lossy transmission line equations on the extended graph Γ_{l_0}, we consider the Zakharov-Shabat equations defined on each branch $e_j, \quad j = 0, \dots, N$ as follows

$$\begin{cases} \partial_x \nu_{1j}(x,k) = (q_{j,d}(x) - ik)\nu_{1j}(x,k) - q_{j,+}(x)\nu_{2j}(x,k), \\ \partial_x \nu_{2j}(x,k) = -q_{j,-}(x)\nu_{1j}(x,k) - (q_{j,d}(x) - ik)\nu_{2j}(x,k), \end{cases} \qquad x \in [0, l_j]. \tag{4.2}$$

with the boundary conditions at the central node

$$\begin{cases} \nu_{10}(0,k) + \nu_{20}(0,k) = \nu_{1j}(0,k) + \nu_{2j}(0,k) \quad \forall j \in \{1, \dots, N\} \\ \sum_{j=1}^{N} \nu_{1j}(0,k) - \nu_{2j}(0,k) = \nu_{10}(0,k) - \nu_{20}(0,k), \end{cases} \tag{4.3}$$

and at all boundary vertices

$$\nu_{1j}(l_j,k) - \nu_{2j}(l_j,k) = 0 \qquad \forall j \in \{1, \dots, N\}, \tag{4.4}$$

$$\nu_{20}(-l_0,k) = \nu_S(k). \tag{4.5}$$

4.2 Direct scattering problem

We will consider the Zakharov-Shabat equations and we prove the existence and the uniqueness of the solution. As for the case of a segment (see Section 1.4), we introduce the Riccati equation in order to define the reflection coefficient $r_0(-l_0; k)$.
Next we construct the scattering data for the extended graph with $l_0 = \infty$. A new reflection coefficient $r(k)$ will be given by asymptotic boundary conditions on the test branch e_0 and we will see how $r(k)$ is related to $r_0(-l_0; k)$.

Lemma 6. *Let Γ_{l_0} be a star-shaped graph. Let $\{q_{j,+}, q_{j,-}, q_{j,d}\}_{j=1}^{N}$ be in the class*

$$C_0^+(\Gamma) = \{q_{j,+}, q_{j,-}, q_{j,d} \in C_0([0, l_j]), \quad \forall j = 1, \dots, N\}.$$

and let $\{q_{0,+}, q_{0,-}, q_{0,d}\}$ be zero on the 0-th branch. The Zakharov-Shabat system (4.2) *with boundary conditions* (4.3),(4.4) *and* (4.5) *admits a unique solution.*

Proof of Lemma 6. In order to prove the well-posedness of the problem defined by (4.2),(4.3),(4.4) and (4.5), we will use the decoupling technique of the invariant imbedding method [8], [59],[7].
Let us introduce the following Riccati equation on Γ_0 defined on each branch e_j as following:

$$\frac{dr_j}{dx}(x,k) = q_{j,-}(x)r_j^2(x,k) + 2(q_{j,d}(x) - ik)r_j(x,k) - q_{j,+}(x), \tag{4.6}$$

with the boundary condition at central node

$$r_0(0,k) = \frac{1 - \sum_{j=1}^{N} \frac{1-r_j(0,k)}{1+r_j(0,k)}}{1 + \sum_{j=1}^{N} \frac{1-r_j(0,k)}{1+r_j(0,k)}}, \tag{4.7}$$

while at the terminal nodes $l_1, \ldots, l_N$ we have

$$r_j(l_j,k) = 1\Big(= \rho_j(k)\Big) \qquad \forall j = 1, \ldots, N. \tag{4.8}$$

We remark that, thanks to Lemma 1, the restriction of solution $r_j(x,k)$ exists and it is unique on each branch e_j. The assumption **C2** satisfies the hypothesis of Corollary 1 (page 41) and consequently the coefficients r_j verify

$$|r_j(0,k)| < 1 \qquad \forall j = 1, \ldots, N,$$

so the boundary condition (4.7) at central node is well-defined for all k in $\mathbb{R}$.
Hence the Riccati equation (4.6) admits a unique global solution defined for all $x \in \Gamma_0$.

Now, we will change the variables in (4.2),(4.3),(4.4) and (4.5), setting

$$\tilde{\nu}_{1j}(x,k) = \nu_{1j}(x,k) - r_j(x,k)\nu_{2j}(x,k).$$

The new equivalent system is given by

$$\begin{cases} \partial_x \tilde{\nu}_{1j}(x,k) = (q_{j,d}(x) - ik + q_{j,-}(x)r_j(x,k))\tilde{\nu}_{1j}(x,k), \\ \partial_x \nu_{2j}(x,k) = -q_{j,-}(x)\tilde{\nu}_{1j}(x,k) - (q_{j,d}(x) - ik + q_{j,-}(x)r_j(x,k))\nu_{2j}(x,k) \end{cases} \tag{4.9}$$

where the boundary conditions at the central node are

$$\begin{cases} \tilde{\nu}_{10}(0,k) + (r_0(0,k)+1)\nu_{20}(0,k) = \tilde{\nu}_{1j}(0,k) + (r_j(0,k)+1)\nu_{2j}(0,k) \\ \tilde{\nu}_{10}(0,k) + (r_0(0,k)-1)\nu_{20}(0,k) = \sum_{j=1}^{N} \tilde{\nu}_{1j}(0,k) + (r_j(0,k)-1)\nu_{2j}(0,k) \end{cases} \tag{4.10}$$

and at the terminal nodes, we have

$$\begin{cases} \tilde{\nu}_{1j}(l_j,k) = 0 \qquad j = 1,\dots,N \\ \nu_{20}(-l_0,k) = \nu_S(k). \end{cases}$$

Note that the system (4.9) is decoupled: the first equation is independent from the second one, because at the central node the boundary conditions involve only the first variable $\tilde{\nu}_{1j}(x,k)$. From (4.7) and (4.10) we obtain

$$\tilde{\nu}_{10}(0,k) = \sum_{j=1}^{N} \frac{r_0(0,k)+1}{r_j(0,k)+1} \tilde{\nu}_{1j}(0,k).$$

Now it is clear that the first equation of (4.9) depends only on the variables $\{\tilde{\nu}_{1j}\}_{j=1}^{n}$ and, being a Cauchy problem, it has a unique solution $\{\tilde{\nu}_{1j}(x,k)\}_{j=0}^{N} \equiv 0$. Indeed, we have $\nu_{1j}(x,k) = r_j(x,k)\nu_{2j}(x,k)$.
The second equation becomes simply

$$\partial_x \nu_{2j}(x,k) = -(q_{j,d}(x) - ik + q_{j,-}(x) r_j(x,k))\nu_{2j}(x,k)$$

with the boundary conditions

$$\begin{cases} \nu_{20}(-l_0,k) = \nu_S(k), \\ \nu_{2j}(0,k) = \dfrac{(r_0(0,k)+1)}{(r_j(0,k)+1)} \nu_{20}(0,k). \end{cases}$$

Also the second equation has also unique solution.

We have shown the existence and the uniqueness of the solutions of (4.9),(4.10). This complete the proof for the well-posedness of (4.2), (4.3), (4.4) and (4.5). □

We define the reflection coefficient for the Zakharov-Shabat system (4.2) on Γ_{l_0} as

$$r_l(k) = r_0(-l_0,k). \tag{4.11}$$

Let Γ^+ be the union of Γ whit the half-line $(-\infty, 0]$, i.e. the length l_0 of the branch indexed by 0 is chosen to be infinite. According to the classical scattering theory, we look for a solution of the Zakharov-Shabat system on Γ^+ such that it verifies the asymptotic limit

$$\begin{pmatrix} \nu_1(x,k) \\ \nu_2(x,k) \end{pmatrix} \sim \begin{pmatrix} 0 \\ 1 \end{pmatrix} e^{ikx} + r(k) \begin{pmatrix} 1 \\ 0 \end{pmatrix} e^{-ikx} \qquad \text{as } x \to +\infty$$

In terms of experiment, we are interested in the scattering solution where a signal of frequency k is applied at the extremity of the test branch e_0. Note that the asymptotic limit is a sum of exponentials and this can be represented as sum of a incident and reflected waves. We are implicitly choosing a normalized incident wave. In this case, the reflection coefficient $r(k)$ is defined by the following proposition

Proposition 7. *Let Γ^+ be the star-shaped graph and let assume that the assumptions **C1** through **C3** hold. Let $\boldsymbol{q} = \otimes_{j=1}^{N}(q_{j,+}, q_{j,-}, q_{j,d})$ be in the class*

$$C_0^+(\Gamma) = \{q_{j,+}, q_{j,-}, q_{j,d} \in C_0([0, l_j]), \quad \forall j = 1, \dots, N\},$$

then there exists a unique continuous (with respect to k) solution

$$\boldsymbol{Y}(x,k) := \{Y_j(x,k)\}_{j=0}^{N} = \left\{ \begin{pmatrix} y_{1j}(x,k) \\ y_{2j}(x,k) \end{pmatrix} \right\}_{j=0}^{N}$$

of the scattering problem. This means that for every $k \in \mathbb{R}$, $\boldsymbol{Y}(x,k)$ satisfies

- *the Zakharov-Shabat equations* (4.2),
- *$\boldsymbol{Y}(x,k)$ satisfies the boundary conditions* (4.3) *and* (4.4)*;*
- *For each $k \in \mathbb{R}$ there exists $r(k)$ such that*

$$Y_0(x,k) = \begin{pmatrix} 0 \\ 1 \end{pmatrix} e^{ikx} + r(k) \begin{pmatrix} 1 \\ 0 \end{pmatrix} e^{-ikx}, \qquad x \to -\infty. \tag{4.12}$$

The reflection coefficient $r(k)$ appears to be unique.

Proof. In order to prove the well-posedness of the problem (4.2)-(4.4) verifying (4.12), we consider the same problem defined on a subgraph and we extend analytically the

solution.
Let fix $l_0 > 0$ and let consider a Zakharov-Shabat system (4.2) defined on the subgraph $\Gamma_{l_0} \subset \Gamma^+$, defined as above, with the boundary conditions at central node (4.3), at the terminal nodes (4.4) and on the 0-th branch

$$\nu_{20}(-l_0, k) = \nu_s(k).$$

Thanks to Lemma 6, the problem is well posed and it admits a unique solution $\otimes_{j=0}^{N}(\nu_{1j}(x,k), \nu_{2j}(x,k))$ and moreover there exists a unique coefficient $r_l(k)$ such that

$$\nu_{10}(-l_0, k) = r_l(k)\nu_{20}(-l_0, k). \tag{4.13}$$

Let's consider the system (4.1) on the half line $(-\infty, -l_0)$, Adding the half line at the node $x = l_0$ of the graph Γ_{l_0} and imposing the continuity of the solution we obtain on the 0-th branch

$$\begin{pmatrix} y_{10}(x,k) \\ y_{20}(x,k) \end{pmatrix} = \nu_{20}(-l_0,k)e^{ikl_0}\begin{pmatrix} 0 \\ 1 \end{pmatrix}e^{ikx} + \nu_{10}(-l_0,k)e^{-ikl_0}\begin{pmatrix} 1 \\ 0 \end{pmatrix}e^{-ikx}.$$

From the boundary condition at $x = -l_0$ and from (4.13), it follows

$$\begin{pmatrix} y_{10}(x,k) \\ y_{20}(x,k) \end{pmatrix} = \nu_S(k)e^{ikl_0}\begin{pmatrix} 0 \\ 1 \end{pmatrix}e^{ikx} + \nu_S(k)e^{-ikl_0}r_l(k)\begin{pmatrix} 1 \\ 0 \end{pmatrix}e^{-ikx}.$$

Normalizing the first vector we obtain

$$\begin{pmatrix} y_{10}(x,k) \\ y_{20}(x,k) \end{pmatrix} = \begin{pmatrix} 0 \\ 1 \end{pmatrix}e^{ikx} + e^{-2ikl_0}r_l(k)\begin{pmatrix} 1 \\ 0 \end{pmatrix}e^{-ikx}.$$

This is equivalent to (4.12), where the reflection coefficient $r(k)$ is related to the coefficients $r_l(k)$ defined in (4.11) by the formula

$$r(k) = e^{-2ikl_0}r_l(k). \tag{4.14}$$

The latter formula is the same as (1.110), where we had shown the equivalence between the engineering scattering data and the theoretic scattering data for the Zakharov-Shabat equations.

□

4.3 Inverse problems and main results

As a first inverse problem, we consider the inversion of the geometry of the graph. We will be able to find the lengths l_j of the branches of a star-shaped graph through the knowledge of the reflection coefficient $r(k)$.

Theorem 6. *Assume for the star-shaped graph Γ^+ that*

B1 *$l_j \neq l_{j'}$ for any $j, j' \in \{1, \cdots, N\}$ such that $j \neq j'$.*

C4 *We assume for the potentials to satisfy*

$$q_{j,+}, q_{j,-}, q_{j,d} \in H^1(0, l_j) \quad \forall j = 1, \ldots, N.$$

The knowledge of the reflection coefficient $r(k)$ determines uniquely the lengths $(l_j)_{j=1}^N$.

Remark 28. As we will see through the proof, the inversion method is constructive: it allows to recover at least approximately the lengths for each branch. A proof of this theorem will be provided in Section 4.4.

A second inverse problem is related to the detection of soft faults in the network. It can be formulated as the identifiability of loss line factors. We will prove the well-posedness of the inverse problem of finding the loss line factors defined as

$$\int_0^{l_j} q_{j,d}(x)dx = \frac{1}{2}\int_0^{l_j} \left(\frac{R_j(x)}{L_j(x)} + \frac{G_j(x)}{C_j(x)}\right) dx$$

on each branch. If any of these quantities changes, we know that there is a variation of the line parameters in the corresponding branch. By performing the inverse scattering technique [62] on the branch we can identify the soft faults causing such variations.

Theorem 7. *Assume for the star-shaped graph Γ^+ that **B1** is valid.*
*If there exist two potentials $\boldsymbol{q} = \otimes_{j=1}^N (q_{j,+}, q_{j,-}, q_{j,d})$ and $\boldsymbol{q'} = \otimes_{j=1}^N (q'_{j,+}, q'_{j,-}, q'_{j,d})$ satisfying **C4** and the condition $Z_{c0j}(0) = Z'_{c0j}(0)$ for all $j = 0, \ldots, N$ and giving rise to the same reflection coefficient, $r(k) \equiv r'(k)$, one necessarily has:*

$$\int_0^{l_j} q_{j,d}(s)ds = \int_0^{l_j} q'_{j,d}(s)ds \qquad j = 1, \cdots, N.$$

Remark 29. The condition about the characteristic impedance $Z_{c0j}(0)$ at the central node excludes faults of the connector.

Defining the following factor

$$Q_{j,d}(x_1, x_2) := \int_{x_1}^{x_2} q_{j,d}(s)ds,$$

we have shown we are able to identify the loss line factor $Q_{j,d}(0, l_j)$. This theorem allows to identify the situations where the soft faults cause a variation of the loss line factor. The proof can be found in Section 4.6.

The last result concerns the identifiability of the line parameters R/L and G/C on the uniform transmission line network. The hypothesis of constant line parameters and their comparison such that $R/L > G/C$ allows to identify two aggregates of line parameters

$$\frac{R}{L} \qquad \text{and} \qquad \frac{G}{C}$$

on each wire of a star-shaped network.

Theorem 8. *Let us consider a star-shaped network* Γ^+ *with the geometric assumption* ***B1****. Let the potentials* $\boldsymbol{q} = \otimes_{j=1}^{N}(q_{j,+}, q_{j,-}, q_{j,d})$ *be of the following forms:*

$$q_{j,d}(x) : \quad = \tfrac{1}{2}\left(\tfrac{R_j}{L_j} + \tfrac{G_j}{C_j}\right), \tag{4.15}$$

$$q_{j,+}(x) : \quad = +\tfrac{1}{2}\left(\tfrac{R_j}{L_j} - \tfrac{G_j}{C_j}\right), \tag{4.16}$$

$$q_{j,-}(x) : \quad = -\tfrac{1}{2}\left(\tfrac{R_j}{L_j} - \tfrac{G_j}{C_j}\right). \tag{4.17}$$

where R_j, L_j, G_j *and* C_j *are constant parameters uniformly defined on each branch. If* $G_j/C_j < R_j/L_j$ *on each branch, then the reflection coefficient* $r(k)$ *allows to identify uniquely these two quantities*

$$\frac{R_j}{L_j} \qquad \textit{and} \qquad \frac{G_j}{C_j}$$

on all branches e_j *of the star-shaped network* Γ.

This theorem investigates the identifiability problem of the "isolation faults". As described in Section 1.1, the french railway's $SNCF$ is interested in the detection of these faults as long as the technique is not invasive. The hypothesis $G_j/C_j < R_j/L_j$

is given by the small influence in the shunt conductance G over the resistance R; in real applications $G_j/C_j \ll R_j/L_j$. This result states the measurement of the reflection coefficient at high frequency is enough to retrieve the quantities R/L and G/C. The proof can be found in Section 4.7.

4.4 Identification of Geometry

Theorem 6 allows us to detect and locate any possible hard faults. Through the analysis of the reflection coefficient $r(k)$ we will be able to compute the position of any eventual hard faults.

This section is devoted to the proof of Theorem 6. The proof is based on an asymptotic analysis in the high frequency regime of the reflection coefficient and some classical results from the theory of the almost periodic functions.
Before proving the theorem, we need to introduce the fundamental solutions of the following Cauchy problem.

Definition 18. Let's consider the potentials $q_{j,+}, q_{j,-}$ and $q_{j,d}$ be in the class $C_0^+(\Gamma)$. The *fundamental solutions* $\Phi_j(x,k) :=(\phi_{1j}(x,k), \phi_{2j}(x,k))$ and $\Psi_j(x,k) := (\psi_{1j}(x,k), \psi_{2j}(x,k))$ are solutions of the same system defined on $[0, l_j]$:

$$\begin{cases} \partial_x \nu_{1j}(x,k) = (q_{j,d}(x) - ik)\nu_{1j}(x,k) - q_{j,+}(x)\nu_{2j}(x,k), \\ \partial_x \nu_{2j}(x,k) = -q_{j,-}(x)\nu_{1j}(x,k) - (q_{j,d}(x) - ik)\nu_{2j}(x,k), \end{cases} \tag{4.18}$$

verifying the initial values at $x = l_j$

$$\begin{cases} \phi_{1j}(l_j,k) = 1, \\ \phi_{2j}(l_j,k) = 1, \end{cases} \qquad \begin{cases} \psi_{1j}(l_j,k) = 1 \\ \psi_{2j}(l_j,k) = -1. \end{cases}$$

Remark 30. In Appendix C, we show that the system of fundamental solutions Φ_j and Ψ_j forms a basis for the vector space of the restrictions to the j-th edge of the solutions of the Zakharov-Shabat system on Γ^+. For any boundary conditions at the external vertices, a solution of the Zakharov-Shabat system on Γ^+ can be described on each branch as a linear combination of the fundamental solutions .
It is not difficult to see that the fundamental solution $\Phi_j(x,k)$ is co-linear with the restriction of the scattering solution $Y_j(x,k)$ for the Zakharov-Shabat system

(4.2),(4.3),(4.4) to the j-branch. Their Wronskian

$$W_j(x) := \nu_{1j}(x,k)\phi_{2j}(x,k) - \phi_{1j}(x,k)\nu_{2j}(x,k) \tag{4.19}$$

is constant along the edge and it is equal to zero because of the boundary conditions at the external vertex l_j and this is enough to guarantee the co-linearity between $Y_j(x,k)$ and $\Phi_j(x,k)$.

Next lemma shows the high-frequency behavior of the fundamental solution.

Lemma 7. *Let $\phi_1(x,k), \phi_2(x,k)$ be a fundamental solution associated to the Zakharov-Shabat system on $[0,l]$ verifying the Cauchy boundary condition*

$$\phi_1(l,k) = 1 \qquad \phi_2(l,k) = 1.$$

We have the following asymptotic behavior as k tends to infinity

$$\begin{aligned} \phi_1(x,k) &= e^{Q_d(x,l)-ik(l-x)} + \mathcal{O}\left(1/k\right), \\ \phi_2(x,k) &= e^{-Q_d(x,l)+ik(l-x)} + \mathcal{O}\left(1/k\right), \end{aligned} \tag{4.20}$$

where the quantity $Q_d(x,l)$ represents the dissipation along the line, i.e.

$$Q_d(x,l) = \int_x^l q_d(s)ds = \int_x^l \frac{1}{2}\left(\frac{R(s)}{L(s)} + \frac{G(s)}{C(s)}\right) ds.$$

Proof. The proof of high frequency behavior can be found in Section C.2 of the Appendix. □

Before passing to the proof of theorems, we further need the following Lemma:

Lemma 8. *Let us consider a star-shaped network Γ^+ satisfying **B1**. Let's assume that the potentials $\boldsymbol{q} = \otimes_{j=1}^N (q_{j,+}, q_{j,-}, q_{j,d})$ are of the following forms*

$$q_{j,d}(x) \in H^1(\Gamma^+), \qquad q_{j,+}(x) = 0, \qquad q_{j,-}(x) = 0. \tag{4.21}$$

Then the knowledge of the reflection coefficient $r(k)$ determines uniquely the parameters $\{l_j\}_{j=1}^N$.

Remark 31. The assumption about potentials corresponds to the situation, where

- the line parameters L and C are constants along the network,

- the loss parameters R_j and L_j are such that on each branch

$$\frac{R_j(x)}{L} = \frac{G_j(x)}{C}, \quad x \in [0, l_j], \qquad \forall j = 1, \dots, N.$$

Proof. From the boundary conditions at the central node (4.3) we have

$$\frac{\nu_{10}(0,k) - \nu_{20}(0,k)}{\nu_{10}(0,k) + \nu_{20}(0,k)} = \sum_{j=1}^{N} \frac{\nu_{1j}(0,k) - \nu_{2j}(0,k)}{\nu_{1j}(0,k) + \nu_{2j}(0,k)}. \tag{4.22}$$

Noting that the solution on each branch is co-linear with $\Phi_j(x,k)$ and the relation (4.12) together with the explicit solutions for $\nu_{10}(x,k)$ and $\nu_{20}(x,k)$, we have

$$\frac{r(k)-1}{r(k)+1} = \sum_{j=1}^{N} \frac{\phi_{1j}(0,k) - \phi_{2j}(0,k)}{\phi_{1j}(0,k) + \phi_{2j}(0,k)}. \tag{4.23}$$

When the potentials $q_{j,+}(x)$ and $q_{j,-}(x)$ are zero, the fundamental solutions $\phi_{1j}(x,k)$ and $\phi_{2j}(x,k)$ write explicitly as

$$\begin{cases} \phi_{1j}(x,k) = e^{Q_{j,d}(x,l_j) - ik(l_j - x)}, \\ \phi_{2j}(x,k) = e^{-Q_{j,d}(x,l_j) + ik(l_j - x)}, \end{cases}$$

therefore we have

$$\frac{r(k)-1}{r(k)+1} = \sum_{j=1}^{N} \frac{e^{Q_{j,d}(0,l_j) - ikl_j} - e^{-Q_{j,d}(0,l_j) + ikl_j}}{e^{Q_{j,d}(0,l_j) - ikl_j} + e^{-Q_{j,d}(0,l_j) + ikl_j}} = \sum_{j=1}^{N} \tanh(Q_{j,d}(0,l_j) - ikl_j). \tag{4.24}$$

The knowledge $r(k)$ determines uniquely the signal

$$f(k) = \sum_{j=1}^{N} \tanh(Q_{j,d}(0,l_j) - ikl_j)$$

For k being real, the hyperbolic tangent is periodic: a fourier transform of the signal $f(k)$ reveals the different periods of the hyperbolic tangents. □

We are ready to prove Theorem 6.

Proof of theorem 6. Let's suppose that there exist two graph settings $\{l_j\}_{j=1}^N$ and $\{l'_j,\}_{j=1}^N$ giving rise to the same reflection coefficient.

Using (4.23), we have

$$\sum_{j=1}^{N} \frac{\phi_{1j}(0,k) - \phi_{2j}(0,k)}{\phi_{1j}(0,k) + \phi_{2j}(0,k)} = \sum_{j=1}^{N} \frac{\phi'_{1j}(0,k) - \phi'_{2j}(0,k)}{\phi'_{1j}(0,k) + \phi'_{2j}(0,k)}.$$

This is equivalent to

$$\prod_{j'=1}^{N} [\phi'_{1j'}(0,k) + \phi'_{2j'}(0,k)] \left(\sum_{j=1}^{N} (\phi_{1j}(0,k) - \phi_{2j}(0,k)) \prod_{p \neq j} (\phi_{1p}(0,k) + \phi_{2p}(0,k)) \right) -$$
$$\prod_{j=1}^{N} [\phi_{1j}(0,k) + \phi_{2j}(0,k)] \left(\sum_{j'=1}^{N} (\phi'_{1j'}(0,k) - \phi'_{2j'}(0,k)) \prod_{p \neq j'} (\phi'_{1p}(0,k) + \phi'_{2p}(0,k)) \right) = 0. \tag{4.25}$$

Now using the asymptotic behavior of the fundamental solutions shown in Lemma 7 and defining the function

$$F(k) := \prod_{j'=1}^{N} \cosh(Q'_{j',d}(0,l'_j) - ikl'_{j'}) \left(\sum_{j=1}^{N} \sinh(Q_{j,d}(0,l_j) - ikl_j) \prod_{p \neq j} \cosh(Q_{p,d}(0,l_j) - ikl_p) \right) +$$
$$- \prod_{j'=1}^{N} \cosh(Q_{j',d}(0,l'_j) - ikl_{j'}) \left(\sum_{j=1}^{N} \sinh(Q'_{j,d}(0,l_j) - ikl'_j) \prod_{p \neq j} \cosh(Q'_{p,d}(0,l_j) - ikl'_p) \right),$$

the formula (4.25) can be written as

$$F(k) = \mathcal{O}\left(\frac{1}{k}\right), \qquad \text{as } k \to \infty.$$

The function $F(k)$ is almost periodic in the Bohr's sense [9] and moreover also $F^2(k)$ is an almost periodic function and its mean value $M(F^2)$ is well defined. Furthermore,

$$M(F^2) := \lim_{k\to\infty} \frac{1}{k} \int_0^k F^2(\xi) d\xi = \lim_{k\to\infty} \frac{1}{k} \left(\int_0^1 F^2(\xi) d\xi + \int_1^k F^2(\xi) d\xi \right) \leq$$
$$\leq \lim_{k\to\infty} \frac{1}{k} \left(C_1 + C_2 \int_1^k \frac{1}{k^2} dk \right) = 0.$$

The mean value equals to zero implies $F(k) = 0$ and so we have for each $k \in \mathbb{R}$

$$\sum_{j=1}^{N} \tanh(Q_{j,d}(0,l_j) - ikl_j) = \sum_{j=1}^{N} \tanh(Q'_{dj}(0,l_j) - ikl'_j).$$

and, therefore, by Lemma 8, the two settings are equivalent. □

4.5 From inverse scattering to inverse spectral problem

Here we present some auxiliary proposition in order to prove Theorem 7 and Theorem 8. With the next proposition we show the equivalence between the inverse scattering problem defined on the extended graph Γ^+ and some inverse spectral problems defined on the compact part Γ.

We will see the knowledge of the reflection coefficient $r(k)$ defined in (4.12) is equivalent to the knowledge of different spectra of a Zakharov-Shabat operator defined for Γ associated to different boundary conditions at the central node.

Let's define the function

$$h(k) = \frac{r(k)-1}{r(k)+1}. \tag{4.26}$$

For fixed $k \in \mathbb{R}$, we define the Zakharov-Shabat operator $\mathcal{L}(k)$ acting on the compact graph Γ

$$\mathcal{L}(k) = \otimes_{j=1}^{N} \begin{pmatrix} -\partial_x + q_{j,d} & -q_{j,+} \\ +q_{j,-} & \partial_x + q_{j,d} \end{pmatrix} \tag{4.27}$$

$$D(\mathcal{L}(k)) = \text{closure of } C_k^\infty(\Gamma) \text{ in } H^1(\Gamma) \times H^1(\Gamma), \tag{4.28}$$

where $C_k^\infty(\Gamma)$ denotes the space of infinitely differentiable functions $\otimes_{j=0}^{N}(f_{1j}, f_{2j})^{tr}$ defined on Γ satisfying the boundary conditions

$$\begin{aligned} f_{11}(0,k) + f_{21}(0,k) &= f_{1j}(0,k) + f_{2j}(0,k) \qquad \forall j \in \{2,\dots,N\} \\ \sum_{i=1}^{N} f_{1j}(0,k) - f_{2j}(0,k) &= h(k)(f_{11}(0,k) + f_{21}(0,k)), \\ f_{1j}(l_j,k) - f_{2j}(l_j,k) &= 0, \qquad j = 1,\cdots,N. \end{aligned} \tag{4.29}$$

Remark 32. The only dependence on k of the operator is through the boundary con-

dition (4.29) at the central node.

Definition 19. An *eigenvalue* of operator $\mathcal{L}(k)$ is a complex number ξ, with $\Im(\xi) \geq 0$, such that there exists a nontrivial solution called *eigensolution*

$$\mathbf{Y}(x,\xi) = \otimes_{j=1}^{N} \begin{pmatrix} y_{1j}(x,\xi) \\ y_{2j}(x,\xi) \end{pmatrix}.$$

verifying

$$\mathcal{L}(k)\mathbf{Y}(x,\xi) = \xi \mathbf{Y}(x,\xi).$$

Proposition 8. *We are able to characterize the set of pure imaginary* eigenvalues *of* $\mathcal{L}(k)$*, denoted by* $\sigma_i(\mathcal{L}(k))$*, as a level set of the function* $h(k)$*:*

$$\sigma_i(\mathcal{L}(k)) = \{\zeta \in \mathbb{C} : \zeta = i\xi, \xi \in \mathbb{R}^+ \text{ such that } h(\xi) = h(k)\}$$

where h *is given by (4.26).*

Proof. We start by proving the inclusion

$$\sigma_i(\mathcal{L}(k)) \subseteq \{\zeta \in \mathbb{C} : \zeta = i\xi, \xi \in \mathbb{R}^+ \text{ such that } h(\xi) = h(k)\}.$$

Let $\zeta \in \sigma_i(\mathcal{L}(k))$, then there exists a non-zero solution associated to the eigenvalue $\zeta = i\xi$. Hence we have

$$\sum_{i=1}^{N} y_{1j}(0,\xi) - y_{2j}(0,\xi) = h(k)(y_{11}(0,\xi) + y_{21}(0,\xi)).$$

We extend this solution to the Zakharov-Shabat equations defined on Γ^+ imposing the boundary condition at the central node

$$h(k)(y_{11}(0,\xi) + y_{21}(0,\xi)) = \sum_{j=1}^{N} y_{1j}(0,\xi) - y_{2j}(0,\xi) = y_{10}(0,\xi) - y_{20}(0,\xi)$$

We use the continuity at the central node, i.e. $y_{11}(0,\xi) + y_{21}(0,\xi) = y_{10}(0,\xi) + y_{20}(0,\xi)$ and therefore

$$h(k)(y_{10}(0,\xi) + y_{20}(0,\xi)) = y_{10}(0,\xi) - y_{20}(0,\xi).$$

Thus

$$h(k) = \frac{y_{10}(0,\xi) - y_{20}(0,\xi)}{y_{10}(0,\xi) + y_{20}(0,\xi)} = \frac{r(\xi) - 1}{r(\xi) + 1} = h(\xi).$$

In the last line, we used the representation (4.12) of the scattering solution for the 0-th branch. This proves the first inclusion.

Now, we prove that

$$\sigma_i(\mathcal{L}(k)) \supseteq \{\zeta \in \mathbb{C} : \zeta = i\xi, \xi \in \mathbb{R}^+ \text{ such that } h(\xi) = h(k)\}.$$

Let $\xi \in \mathbb{R}$ be such that $h(\xi) = h(k)$. We consider a scattering solution of Zakharov-Shabat equations on Γ^+ associated to the frequency ξ and we prove that the restriction of this scattering solution to $\mathcal{L}$ is an eigen-solution of eigenvalue $i\xi$.
In this aim we only need to show that this restriction is in the domain $D(\mathcal{L}(k))$. The boundary conditions (4.29) are verified:

$$\begin{aligned}
\sum_{j=1}^{N} y_{1j}(0,\xi) - y_{2j}(0,\xi) &= y_{10}(0,\xi) - y_{20}(0,\xi) \\
&= \frac{y_{10}(0,\xi) - y_{20}(0,\xi)}{y_{10}(0,\xi) + y_{20}(0,\xi)}(y_{10}(0,\xi) + y_{20}(0,\xi)) \\
&= \frac{r(\xi) - 1}{r(\xi) + 1}(y_{11}(0,\xi) + y_{21}(0,\xi)) = h(\xi)(y_{11}(0,\xi) + y_{21}(0,\xi)).
\end{aligned}$$

This concludes the proof. □

Now we provide the characteristic equation for the operator $\mathcal{L}(k)$. In order to complete this task, we need to use the fundamental solutions defined in (4.18).

Proposition 9. *Let k be a real positive number. Then ik is an eigenvalue of the operator $\mathcal{L}(k)$ if and only if*

$$h(k) = \sum_{j=1}^{N} \frac{\phi_{1j}(0,k) - \phi_{2j}(0,k)}{\phi_{1j}(0,k) + \phi_{2j}(0,k)}, \tag{4.30}$$

where $\Phi_j(x,k) = (\phi_{1j}(x,k), \phi_{2j}(x,k))$ are the fundamental solutions on different branches.

Proof. Assume that ik is a pure imaginary eigenvalue of $\mathcal{L}(k)$, then the associated eigenfunction $\otimes_{j=1}^{N}(y_{1j}(x,k), y_{2j}(x,k))$ has necessarily the form:

$$(y_{1j}(x,k), y_{2j}(x,k)) = \alpha_j(\phi_{1j}(x,k), \phi_{2j}(x,k)),$$

where α_j are real constants and the vector $(\alpha_1, \ldots, \alpha_N)$ is different from zero. The function $\otimes_{j=1}^N(\nu_{1j}(x,k), \nu_{2j}(x,k))$ should satisfy the associated boundary conditions at the central node, or equivalently the vector $(\alpha_1, \ldots, \alpha_N)$ is in the kernel of the matrix associated to the boundary conditions at the central node :

$$M := \begin{pmatrix} \phi_{11}(0)+\phi_{21}(0) & -\phi_{12}(0)-\phi_{22}(0) & 0 & \cdots & 0 \\ 0 & \phi_{12}(0)+\phi_{22}(0) & -\phi_{13}(0)-\phi_{23}(0) & \cdots & 0 \\ 0 & 0 & \phi_{13}(0)+\phi_{23}(0) & \cdots & 0 \\ \cdots & \cdots & \cdots & \cdots & \cdots \\ \begin{array}{l} -h(k)(\phi_{11}(0)+\phi_{21}(0)) \\ +\phi_{11}(0)-\phi_{21}(0) \end{array} & \phi_{12}(0)-\phi_{22}(0) & \phi_{13}(0)-\phi_{23}(0) & \ldots & \phi_{1N}(0)-\phi_{2N}(0) \end{pmatrix}$$

where for simplicity of notations we have removed the dependence on k of the fundamental solutions, i.e. $\phi_{ij}(0) = \phi_{ij}(0,k)$. The determinant of M has to be zero:

$$\sum_{j=1}^N(\phi_{1j}(0,k)-\phi_{2j}(0,k))\prod_{i\neq j}(\phi_{1i}(0,k)+\phi_{2i}(0,k) = h(k)\prod_{j=1}^N(\phi_{1j}(0,k)+\phi_{2j}(0,k)). \tag{4.31}$$

Let's denote by $\Psi(k)$ and $\Phi(k)$ the following expressions

$$\begin{aligned} \Psi(k) &= \sum_{j=1}^N(\phi_{1j}(0,k)-\phi_{2j}(0,k))\prod_{i\neq j}(\phi_{1i}(0,k)+\phi_{2i}(0,k)), \\ \Phi(k) &= \prod_{j=1}^N(\phi_{1j}(0,k)+\phi_{2j}(0,k)). \end{aligned}$$

The equation (4.31) can be written simply as

$$\Psi(k) = h(k)\Phi(k).$$

□

Corollary 3. Let us consider two potentials $\mathbf{q} = \otimes_{j=1}^N(q_{j,+}, q_{j,-}, q_{j,d})$ and $\mathbf{q}' = \otimes_{j=1}^N(q'_{j,+}, q'_{j,-}, q'_{j,d})$ and denote by $\mathcal{L}^+$ and $\mathcal{L}'^+$, the associated Zakharov-Shabat systems defined on the extended graph Γ^+. Assuming that the reflection coefficients $r(k)$ and $r'(k)$ are equivalent

$$r(k) \equiv r'(k),$$

then we have

$$\Phi'(k)\Psi(k) = \Psi'(k)\Phi(k), \qquad \forall k \in \mathbb{R}^+. \tag{4.32}$$

Proof. By Proposition 8, ik is an eigenvalue of the operators $\mathcal{L}(k)$ and $\mathcal{L}'(k)$. Applying Proposition 9, we have

$$\Psi'(k) = h'(k)\Phi'(k) \quad \text{and} \quad \Psi(k) = h(k)\Phi(k).$$

As the reflection coefficients are the same $r(k) = r'(k)$ and consequently $h(k) = h'(k)$, the above equation yields to (4.32). □

Eventually we arrive at the following proposition concerning the error between $\mathbf{q}$ and $\mathbf{q}'$.

Proposition 10. *Consider two potentials $\boldsymbol{q} = \otimes_{j=1}^{N}(q_{j,+}, q_{j,-}, q_{j,d})$ and $\boldsymbol{q'} = \otimes_{j=1}^{N}(q'_{j,+}, q'_{j,-}, q'_{j,d})$ and denote by $\mathcal{L}^+$ and $\mathcal{L}'^+$ the associated Zakharov-Shabat systems defined on the extended graph Γ^+. Assuming that the reflection coefficients $r(k)$ and $r'(k)$ are equivalent $r(k) \equiv r'(k)$, we have for all $k \in \mathbb{R}^+$*

$$\begin{aligned} &\sum_{j=1}^{N} \prod_{i \neq j} (\phi'_{1i}(0,k) + \phi'_{2i}(0,k))(\phi_{1i}(0,k) + \phi_{2i}(0,k)) \times \\ &\times \left[\int_0^{l_j} \tilde{q}_{j,d}(x) \Big(\phi_{1j}(x,k)\phi'_{2j}(x,k) + \phi'_{1j}(x,k)\phi_{2j}(x,k) \Big) dx + \right. \\ &\left. + \int_0^{l_j} \tilde{q}_{j,-}(x)\phi_{1j}(x,k)\phi'_{1j}(x,k) - \tilde{q}_{j,+}(x)\phi_{2j}(x,k)\phi'_{2j}(x,k) dx \right] = 0. \end{aligned} \tag{4.33}$$

where the sign $\sim$ denotes the error terms:

$$\tilde{q}_{j,x} = q_{j,x} - q'_{j,x}, \qquad x := +, -, d.$$

Proof. From Corollary 3, we have

$$\Psi(k)\Phi'(k) - \Psi(k)\Phi'(k) = 0$$

or equivalently

$$\sum_{j=1}^{N}\prod_{i\neq j}(\phi'_{1i}(0,k)+\phi'_{2i}(0,k))(\phi_{1i}(0,k)+\phi_{2i}(0,k))\times$$
$$\times\Big[\phi_{1j}(0,k)-\phi_{2j}(0,k))(\phi'_{1j}(0,k)+\phi'_{2j}(0,k))+$$
$$-(\phi_{1j}(0,k)+\phi_{2j}(0,k))(\phi'_{1j}(0,k)-\phi'_{2j}(0,k)\Big]=0. \quad (4.34)$$

Now we develop the terms between square brackets. Let us fix a single branch, omitting the index j and the dependence of k, i.e. $\phi_1(0)=\phi_{1j}(0,k)$ and $\phi_2(0)=\phi_{2j}(0,k)$ we have

$$\begin{aligned}(\phi_1(0)-\phi_2(0))(\phi'_1(0)+\phi'_2(0))-(\phi_1(0)+\phi_2(0))(\phi'_1(0)-\phi'_2(0))=\\ =\int_0^l\frac{d}{dx}[(\phi_1(x)-\phi_2(x))(\phi'_1(x)+\phi'_2(x))-(\phi_1(x)+\phi_2(x))(\phi'_1(x)-\phi'_2(x))]dx\\ =\int_0^l\frac{d}{dx}[-2\phi'_1(x)\phi_2(x)+2\phi_1(x)\phi'_2(x)]dx.\end{aligned}$$

Now we note that fundamental solutions $\Phi(x,k)$ and $\Phi'(x,k)$ solve the Zakharov-Shabat system (4.18), hence

$$\begin{aligned}(\phi_1(0)-\phi_2(0))(\phi'_1(0)+\phi'_2(0))-(\phi_1(0)+\phi_2(0))(\phi'_1(0)-\phi'_2(0))=\\ =2\int_0^l[-(q'_d-ik)\phi'_1\phi_2+q'_+\phi_2\phi'_2+q_-\phi_1\phi'_1-(-q_d+ik)\phi'_1\phi_2+\\ +(q_d-ik)\phi_1\phi'_2-q_+\phi_2\phi'_2-q'_-\phi_1\phi'_1+(-q'_d+ik)\phi_1\phi'_2\\ =2\int_0^l\tilde{q}_d(x)\phi'_1(x,k)\phi_2(x,k)dx+2\int_0^l\tilde{q}_d(x)\phi_1(x,k)\phi'_2(x,k)dx+\\ -2\int_0^l\tilde{q}_+(x)\phi_2(x,k)\phi'_2(x,k)dx+2\int_0^l\tilde{q}_-(x)\phi_1(x,k)\phi'_1(x,k)dx.\end{aligned}$$

The formula (4.34) writes for any $k \in \mathbb{R}^+$

$$2\sum_{j=1}^{N}\prod_{i\neq j}(\phi'_{1i}(0)+\phi'_{2i}(0))(\phi_{1i}(0)+\phi_{2i}(0))\times \\ \left[\int_0^{l_j}\tilde{q}_{j,d}(x)\Big(\phi_{1j}(x,k)\phi'_{2j}(x,k)+\phi'_{1j}(x,k)\phi_{2j}(x,k)\Big)dx+ \right. \\ \left.\int_0^{l_j}-\tilde{q}_{j,+}(x)\phi_{2j}(x,k)\phi'_{2j}(x,k)+\tilde{q}_{j,-}(x)\phi_{1j}(x,k)\phi'_{1j}(x,k)dx\right]=0. \quad (4.35)$$

This concludes the proof. □

We are now ready to prove Theorems 7 and 8.

4.6 Identification of the line loss factor

In this section we prove the identifiability of the line loss factor defined as

$$Q_{j,d}(0,l_j)=\int_0^{l_j}q_{j,d}(s)ds$$

for each branch e_j.

Here we prove Theorem 7 applying the characteristic equation (4.35) and the high-frequency behaviors of $\Phi_j(x,k)$ (see Lemma 7).

We define the function:

$$F(k):=\sum_{j=1}^{N}\prod_{n\neq j}(e^{Q_{n,d}(0,l_n)-ikl_n}+e^{-Q_{n,d}(0,l_n)+ikl_n})(e^{Q'_{n,d}(0,l_n)-ikl_n}+e^{-Q'_{n,d}(0,l_n)+ikl_n})\times \\ \times\int_0^{l_j}\tilde{q}_{j,d}(x)(e^{\tilde{Q}_{j,d}(x,l_j)}+e^{-\tilde{Q}_{j,d}(x,l_j)})dx,$$

where $\tilde{Q}_{j,d}(x,l_j)$ denotes the difference $Q_{j,d}(x,l_j)-Q'_{j,d}(x,l_j)$. The asymptotic formula (4.20) applied to the equation (4.35) implies

$$F(k)=\mathcal{O}\left(\frac{1}{k}\right) \qquad \text{as } k\to\infty.$$

Since $F(k)$ is almost periodic function with respect to the frequency k, the behavior at infinity as $1/k$ implies $F(k)=0$ and this is equivalent to

$$\sum_{j=1}^{N}\prod_{n\neq j}(e^{Q_{n,d}(0,l_n)-ikl_n}+e^{-Q_{n,d}(0,l_n)+ikl_n})(e^{Q'_{n,d}(0,l_n)-ikl_n}+e^{-Q'_{n,d}(0,l_n)+ikl_n})\times$$
$$\times\int_0^{l_j}\tilde{q}_{j,d}(x)\cosh(\tilde{Q}_{j,d}(x,l_j))dx=0.$$

The integral can be easily calculated, hence we have for all $k\in\mathbb{R}^+$

$$\sum_{j=1}^{N}\prod_{n\neq j}(e^{Q_{n,d}(0,l_n)-ikl_n}+e^{-Q_{n,d}(0,l_n)+ikl_n})(e^{Q'_{n,d}(0,l_n)-ikl_n}+e^{-Q'_{n,d}(0,l_n)+ikl_n})\times$$
$$\times(\sinh(\tilde{Q}_{j,d}(0,l_j)))=0. \quad (4.36)$$

Under the assumption **B1** and ordering the branch lengths so that $l_1<l_2<\ldots<l_N$, there is only one term in the expression (4.35) whose frequency is given by $2(l_2+\ldots+l_N)$. Considering this term and indentifying it to zero, we have easily $\sinh(\tilde{Q}_{1,d}(0,l_1))=0$ which implies

$$\tilde{Q}_{1,d}(0,l_1)=0.$$

Consequently we can identify the quantity

$$\int_0^{l_1}q_{1,d}(s)ds=\int_0^{l_1}q'_{1,d}(s)ds.$$

Now the equation (4.35) can be simplified to:

$$\sum_{j=2}^{N}\prod_{n\neq j}(e^{Q_{n,d}(0,l_n)-ikl_n}+e^{-Q_{n,d}(0,l_n)+ikl_n})(e^{Q'_{n,d}(0,l_n)-ikl_n}+e^{-Q'_{n,d}(0,l_n)+ikl_n})\times$$
$$\times(\sinh(\tilde{Q}_{j,d}(0,l_j))=0.$$

and we conclude the proof of Theorem 7 repeating the same argument $N-1$ times.

Remark 33. We have identified the quantity $Q_{j,d}(0,l_j)$ for each branch. Getting back

to the line parameters, it writes

$$Q_{j,d}(0,l_j) = \int_0^{l_j} \frac{1}{2}\left(\frac{R_j(x)}{L_j(x)} + \frac{G_j(x)}{C_j(x)}\right) dx$$

and this is called the *line loss factor*.

4.7 Identifiability of $\frac{R}{L}$ and $\frac{G}{C}$

In this section we examine the case of a uniform transmission line network and we show that under the assumption of weak conductance

$$\frac{G}{C} < \frac{R}{L},$$

we can identify these two parameter ratios.
In order to prove Theorem 8, we introduce an auxiliary proposition:

Proposition 11. *Consider a star-shaped graph Γ satisfying the geometrical assumptions **B1**. Let's consider two potential sets $\boldsymbol{q} = \otimes_{j=1}^N (q_{j,+}, q_{j,-}, q_{j,d})$ and $\boldsymbol{q'} = \otimes_{j=1}^N (q'_{j,+}, q'_{j,-}, q'_{j,d})$ satisfying the hypothesis:*

C5 *At the extremities $x = l_j$ and $x = 0$, the potentials verify*

$$\begin{cases} q_{j,+}(l_j) = -q_{j,-}(l_j) = \mathfrak{a}_j^l, \\ q_{j,+}(0) = -q_{j,-}(0) = \mathfrak{a}_j^0. \end{cases} \qquad j = 1, \dots, N$$

C6 *We assume for the potentials to satisfy:*

$$q_{j,-}, q_{j,+}, q_{j,d} \in H^2(0, l_j) \qquad \forall j = 1, \dots, N.$$

If they give rise to the same reflection coefficients $r(k) \equiv r'(k)$, then the following quantity

$$\tilde{\mathcal{Q}}_j(\boldsymbol{q}, \boldsymbol{q'}) := \int_0^{l_j} \cosh(\tilde{Q}_{j,d}(0,x))\Big(q'_{j,+}(x)q'_{j,-}(x) - q_{j,+}(x)q_{j,-}(x)\Big)dx. \tag{4.37}$$

is equal to zero on each branch. Here

$$\tilde{Q}_{j,d}(0,x) = Q_{j,d}(0,x) - Q'_{j,d}(0,x) = \int_0^x (q_{j,d}(s) - q'_{j,d}(s))ds.$$

Remark 34. The auxiliary proposition is a generalization of Theorem 7. Indeed, in order to obtain (4.37), we will need to simplify (4.35) within high-frequency regimes by considering higher order approximation of $(\phi_{1j}(x,k), \phi_{2j}(x,k))$ than (4.20).

Remark 35. The condition **C5** represents the case where at the extremities, the transmission lines are uniform, i.e. the line parameters R, L, C and G are constant. In this case we are implicitly excluding any possible electric fault of the connectors.

Before passing to the proof of the proposition, we further need a lemma on the fundamental solutions and their asymptotic behaviors. For simplicity's sake, let's parametrize each branch in the opposite sense $x \mapsto l_j - x$. This choice is useful, since we are dealing with fundamental solutions. In the new coordinates 0 represents the terminal node, while l_j is the central node.
The lemma describes the high frequency behavior of the fundamental solutions up to the second order on a segment $[0, l]$.

Lemma 9. *Let $\phi_1(x,k)$ and $\phi_2(x,k)$ be the fundamental solution associated to the Zakharov-Shabat system defined on the interval $[0,l]$ with the Cauchy boundary condition*

$$\phi_1(0,k) = 1 \qquad \phi_2(0,k) = 1.$$

Moreover let's suppose that the potentials (q_+, q_-, q_d) verify the following condition

C5.I *At the extremity $x = 0$, the potentials verify*

$$q_+(0) = -q_-(0) = \mathfrak{a}.$$

Their asymptotic behavior at the second order is given by

$$\begin{cases} \phi_1(x,k) = e^{Q_d(0,x)-ikx}\left[1 + \frac{\mathfrak{a}}{2ik}\right] - \frac{1}{2ik}e^{-Q_d(0,x)+ikx}q_+(x) + \mathcal{O}\left(\frac{1}{k^2}\right) \\ \\ \phi_2(x,k) = e^{-Q_d(0,x)+ikx}\left[1 + \frac{\mathfrak{a}}{2ik}\right] + \frac{1}{2ik}e^{+Q_d(0,x)-ikx}q_-(x) + \mathcal{O}\left(\frac{1}{k^2}\right) \end{cases} \tag{4.38}$$

where $Q_d(0,x) = \int_0^x q_d(s)ds$.

We also have the following high frequency behaviors for k tending to $+\infty$:

$$\begin{aligned}
\phi_1(x)\phi_2'(x)+\phi_1'(x)\phi_2(x) &= \left[e^{\tilde{Q}_d(0,x)}+e^{-\tilde{Q}_d(0,x)}\right]\left(1+\frac{\mathfrak{a}}{ik}\right)+\mathcal{O}\left(\frac{1}{k^2}\right), \quad (4.39)\\
\phi_2(x)\phi_2'(x) &= e^{-(Q_d(0,x)+Q_d'(0,x)+2ikx)}+\frac{1}{2ik}e^{-\tilde{Q}_d(0,x)}q_-'(x)\\
&\quad +\frac{1}{2ik}e^{\tilde{Q}_d(0,x)}q_-(x)+\mathcal{O}\left(\frac{1}{k^2}\right), \quad (4.40)\\
\phi_1(x)\phi_1'(x) &= e^{(Q_d(0,x)+Q_d'(0,x)-2ikx)}-\frac{1}{2ik}e^{\tilde{Q}_d(0,x)}q_+'(x)\\
&\quad -\frac{1}{2ik}e^{-\tilde{Q}_d(0,x)}q_+(x)+\mathcal{O}\left(\frac{1}{k^2}\right). \quad (4.41)
\end{aligned}$$

As usual, the symbol $\sim$ denotes the error terms.

Proof. The proof can be found in the Appendix C.2. □

Proof of Proposition 11. The idea of the proof is basically the same as Theorem 7: we apply to the characteristic equation (4.35) the asymptotic behavior of the fundamental solutions up to the second order. The characteristic equation for Zakharov-Shabat system write for all $k\in\mathbb{R}^+$

$$\begin{aligned}
&\sum_{j=1}^{N}\prod_{i\neq j}(\phi_{1i}'(l_i,k)+\phi_{2i}'(l_i,k))(\phi_{1i}(l_i,k)+\phi_{2i}(l_i,k))\times\\
&\left[\int_0^{l_j}\tilde{q}_{j,d}(x)\Big(\phi_{1j}(x,k)\phi_{2j}'(x,k)+\phi_{1j}'(x,k)\phi_{2j}(x,k)\Big)dx+\right.\\
&\left.\int_0^{l_j}-\tilde{q}_{j,+}(x)\phi_{2j}(x,k)\phi_{2j}'(x,k)+\tilde{q}_{j,-}(x)\phi_{1j}(x,k)\phi_{1j}'(x,k)dx\right]=0.
\end{aligned}$$

Applying (4.39),(4.40) and (4.41), the latter expression becomes

$$\begin{aligned}
&\sum_{j=1}^{N}\prod_{n\neq j}(e^{Q_{n,d}(0,l_n)-ikl_n}+e^{-Q_{n,d}(0,l_n)+ikl_n})(e^{Q_{n,d}'(0,l_n)-ikl_n}+e^{-Q_{n,d}'(0,l_n)+ikl_n})\times\\
&\times\left\{\left(1+\frac{\mathfrak{a}}{ik}\right)\int_0^{l_j}\tilde{q}_{j,d}(x)\left(e^{\tilde{Q}_{j,d}(0,x)}+e^{-\tilde{Q}_{j,d}(0,x)}\right)dx+\right.\\
&-\int_0^{l_j}\tilde{q}_{j,+}(x)\left[e^{Q_{j,d}(0,x)+Q_{j,d}'(0,x)+2ikx}+\frac{e^{\tilde{Q}_{j,d}(0,x)}}{2ik}q_{j,-}(x)+\frac{e^{-\tilde{Q}_{j,d}(0,x)}}{2ik}q_{j,-}'(x)\right]dx\\
&\left.+\int_0^{l_j}\tilde{q}_{j,-}(x)\left[e^{Q_{j,d}(0,x)+Q_{j,d}'(0,x)-2ikx}-\frac{e^{\tilde{Q}_{j,d}(0,x)}}{2ik}q_{j,+}'(x)-\frac{e^{-\tilde{Q}_{j,d}(0,x)}}{2ik}q_{j,+}(x)\right]dx\right\}=\mathcal{O}\left(\frac{1}{k^2}\right).
\end{aligned}$$

We note that the second line is zero. In fact, the integral can be computed explicitly, applying the results of Theorem 7,

$$\left(1+\frac{\mathfrak{a}}{ik}\right)\int_0^{l_j}\tilde{q}_{j,d}(x)\left(e^{\tilde{Q}_{j,d}(0,x)}+e^{-\tilde{Q}_{j,d}(0,x)}\right)dx=\left(1+\frac{\mathfrak{a}}{ik}\right)\sinh(\tilde{Q}_{j,d}(0,l_j))=0.$$

Re-ordering the terms, the characteristic equation can be simplified to:

$$\begin{aligned}\sum_{j=1}^{N}\prod_{n\neq j}&(e^{Q_{n,d}(0,l_n)-ikl_n}+e^{-Q_{n,d}(0,l_n)+ikl_n})(e^{Q'_{n,d}(0,l_n)-ikl_n}+e^{-Q'_{n,d}(0,l_n)+ikl_n})\times\\&+\left\{\int_0^{l_j}\left(-\tilde{q}_{j,+}(x)e^{-Q_{j,d}(0,x)-Q'_{j,d}(0,x)+2ikx}+\tilde{q}_{j,-}(x)e^{Q_{j,d}(0,x)+Q'_{j,d}(0,x)-2ikx}\right)dx+\right.\\&\qquad-\int_0^{l_j}\frac{\tilde{q}_{j,+}(x)}{2ik}\left[e^{-\tilde{Q}_{j,d}(0,x)}q'_{j,-}(x)+e^{\tilde{Q}_{j,d}(0,x)}q_{j,-}(x)\right]dx+\\&\left.-\int_0^{l_j}\frac{\tilde{q}_{j,-}(x)}{2ik}\left[+e^{\tilde{Q}_{j,d}(0,x)}q'_{j,+}(x)+e^{-\tilde{Q}_{j,d}(0,x)}q_{j,+}(x)\right]dx\right\}=\mathcal{O}\left(\frac{1}{k^2}\right).\end{aligned}\tag{4.42}$$

We define

$$\tilde{\mathcal{B}}_j(\mathbf{q},\mathbf{q}';k):=\int_0^{l_j}\left(-\tilde{q}_{j,+}(x)e^{-Q_{j,d}(0,x)-Q'_{j,d}(0,x)+2ikx}+\tilde{q}_{j,-}(x)e^{Q_{j,d}(0,x)+Q'_{j,d}(0,x)-2ikx}\right)dx.$$

and

$$\begin{aligned}\tilde{\mathcal{Q}}^1_j(\mathbf{q},\mathbf{q}'):=&-\int_0^{l_j}\tilde{q}_{j,+}(x)\left[e^{-\tilde{Q}_{j,d}(0,x)}q'_{j,-}(x)+e^{\tilde{Q}_{j,d}(0,x)}q_{j,-}(x)\right]dx+\\&-\int_0^{l_j}\tilde{q}_{j,-}(x)\left[+e^{\tilde{Q}_{j,d}(0,x)}q'_{j,+}(x)+e^{-\tilde{Q}_{j,d}(0,x)}q_{j,+}(x)\right]dx.\end{aligned}$$

The equation (4.42) can be rewritten as

$$\sum_{j=1}^{N}\prod_{n\neq j}\cosh^2(Q_{n,d}(0,l_n)-ikl_n)\left[\tilde{\mathcal{B}}_j(\mathbf{q},\mathbf{q}';k)+\frac{1}{2ik}\tilde{\mathcal{Q}}^1_j(\mathbf{q},\mathbf{q}')\right]=\mathcal{O}\left(\frac{1}{k^2}\right).$$

A simple integration by parts togher with the assumptions **C5** and **C6** implies

$$\tilde{\mathcal{B}}_j(\mathbf{q},\mathbf{q}';k)=\mathcal{O}\left(\frac{1}{k^2}\right).$$

Therefore we have

$$\sum_{j=1}^{N}\prod_{n\neq j}\cosh^2(Q_{n,d}(0,l_n)-ikl_n)\left[\tilde{\mathcal{Q}}_j^1(\mathbf{q},\mathbf{q}')\right]=0. \tag{4.43}$$

As in the proof of Theorem 7, we suppose that $l_1<\ldots<l_N$. We note that there is only one term in expression (4.43) whose frequency is given by $2(l_2+\ldots+l_N)$. Considering this term and identifying it to zero, we arrive to

$$\tilde{\mathcal{Q}}_1^1(\mathbf{q},\mathbf{q}')=0.$$

Now the expression (4.43) can be simplified as

$$\sum_{j=2}^{N}\prod_{n\neq j}\cosh^2(Q_{n,d}(0,l_n)-ikl_n)\left[\tilde{\mathcal{Q}}_j^1(\mathbf{q},\mathbf{q}')\right]=0. \tag{4.44}$$

Repeating this argument $N-1$ times, we obtain

$$\tilde{\mathcal{Q}}_j^1(\mathbf{q},\mathbf{q}')=0,\qquad \forall j=1,\ldots,N.$$

It remains to show that

$$\tilde{\mathcal{Q}}_j^1(\mathbf{q},\mathbf{q}')=\tilde{\mathcal{Q}}_j(\mathbf{q},\mathbf{q}').$$

Developing the $\tilde{\mathcal{Q}}_j^1(\mathbf{q},\mathbf{q}')$ we have:

$$\tilde{\mathcal{Q}}_j^1=\int_0^{l_j}e^{\tilde{Q}_{j,d}(0,x)}\Big(-\tilde{q}_{j,+}(x)q_{j,-}(x)-\tilde{q}_{j,-}(x)q'_{j,+}(x)\Big)+$$
$$+e^{-\tilde{Q}_{j,d}(0,x)}\Big(-\tilde{q}_{j,+}(x)q'_{j,-}(x)-\tilde{q}_{j,-}(x)q_{j,+}(x)\Big)dx.$$

For simplicity's sake, we look only at the integrands omitting the index j and the

dependence on the variable x, i.e. $q_{j,+}(x) = q_+$, $q_{j,-}(x) = q_-$, and $Q_{j,d}(0,x) = Q_d$

$$
\begin{aligned}
e^{\tilde{Q}_d}\Big(&- \tilde{q}_+ q_- - \tilde{q}_- q'_+\Big) + e^{-\tilde{Q}_d}\Big(- \tilde{q}_+ q'_- - \tilde{q}_- q_+\Big) = \\
&= e^{\tilde{Q}_d}\Big(- (q_+ - q'_+)q_- - (q_- - q'_-)q'_+\Big) + e^{-\tilde{Q}_d}\Big(- (q_+ - q'_+)q'_- - (q_- - q'_-)q_+\Big) \\
&= e^{\tilde{Q}_d}\Big(- q_+ q_- + q'_+ q'_-\Big) + e^{-\tilde{Q}_d}\Big(+ q'_+ q'_- - q_- q_+\Big) \\
&= (e^{-\tilde{Q}_d} + e^{\tilde{Q}_d})\Big(q'_+ q'_- - q_- q_+\Big) = \cosh(\tilde{Q}_d(0,x))\Big(q'_+(x)q'_-(x) - q_-(x)q_+(x)\Big).
\end{aligned}
$$

So this concludes the proof of the proposition. □

In terms of line parameters the quantity (4.37) represents

$$
\begin{aligned}
\tilde{\mathcal{Q}}_j(\mathbf{q},\mathbf{q}') = \int_0^{l_j} \cosh(\int_0^x \left(\frac{\tilde{R}(s)}{L(s)} + \frac{\tilde{G}(s)}{C(s)}ds\right)) \Bigg[&\frac{1}{16}\left(\frac{d}{dx}\log\frac{L(x)}{C(x)}\right)^2 + \\
&-\frac{1}{16}\left(\frac{d}{dx}\log\frac{L'(x)}{C'(x)}\right)^2 + \left(\frac{R'(x)}{L'(x)} - \frac{G'(x)}{C'(x)}\right)^2 - \left(\frac{R(x)}{L(x)} - \frac{G(x)}{C(x)}\right)^2\Bigg] dx
\end{aligned}
$$

Remark 36. If we are restrained to the lossless network, the expression (4.37) is equivalent to the result obtain in Theorem 4 of Chapter 3. Imposing the potentials $q_{j,d} \equiv 0$ and $q_{j,-} = q_{j,+} := q_j$, $\mathcal{Q}_j = 0$ implies that

$$
\int_0^{l_j}\left(\frac{d}{dx}\log Z_{c,j}(x)\right)^2 dx = \int_0^{l_j}\left(\frac{d}{dx}\log Z'_{c,j}(x)\right)^2 dx,
$$

We finish this section giving the proof of Theorem 8. We are in the case where the network transmission line are uniform and we want to prove the identifiability of two aggregates of line parameters.

Proof of Theorem 8. We recall that the potentials for a uniform network are given by

$$
q_{j,d}(x) = +\frac{1}{2}\left(\frac{R_j}{L_j} + \frac{G_j}{C_j}\right), \tag{4.15}
$$

$$
q_{j,-}(x) = -\frac{1}{2}\left(\frac{R_j}{L_j} - \frac{G_j}{C_j}\right), \tag{4.17}
$$

$$
q_{j,+}(x) = +\frac{1}{2}\left(\frac{R_j}{L_j} - \frac{G_j}{C_j}\right). \tag{4.16}
$$

Theorem 7 states the identifiability of the loss line factor

$$\int_0^{l_j} q_{j,d} dx = \frac{l_j}{2}\left(\frac{R_j}{L_j} + \frac{G_j}{C_j}\right) = \alpha_j, \qquad \forall j = 1, \ldots, N$$

The uniform parameters verify the conditions **C5** and **C6** and, thanks to Proposition 11, we have

$$\int_0^{l_j} \cosh(\alpha_j)(q_{lj}^2) dx = \int_0^{l_j} \cosh(\alpha_j)\frac{1}{4}\left(\frac{R_j}{L_j} - \frac{G_j}{C_j}\right)^2 dx = \beta_j, \qquad j = 1, \ldots, N$$

for some β_j.
To identify the two aggregate parameters R/L and G/C, we have to show the uniqueness of the solution of the following system:

$$\begin{cases} \frac{l_j}{2}\left(\frac{R_j}{L_j} + \frac{G_j}{C_j}\right) = \alpha_j, \\ \frac{l_j}{4}\cosh(\alpha_j)\left(\frac{R_j}{L_j} - \frac{G_j}{C_j}\right)^2 = \beta_j. \end{cases}$$

The above system is equivalent to the two systems of equations

$$\mathcal{S}^{\pm} := \begin{cases} \frac{R_j}{L_j} + \frac{G_j}{C_j} = \check{\alpha}_j \\ \frac{R_j}{L_j} - \frac{G_j}{C_j} = \pm\check{\beta}_j \end{cases} \tag{4.45}$$

where $\check{\alpha}_j = 2\alpha_j/l_j$ and $(\check{\beta}_j)^2 = 4\beta_j/(\cosh(\alpha_j)l_j)$. A priori we have two possible solutions, but only the solution of $\mathcal{S}^+$ given by

$$\frac{R_j}{L_j} = \frac{1}{2}(\check{\alpha}_j + \check{\beta}_j);$$
$$\frac{G_j}{C_j} = \frac{1}{2}(\check{\alpha}_j - \check{\beta}_j);$$

verifies the condition

$$\frac{G_j}{C_j} < \frac{R_j}{L_j}.$$

Hence it is the only admissible solution. □

4.8 Summary and further directions

In this chapter we have presented some results for the inverse scattering problem on the lossy transmission network.

We have shown the direct scattering problem for both lossy transmission network: the transmission line parameters determine uniquely the reflection coefficient $r(k)$. The proof can be easily adapted to the case of a tree network.
For the lossy case, the presence of dissipation avoids the phenomenon of resonant frequencies: we have shown that the condition

$$\min_{x\in I_1}\left(\frac{G(x)}{C(x)},\frac{R(x)}{L(x)}\right)=\mathfrak{c}>0, \tag{1.77}$$

is necessary for the well-posedness of the direct scattering problem. A further direction could be to investigate on the sufficient condition to have no resonant phenomenon.

The first result concerns the identification problem related to the geometry of the star-shape network. Once again, the knowledge of the reflection coefficient allows to identify the lengths of the branch of the network.

Theorem (Theorem 6)**.** *Assume for the star-shaped graph* Γ^+ *that*

B1 $l_j \neq l_{j'}$ *for any* $j, j' \in \{1, \cdots, N\}$ *such that* $j \neq j'$.

C4 *We assume for the potentials to satisfy*

$$q_{j,+}, q_{j,-}, q_{j,d} \in H^1(0, l_j) \quad \forall j = 1, \ldots, N.$$

The knowledge of the reflection coefficient $r(k)$ *determines uniquely the lengths* $(l_j)_{j=1}^N$.

A possible application is the detection and localization of hard faults, appearing as open circuits, on a star-shaped wired network.

This result improves the engineering state of art: Furse [21] retrieve the position of a load (open, short or resistive) on a single uniform transmission line through a PDFDR system.

We have studied the identifiability of the potential on each line: through the analysis of the reflection coefficient $r(k)$ we can retrieve the loss line factor defined

$$Q_{j,d}(0,l_j) = \int_0^{l_j} \left(\frac{R_j}{L_j}(x) + \frac{G_j}{C_j}(x) \right) dx$$

on each line.

Theorem (Theorem 7)**.** *Assume for the star-shaped graph Γ^+ that **B1** is valid. If there exist two potentials $\boldsymbol{q} = \otimes_{j=1}^N (q_{j,+}, q_{j,-}, q_{j,d})$ and $\boldsymbol{q'} = \otimes_{j=1}^N (q'_{j,+}, q'_{j,-}, q'_{j,d})$ satisfying **C4** and the condition $Z_{c0j}(0) = Z'_{c0j}(0)$ for all $j = 0, \ldots, N$ and giving rise to the same reflection coefficient, $r(k) \equiv r'(k)$, one necessarily has:*

$$\int_0^{l_j} q_{j,d}(s)ds = \int_0^{l_j} q'_{j,d}(s)ds \qquad j = 1, \cdots, N.$$

Supposing the reliability of the connectors at the central node $Z_{c0j}(0) = Z'_{c0j}(0)$, the measurement of a reflection coefficient allows to identify all soft faults causing line parameters variations. This test classify all soft faults with respect the quantity $Q_j(0, l_j)$.

A third result is the identifiability of two parameter aggregates

$$\frac{R_j}{L_j} \text{ and } \frac{G_j}{C_j}$$

for the case of the uniform transmission network. For the railway's maintenance operation, the detection of the isolation faults is related to the identification of the quantity G_j/C_j: the main difficult is due to the fact this term has a weak influence on the electric transmission.

Theorem (Theorem 8)**.** *Let us consider a star-shaped network Γ^+ with the geometric assumption **B1**. Let the potentials $\boldsymbol{q} = \otimes_{j=1}^N (q_{j,+}, q_{j,-}, q_{j,d})$ be of the following forms:*

$$q_{j,d}(x) := \frac{1}{2} \left(\frac{R_j}{L_j} + \frac{G_j}{C_j} \right), \tag{4.15}$$

$$q_{j,+}(x) := +\frac{1}{2} \left(\frac{R_j}{L_j} - \frac{G_j}{C_j} \right), \tag{4.16}$$

$$q_{j,-}(x) := -\frac{1}{2} \left(\frac{R_j}{L_j} - \frac{G_j}{C_j} \right). \tag{4.17}$$

where R_j, L_j, G_j and C_j are constant parameters uniformly defined on each branch. If $G_j/C_j < R_j/L_j$ on each branch, then the reflection coefficient $r(k)$ allows to identify uniquely these two quantities

$$\frac{R_j}{L_j} \qquad \textit{and} \qquad \frac{G_j}{C_j}$$

on all branches e_j of the star-shaped network Γ.

The assumption $\frac{G}{C} < \frac{R}{L}$ becomes natural in the context of Theorem 8 . The measurement of one reflection coefficient determines uniquely these two quantities.

Chapter 5

Conclusions and Perspectives

The initial goal of this thesis was to determine the information contained in the reflectometry measurements used for fault-detection and fault diagnosis on electrical networks. This led us to formulate the basic reflectometry technique as a mathematical inverse problem and to study its wellposedness. Following [30], we have been able to model the reflectometry experiments through the inverse scattering for Zakharov-Shabat system and $1-d$ Schrödinger equation. Motivated by some industrial problems, we have considered the reflectometry experiment on networks: we restrict ourself to the case where we have only one reflectometer on a star-shaped network.
This manuscript presents multiple results for the inverse scattering problems on a star-shaped graph for both Zakharov-Shabat system and Schrödinger equation: we have studied the identifiability of potentials and geometric parameters.

Despite our results on the identifiability of hard and soft faults, fault detection and diagnosis require significant improvements. While we have discussed the identification of potential from a single reflection coefficient, it is necessary to find a method for the reconstruction of the potentials from a larger scattering data set. An interesting direction of research could be expanding the scattering data for a network: we have considered only one plug-in port for reflectometry measurements omitting measurements for transmitted signals. A larger scattering data set, including other reflection and *transmission* coefficients could lead to better results in the identification problems.

Hard faults detection problem has been solved in the lossy case for a star-shaped network. Research needs to be performed toward the generalization of this results on

a tree. It seems that the number of matched load branches can be retrieved using a high frequency analysis of reflection coefficient.

We suggest, also, to develop a numerical algorithm to retrieve hard faults on a star shaped graph. In real application, only a limited frequency range is available and so, it would be interesting to investigate what result can be obtained from a partial knowledge of reflection coefficients for a possible implementation on the on-board diagnosis device.

The results for the identification of soft faults improve in a significant way the state of art of research. On the other hand, these identifications together with technical limitations are not yet sufficient for a real industrial application.

Looking at the reflectometry applications, we propose to find an algorithm to retrieve from the reflection coefficient information on potential such as the loss line factor or, for the lossless case, the quantity $\int_0^{l_j} q_j(s)ds$. The knowledge of such information allows to detect, at least, a certain class of soft faults.

In this thesis, we have always supposed the continuity of the line parameters (see assumption $A1$ and $C1$), while in the real setting it is common to have piecewise continuous transmission line parameters. As for the future research, it would be fruitful to relax the potential's hypothesis.

Finally, another limitation for the applicability of all the results of this manuscript is due to the fact that we are generally interested in non-invasive fault detection. Indeed, one would like to be able to detect and localize the faults without disturbing the normal activity of the network. However, the tests proposed in this chapter assume open or short circuit boundary conditions at the extremities of the branches. One should be able to replace two such experiments by two less invasive ones. This idea has been discussed in Remark 24 of Chapter 3 and should be studied in a future work.

Appendix A

Useful Formulas

Generic boundary conditions

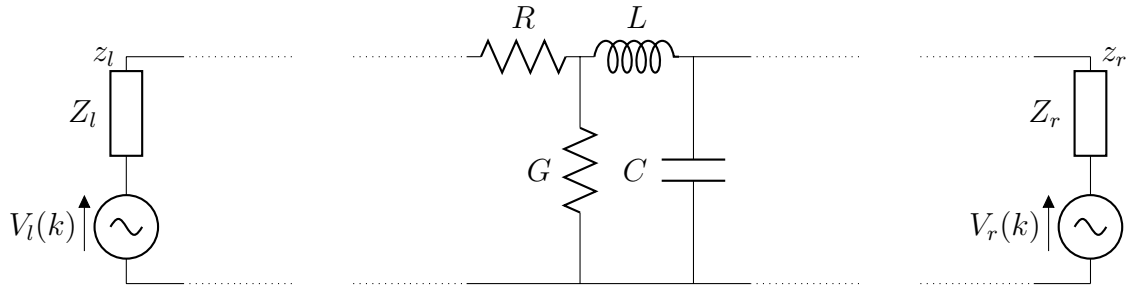

Figure A.1: Transmission line model with two source generators

- Telegrapher's equation in harmonic regime of frequencies k

$$\begin{cases} \partial_x V(k,z) + ikL(z)I(k,z) + R(z)I(k,z) = 0, \\ \partial_x I(k,z) + ikC(z)V(k,z) + G(z)V(k,z) = 0. \end{cases} \tag{1.33}$$

- Telegrapher's generic boundary conditions:

$$\begin{cases} V(k,z_l) + Z_l(k)I(k,z_l) = V_l(k), \\ V(k,z_r) - Z_r(k)I(k,z_r) = V_r(k). \end{cases} \tag{1.34}$$

One source $V_s(k)$ (after the Liouville transformation)

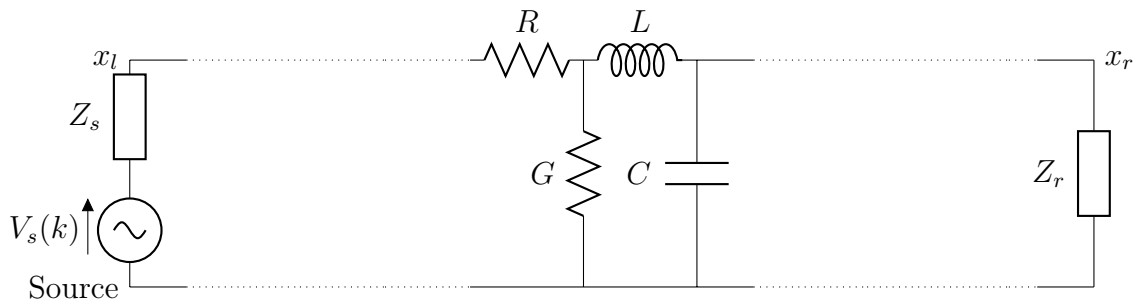

Figure A.2: Transmission line model with one source generator

- Zakharov-Shabat variables

$$\begin{cases} \nu_1(x,k) = \frac{1}{\sqrt{2}}\left[Z_{c0}^{-1/2}(x)V(k,x) - Z_{c0}^{1/2}(x)I(k,x)\right], \\ \\ \nu_2(x,k) = \frac{1}{\sqrt{2}}\left[Z_{c0}^{-1/2}(x)V(k,x) + Z_{c0}^{1/2}(x)I(k,x)\right]. \end{cases} \tag{1.45}$$

- Zakharov-Shabat system

$$\begin{cases} \partial_x\nu_1(x,k) + ik\nu_1(x,k) = q_d(x)\nu_1(x,k) - q_+(x)\nu_2(x,k), \\ \partial_x\nu_2(x,k) - ik\nu_2(x,k) = -q_d(x)\nu_2(x,k) - q_-(x)\nu_1(x,k), \end{cases} \tag{1.46}$$

- Zakharov-Shabat potentials

$$q_d(x) = \frac{1}{2}\left(\frac{R(x)}{L(x)} + \frac{G(x)}{C(x)}\right), \tag{1.47}$$

$$q_-(x) = \frac{1}{4}\frac{d}{dx}\left[\log\frac{L(x)}{C(x)}\right] - \frac{1}{2}\left(\frac{R(x)}{L(x)} - \frac{G(x)}{C(x)}\right), \tag{1.48}$$

$$q_+(x) = \frac{1}{4}\frac{d}{dx}\left[\log\frac{L(x)}{C(x)}\right] + \frac{1}{2}\left(\frac{R(x)}{L(x)} - \frac{G(x)}{C(x)}\right). \tag{1.49}$$

- Boundary parameters

$$\begin{aligned} \rho_r(k) &= \frac{Z_r(k) - Z_{c0}(x_r)}{Z_r(k) + Z_{c0,}(x_r)}, \\ \rho_s(k) &= \frac{Z_s(k) - Z_{c0}(x_l)}{Z_s(k) + Z_{c0}((x_l)}, \\ \nu_s(k) &= \frac{V_s(k)}{\sqrt{2Z_{c0}(x_l)}}. \end{aligned}$$

- Boundary conditions for the Zakharov-Shabat system

$$\begin{aligned} \nu_1(x_r,k) - \rho_r(k)\nu_2(x_r,k) &= 0, \\ \nu_2(x_l,k) - \rho_s(k)\nu_1(x_l,k) &= (1-\rho_s(k))\nu_s(k). \end{aligned}$$

Case	**Physical interpretation**	**Boundary parameters for Telegrapher's equations**	**Boundary parameters for Zakharov-Shabat equations**	**Boundary conditions**
Short circuit	$V(x_r) = 0$	$Z_r(k) = 0$	$\rho_r(k) = -1$	$\nu_1(x_r, k) + \nu_2(x_r, k) = 0$
Open circuit	$I(x_r) = 0$	$Z_r(k) = +\infty$	$\rho_r(k) = 1$	$\nu_1(x_r, k) - \nu_2(x_r, k) = 0$
Matching impedance at right end		$Z_r(k) = Z_{c0}(x_r)$	$\rho_r(k) = 0$	$\nu_1(x_r, k) = 0$
Matching impedance at the source generator		$Z_r(k) = Z_{c0}(x_r)$	$\rho_s(k) = 0$	$\nu_2(x_l, k) = \nu_s(k)$

Table A.1: Experiment's conditions

Appendix B

Asymptotic behavior of eigen-values for Schrödinger equations

B.1 Proof of Lemma 3

In this section we are going to prove Lemma 3 of the Chapter 3. We recall it.

Lemma 10. *Assume for the potential $q(x) \in H^1(0,l)$ that $q(0) = 0$, that $\|q\|_{L^\infty(0,l)} < \frac{\pi^2}{4l^2}$ and that $\int_0^l q(s)ds = 0$. Then, there exists a constant $C_0(l)$ such that λ_n, the n-th eigenvalue of the operator $-\frac{\partial^2}{\partial x^2} + q(x)$ on the segment $[0,l]$, with Dirichlet boundary condition at 0 and Neumann boundary condition at l, satisfies*

$$\left|\lambda_n - \frac{(2n-1)^2\pi^2}{4l^2}\right| \leq C_0(l)\frac{\|q\|_{H^1(0,l)}}{2n-1}.$$

Proof. We, basically, use a classical result from the perturbation theory of linear operators (see [32], Chapter VII, Example 2.17). The assumption $\|q\|_{L^\infty(0,l)} < \frac{\pi^2}{4l^2}$ allows us to apply the Taylor expansion of the eigenvalues of the above operator as a perturbation of the Laplacian operator with the same boundary conditions. Therefore, following [32], we have

$$\left|\lambda_n - \frac{(2n-1)^2\pi^2}{4l^2} + 2\int_0^l q(s)\sin^2\left(\frac{(2n-1)\pi}{2l}s\right)ds\right| \leq c_0(l)\frac{\|q\|_{L^\infty}^2}{2n-1},$$

for some constant $c_0(l)$, only depending on the length l. This leads to

$$\begin{aligned}\left|\lambda_n - \frac{(2n-1)^2\pi^2}{4l^2}\right| &\leq c_0(l)\frac{\|q\|^2_{L^\infty}}{2n-1} + 2\left|\int_0^l q(s)\sin^2\left(\frac{(2n-1)\pi}{2l}s\right)ds\right| = \\ &= c_0(l)\frac{\|q\|^2_{L^\infty}}{2n-1} + 2\left|\int_0^l q(s)\frac{1-\cos\left(\frac{(2n-1)\pi}{l}s\right)}{2}ds\right| < \\ &< c_0(l)\frac{\pi^2}{4l^{3/2}}\frac{\|q\|_{H^1(0,l)}}{2n-1} + \left|\int_0^l q(s)\cos\left(\frac{(2n-1)\pi s}{l}\right)ds\right| = \\ &= c_0(l)\frac{\pi^2}{4l^{3/2}}\frac{\|q\|_{H^1(0,l)}}{2n-1} + \frac{l}{(2n-1)\pi)}\left|\int_0^l q'(s)\sin(\frac{(2n-1)\pi s}{l})ds\right| \leq \\ &\leq \left(c_0(l)\frac{\pi^2}{4l^{3/2}} + \frac{l^{3/2}}{\pi\sqrt{2}}\right)\frac{\|q\|_{H^1(0,l)}}{2n-1}.\end{aligned}$$

In the above computations, for passing from the second to the third line, we have applied the facts that $\|q\|_{L^\infty} < \frac{\pi^2}{4l^2}$, that $\|q\|_{L^\infty} \leq \sqrt{l}\|q\|_{H^1}$ (as $q(0) = 0$) and that $\int_0^l q(s)ds = 0$. For passing from the third to the fourth line, we have integrated by parts and finally for passing from the fourth line to last one, we have applied a Cauchy-Schwartz inequality. Therefore, the constant $C_0(l)$ of the Lemma is given as follows:

$$C_0(l) = c_0(l)\frac{\pi^2}{4l^{3/2}} + \frac{l^{3/2}}{\pi\sqrt{2}}.$$

□

Appendix C

Complement to the Zakharov-Shabat system

C.1 Fundamental solutions associated to the Zakharov-Shabat system

In this section we study the fundamental solutions $\Phi(x,k) := (\phi_1(x,k), \phi_2(x,k))$ and $\Psi(x,k) := (\psi_1(x,k), \psi_2(x,k))$ for the following system defined on the interval $[0,l]$

$$\begin{cases} \partial_x \phi_1(x,k) = (q_d(x) - ik)\phi_1(x,k) - q_+(x)\phi_2(x,k), \\ \partial_x \phi_2(x,k) = -q_-(x)\phi_1(x,k) - (q_d(x) - ik)\phi_2(x,k), \end{cases} \tag{C.1}$$

with the Cauchy boundary conditions

$$\begin{aligned} \phi_1(0,k) &= 1 \qquad \phi_2(0,k) = 1. \\ \psi_1(0,k) &= 1 \qquad \psi_2(0,k) = -1. \end{aligned}$$

Proposition 12. *Let $\Phi(x,k)$ and $\Psi(x,k)$ be the fundamental solutions defined above, then they form a basis for the space of solutions of the Zakharov-Shabat system*

$$\partial_x \begin{pmatrix} \nu_1 \\ \nu_2 \end{pmatrix} = -ik\sigma_3 \begin{pmatrix} \nu_1 \\ \nu_2 \end{pmatrix} + \begin{pmatrix} q_d & -q_+ \\ -q_- & -q_d \end{pmatrix} \begin{pmatrix} \nu_1 \\ \nu_2 \end{pmatrix} \qquad \sigma_3 = \begin{pmatrix} 1 & 0 \\ 0 & -1 \end{pmatrix}. \tag{C.2}$$

$$\begin{aligned} \nu_1(l,k) - \rho_s(k)\nu_2(l,k) &= (1-\rho_s(k))\nu_s(k), \\ \nu_2(0,k) - \rho_l(k)\nu_1(0,k) &= 0. \end{aligned} \tag{C.3}$$

Proof. The solutions Φ and Ψ are linearly independent, because the wronskian

$$W(\Phi,\Psi)(x) = \phi_1(x,k)\psi_2(x,k) - \psi_1(x,k)\phi_2(x,k)$$

is always different from zero.
To see $W(\Phi,\Psi) \neq 0$, it is enough to compute the derivative with respect to the x and observe that

$$\frac{d}{dx}W(\Phi,\Psi)(x) \equiv 0 \qquad \forall x \in [0,l].$$

Hence

$$W(\Phi,\Psi)(x) \equiv W(\Phi,\Psi)(l) = -2 \neq 0 \qquad \forall x \in [0,l].$$

The dimension of the solution's space of the Zakharov-Shabat system (C.2)-(C.3) is two, so consequently any solution $Y(x,k)$ can be written as

$$Y(x,k) = \alpha(k)\Phi(x,k) + \beta(k)\Psi(x,k),$$

with α and β are real value functions depending from the frequency k. The proof is complete. □

We have chosen the Cauchy boundary conditions

$$\Phi(0,k) = \begin{pmatrix} 1 \\ 1 \end{pmatrix}, \qquad \Psi(0,k) = \begin{pmatrix} 1 \\ -1 \end{pmatrix},$$

but we could have chosen any other linearly independent couples. The more conventional choice is

$$\tilde{\Phi}(0,k) = \begin{pmatrix} 1 \\ 0 \end{pmatrix}, \qquad \tilde{\Psi}(0,k) = \begin{pmatrix} 0 \\ 1 \end{pmatrix},$$

but in our case the physical interpretation plays a crucial role. The fundamental solutions Φ and Ψ correspond to the situation when there is respectively an open and short circuits.
The fundamental solutions $\tilde{\Phi}$ and $\tilde{\Psi}$ represents physically the adaptation of line. In fact the $\tilde{\Phi}(x,k)$ behaves as the load at the right end $x = 0$ is matched, while the

fundamental solution $\tilde{\Psi}(x,k)$ is equivalent to the matched load at the left end $x = l$.

C.2 High frequency behavior of fundamental solutions for Zakharov-Shabat system

In this section we study the behavior at high frequency for the solutions of the Zakharov-Shabat system (1.46) with three potentials and so we will be able to prove the Lemma 9 of Chapter 4.

For simplicity sakes, we will split the result in two propositions: in the first proposition we are going to show the asymptotic behavior of solutions to the Zakharov-Shabat system. Next we are going to prove the Lemma 9 applying the previous results to the fundamental solutions

Proposition 13. *Let $\nu_1(x,k)$ and $\nu_2(x,k)$ a solution of the Zakharov Shabat equations verifying the Cauchy boundary conditions*

$$\nu_1(0,k) = \nu_1, \qquad \nu_2(0,k) = \nu_2, \tag{C.4}$$

for some real ν_1 and ν_2. Their asymptotic behavior at the second order is given by

$$\begin{aligned} \nu_1(x,k) = \quad & e^{Q_d(0,x)-ikx}\nu_1 - \tfrac{1}{2ik}e^{-Q_d(0,x)+ikx}q_+(x)\nu_2 \\ & + \tfrac{e^{Q_d(0,x)-ikx}}{2ik}q_+(0)\nu_2 + \mathcal{O}\left(\tfrac{1}{k^2}\right), \qquad \text{(C.5)} \\ \nu_2(x,k) = \quad & e^{-Q_d(0,x)+ikx}\nu_2 + \tfrac{1}{2ik}e^{+Q_d(0,x)-ikx}q_-(x)\nu_1 \\ & - \tfrac{e^{-Q_d(0,x)+ikx}}{2ik}q_-(0)\nu_1 + \mathcal{O}\left(\tfrac{1}{k^2}\right). \qquad \text{(C.6)} \end{aligned}$$

where $Q_d(0,x) = \int_0^x q_d(s)ds$.

Proof. In order to compute the asymptotic limit of fundamental solutions for three potentials Zakharov-Shabat system (q_+, q_-, q_d), we study first the solutions of the classical Zakharov-Shabat equations with two potentials $r(x)$ and $q(x)$ and through the change of variable proposed by Jaulent [30] seen in Chapter 2 we will arrive to (C.5) and (C.6).

Let $Y(x,k)$ be the solution vector $(y_1(x,k), y_2(x,k))^{tr}$ and let σ_3 be the Pauli matrix

defined in (1.55), the two-potential Zakharov-shabat equation is

$$\frac{d}{dx}Y(x,k) + ik\sigma_3 Y(x,k) = \begin{pmatrix} 0 & q \\ r & 0 \end{pmatrix} Y(x,k). \tag{C.7}$$

The Duhamel's formula is

$$\begin{pmatrix} y_1(x,k) \\ y_2(x,k) \end{pmatrix} = e^{-ik\sigma_3 x} \begin{pmatrix} y_1(0,k) \\ y_2(0,k) \end{pmatrix} + \int_0^x e^{-ik\sigma_3(x-s)} \begin{pmatrix} 0 & q \\ r & 0 \end{pmatrix} \begin{pmatrix} y_1(s,k) \\ y_2(s,k) \end{pmatrix} ds. \tag{C.8}$$

Noting that

$$e^{ik\sigma_3 x} = \cos(kx)Id + i\sin(kx)\sigma_3.$$

the explicit integral solutions are

$$\begin{cases} y_1(x,k) = e^{-ikx}y_1(0,k) + \int_0^x q(s)e^{-ik(x-s)}y_2(s,k)ds \\ y_2(x,k) = e^{ikx}y_2(0,k) + \int_0^x r(s)e^{ik(x-s)}y_1(s,k)ds. \end{cases} \tag{C.9}$$

Integrating by parts, we find that for $k \mapsto \infty$ the development of a solution to the two-potential Zakharov-Shabat system is

$$\begin{aligned} y_1(x,k) &= e^{-ikx}y_1(0,k) + \frac{e^{ikx}}{2ik}q(x)y_2(0,k) - \frac{e^{-ikx}}{2ik}q(0)y_2(0,k) + \mathcal{O}\left(\frac{1}{k^2}\right) \\ y_2(x,k) &= e^{ikx}y_2(0,k) - \frac{e^{-ikx}}{2ik}r(x)y_1(0,k) + \frac{e^{ikx}}{2ik}r(0)y_1(0,k) + \mathcal{O}\left(\frac{1}{k^2}\right). \end{aligned}$$

Using the Jaulent change of variables, we write the solution to the Zakharov-Shabat equations (1.46) in terms of two-potential Zakharov-Shabat equations.
Setting

$$M^-(x) = \begin{pmatrix} exp(+\int_0^x q_d(s)ds) & 0 \\ 0 & exp(-\int_0^x q_d(s)ds) \end{pmatrix},$$

we have that

$$\begin{pmatrix} \nu_1(x,k) \\ \nu_2(x,k) \end{pmatrix} = M^-(x)\mathbf{Y}(x,k)$$

are solutions of the Zakharov-Shabat system (1.46) with boundary condition (C.4).

In particular we have the following equivalences between the potentials

$$r(x) = -e^{2Q_d(0,x)} q_-(x),$$
$$q(x) = -e^{-2Q_d(0,x)} q_+(x),$$

where $Q_d(0,x) = \int_0^x q_d(s)ds$.

We are able to write the asymptotic behavior of the solutions of the Zakharov-Shabat system. As k goes to ∞

$$\begin{aligned}
\nu_1(x,k) &= e^{Q_d(0,x)-ikx}\nu_1 - \frac{1}{2ik}e^{-Q_d(0,x)+ikx}q_+(x)\nu_2 + \frac{e^{Q_d(0,x)-ikx}}{2ik}q_+(0)\nu_2 + \mathcal{O}\left(\frac{1}{k^2}\right),\\
\nu_2(x,k) &= e^{-Q_d(0,x)+ikx}\nu_2 + \frac{1}{2ik}e^{+Q_d(0,x)-ikx}q_-(x)\nu_1 - \frac{e^{-Q_d(0,x)+ikx}}{2ik}q_-(0)\nu_1 + \mathcal{O}\left(\frac{1}{k^2}\right),
\end{aligned}$$

and this concludes the proof. □

We are now able to prove the Lemma 9 used in Chapter 4.

Lemma 11. *Let $(\phi_1(x,k), \phi_2(x,k))$ be the fundamental solution of the Zakharov-Shabat system defined on $[0,l]$ satisfying with the boundary condition*

$$\Phi(0,k) = \begin{pmatrix} 1 \\ 1 \end{pmatrix}.$$

Let assume that the potentials q_- and q_+ verify

C5.I $q_{+j}(0) = -q_{-j}(0) = \mathfrak{a}$.

We have the following high frequency behaviors for the fundamental solution

$$\phi_1(x,k) = e^{Q_d(0,x)-ikx}\left[1 + \frac{\mathfrak{a}}{2ik}\right] - \frac{1}{2ik}e^{-Q_d(0,x)+ikx}q_+(x) + \mathcal{O}\left(\frac{1}{k^2}\right) \quad \text{(C.10)}$$
$$\phi_2(x,k) = e^{-Q_d(0,x)+ikx}\left[1 + \frac{\mathfrak{a}}{2ik}\right] + \frac{1}{2ik}e^{+Q_d(0,x)-ikx}q_-(x) + \mathcal{O}\left(\frac{1}{k^2}\right). \quad \text{(C.11)}$$

Let $\Phi'(x,k)$ be a fundamental solution associated to the Zakharov-Shabat system

$$\begin{cases}
\partial_x\phi_1'(x,k) = (q_d'(x) - ik)\phi_1'(x,k) - q_+'(x)\phi_2'(x,k),\\
\partial_x\phi_2'(x,k) = -q_-'(x)\phi_1'(x,k) - (q_d'(x) - ik)\phi_2'(x,k),
\end{cases}$$

verifying the same Cauchy boundary conditions $\Phi(0,k) = \begin{pmatrix} 1 \\ 1 \end{pmatrix}$. *We have the following asymptotic behaviors as* $k \to +\infty$

$$\begin{aligned}
\phi_1(x)\phi_2'(x) + \phi_1'(x)\phi_2(x) &= \left[e^{Q_d'(0,x)} + e^{-Q_d'(0,x)}\right]\left(1 + \frac{\mathfrak{a}}{ik}\right) + \mathcal{O}\left(\frac{1}{k^2}\right), \quad \text{(C.12)} \\
\phi_2(x)\phi_2'(x) &= e^{-(Q_d(0,x)+Q_d'(0,x)+2ikx)} + \frac{1}{2ik}e^{-Q_d'(0,x)}\tilde{q}_-(x) \\
&\quad -\frac{1}{2ik}e^{Q_d'(0,x)}q_-(x) + \mathcal{O}\left(\frac{1}{k^2}\right), \quad \text{(C.13)} \\
\phi_1(x)\phi_1'(x) &= e^{(Q_d(0,x)+Q_d'(0,x)-2ikx)} - \frac{1}{2ik}e^{Q_d'(0,x)}\tilde{q}_+(x) \\
&\quad -\frac{1}{2ik}e^{-Q_d'(0,x)}q_+(x) + \mathcal{O}\left(\frac{1}{k^2}\right). \quad \text{(C.14)}
\end{aligned}$$

Proof. For the behavior of the fundamental solution $\Phi(x,k)$ it is enough to apply the boundary conditions to (C.5) and (C.6). The asymptotic limit of the products of fundamental solutions are given by

$$\begin{aligned}
&\phi_1(x)\phi_2'(x) + \phi_1'(x)\phi_2(x) = \\
&\quad = \left(e^{Q_d(0,x)-ikx}\left[1 + \frac{\mathfrak{a}}{2ik}\right] - \frac{1}{2ik}e^{-Q_d(0,x)+ikx}q_+(x)\right) \\
&\quad \times \left(e^{-Q_d'(0,x)+ikx}\left[1 + \frac{\mathfrak{a}}{2ik}\right] + \frac{1}{2ik}e^{+Q_d'(0,x)-ikx}\tilde{q}_-(x)\right) \\
&\quad + \left(e^{Q_d'(0,x)-ikx}\left[1 + \frac{\mathfrak{a}}{2ik}\right] - \frac{1}{2ik}e^{-Q_d'(0,x)+ikx}q_+(x)\right) \\
&\quad \times \left(e^{-Q_d(0,x)+ikx}\left[1 + \frac{\mathfrak{a}}{2ik}\right] + \frac{1}{2ik}e^{+Q_d(0,x)-ikx}q_-(x)\right) \\
&\quad = \left[e^{Q_d'(0,x)} + e^{-Q_d'(0,x)}\right]\left(1 + \frac{\mathfrak{a}}{2ik}\right)^2 + \mathcal{O}\left(\frac{1}{k^2}\right) \\
&\quad = \left[e^{Q_d'(0,x)} + e^{-Q_d'(0,x)}\right]\left(1 + \frac{\mathfrak{a}}{ik}\right) + \mathcal{O}\left(\frac{1}{k^2}\right).
\end{aligned}$$

$$\phi_2(x)\phi_2'(x) =$$
$$= \left(e^{-Q_d'(0,x)+ikx}\left[1+\frac{\mathfrak{a}}{2ik}\right]+\frac{1}{2ik}e^{+Q_d'(0,x)-ikx}\tilde{q}_-(x)\right)$$
$$\times\left(e^{-Q_d(0,x)+ikx}\left[1+\frac{\mathfrak{a}}{2ik}\right]+\frac{1}{2ik}e^{+Q_d(0,x)-ikx}q_-(x)\right)$$
$$= e^{-(Q_d(0,x)+Q_d'(0kx)+2ikx)}\left(1+\frac{\mathfrak{a}}{2ik}\right)^2$$
$$+\frac{1}{2ik}\left(e^{-Q_d'(0,x)}\tilde{q}_-(x)+e^{+Q_d'(0,x)}q_-(x)\right)\left[1+\frac{\mathfrak{a}}{2ik}\right]+\mathcal{O}\left(\frac{1}{k^2}\right)$$
$$= e^{-(Q_d(0,x)+Q_d'(0,x)+2ikx)}+\frac{1}{2ik}\left(e^{-Q_d'(0,x)}\tilde{q}_-(x)+e^{Q_d'(0,x)}q_-(x)\right)+\mathcal{O}\left(\frac{1}{k^2}\right)$$

$$\phi_1(x)\phi_1'(x) =$$
$$= \left(e^{Q_d(0,x)-ikx}\left[1+\frac{\mathfrak{a}}{2ik}\right]-\frac{1}{2ik}e^{-Q_d(0,x)+ikx}q_+(x)\right)\cdot$$
$$\cdot\left(e^{Q_d'(0,x)-ikx}\left[1+\frac{\mathfrak{a}}{2ik}\right]-\frac{1}{2ik}e^{-Q_d'(0,x)+ikx}\tilde{q}_+(x)\right)=$$
$$= e^{(Q_d(0,x)+Q_d'(0,x)-2ikx)}\left(1+\frac{\mathfrak{a}}{2ik}\right)^2-\frac{1}{2ik}\left(e^{Q_d'(0,x)}\tilde{q}_+(x)+e^{-Q_d'(0,x)}q_+(x)\right)\left[1+\frac{\mathfrak{a}}{2ik}\right]+\mathcal{O}\left(\frac{1}{k^2}\right)=$$
$$= e^{(Q_d(0,x)+Q_d'(0,x)-2ikx)}-\frac{1}{2ik}\left(e^{Q_d'(0,x)}\tilde{q}_+(x)+e^{-Q_d'(0,x)}q_+(x)\right)+\mathcal{O}\left(\frac{1}{k^2}\right).$$

This concludes the proof. □

Bibliography

[1] M. Ablowitz, D. Kaup, C. Newell, and H. Segur. The inverse scattering trasform-fourier analysis for non linear problems. *Studies in Applied Mathematics*, LIII:249–315, 1974.

[2] S. Avdonin and P. Kurasov. Inverse problems for quantum trees. *Inverse problems and imaging web*, 1:1–21, 2008.

[3] S. Avdonin, P. Kurasov, and M. Nowaczyk. On the reconstruction of boundary conditions for star graphs. *Inverse Problems and Imaging*, 4(4):579–598, 2010.

[4] S. Avdonin, G. Leugering, and V. Mikhaylov. On an inverse problem for tree-like networks of elastic strings. *Zeit. Angew. Math. Mech.*, 90(2):136–150, 2010.

[5] M. Belishev. Boundary spectral inverse problem on a class of graphs (trees) by the BC method. *Inverse Problems*, 20:642–672, 2004.

[6] M. Belishev and A. Vakulenko. Inverse problems on graphs: recovering the tree of strings by the BC-method. *J. Inv. Ill-Posed Problems*, 14:29–46, 2006.

[7] R. Bellman, J. Bentsman, and S.M. Meerkov. Invariant imbedding and the reduction of two point boundary value problems to initial value problems. *Proc Natl Acad Sci U S A*, 46(12):1646–1649, 1960.

[8] R. Bellman and Wing G.M. *An introduction to invariant imbedding.* Society for Industrial Mathematics, 1992.

[9] A.S. Besicovitch. *Almost periodic functions.* Dover, Cambridge, 1954.

[10] G. Borg. Eine Umkehrung des Sturm-Liouvilleschen Eigenweraufgabe. *Acta Mathematica*, 78:1–96, 1946.

[11] S Boyd and L.O Chua. On the passivity criterion for lti n,Äêports. *International Journal of Circuit Theory and Applications*, 10(4):323–333, 1982.

[12] O. Boyko and V. Pivovarchik. Inverse spectral problem for a star graph of stieltjes strings. *Methods Funct. Anal. Topology*, 14:148–151, 2008.

[13] R. Carlson. Adjoint and self-adjoint differential operators on graphs. *Electronic Journal of Differential Equations*, 6:1–10, 1998.

[14] R. Carlson. Inverse eigenvalue problems on directed graphs. *Trans. Amer. Math. Soc.*, 351:4069–4088, 1999.

[15] E. A. Coddington and N. Levinson. *Theory of Ordinary Differential Equations*. McGraw-Hill, 1955.

[16] C. Corduneanu. *Integral equations and application*. Cambridge University Press, 2008.

[17] P. Deift and E.Trubowitz. Inverse scattering on the line. *Communications on Pure and Applied Mathematics*, 32(2):121–251, 1979.

[18] L.D. Faddevv. Properties of the s-matrix of the one-dimensional schrödinger equation. *Trduy Mat. Inst. Steklov*, 73:314–333, 1964.

[19] G. Freiling and V. Yurko. *Inverse Sturm-Liouville problems and their applications*. NOVA Science Publishers, 2008.

[20] D.A Frickey. Conversions between S, Z, Y, h, ABCD, and T parameters which are valid for complex source and load impedances. *Microwave Theory and Techniques, IEEE Transactions on*, 42(2):205–211, 1994.

[21] C. Furse, Y.C. Chung, and R. Dangol. Frequency domain reflectometry for on board testing of aging aircraft wiring. *IEEE Trans. EMC*, 45(2), 2003.

[22] C. Furse and N. Kamdar. An inexpensive distance measuring system for navigation of robotic vehicle. *Microwave Opt. Technol. Lett.*, 33(2):84–97, 2002.

[23] C. Gardner, J. Green, M. Kruskal, and R. Miura. Method for solving korteweg–de vries equation. *Phys. Rev. Lett.*, 19:1095—-1098, 1967.

[24] N.I. Gerasimenko. The inverse scattering problem on a noncompact graph. *Theoret. and Math. Phys.*, 75(2):230–240, 1988.

[25] N.I. Gerasimenko and B.S. Pavlov. A scattering problem on noncompact graphs. *Theoret. and Math. Phys.*, 74:345–359, 1988.

[26] L.A. Griffiths, R. Parakh, C. Furse, and B. Baker. The invisible fray: a critical analysis of the use of reflectometry for fray location. *IEEE Sensor Journal*, 6(3), 2006.

[27] B. Gutkin and U. Smilansky. Can one hear the shape of a graph? *J. Phys. A*, 34(31), 2001.

[28] Hewlett Packard. *S-parameters technique for faster, more accurate network design*, 1996.

[29] C. Hochstad and B. Lieberman. An inverse sturm-liouville problem with mixed given data. *SIAM J. Appl. Math.*, 34(4):676–680, 1978.

[30] M. Jaulent. The inverse scattering problem for LCRG transmission lines. *J. Math. Phys.*, 23(12):2286–2290, 1982.

[31] K. Jones and al. Adaptive method and apparatus for transmission line analysis. *U.S. Patent 20 020 169 585*, mar 2002.

[32] T. Kato. *Perturbation Theory for Linear Operators*. Springer, 1980.

[33] I. Kay. The inverse scattering problems for transmission lines. In L. Collin, editor, *Mathematics for Profile inversion-NASA Tech. Mem. TM X-62*, volume 150, pages 6–2–6–17, 1972.

[34] I. Kay and H.E. Moses. The determination of the scattering potential from the spectral measure function,iii: Calculation of the scattering potential from the scattering operator for the one-dimensional schrödinger equation. *Nuovo Cimento*, 10:276–304, 1956.

[35] E. Koelink. Scattering theory. Notes de cours, `http://fa.its.tudelft.nl/ koelink/dictaat-scattering.pdf`, T.U.Delft, 2006.

[36] P. Kurasov and M. Nowaczyk. Inverse spectral problem for quantum graphs. *J. Phys. A*, 38(22), 2005.

[37] P. Kurasov and M. Nowaczyk. Geometric properties of quantum graphs and vertex scattering matrices, 2007. Preprint, Center for Mathematical Sciences, Lund University.

[38] P. Kurasov and F. Stenberg. On the inverse scattering problem on branching graphs. *J. Phys. A*, 35(1), 2002.

[39] K. Kurokawa. Power waves and the scattering matrix. *Microwave Theory and Techniques, IEEE Transactions on*, 13(2), 1965.

[40] P. Lax. Integrals of nonlinear equations of evolution and solitary waves. *Comm. on Pure and Applied Math.*, XXI:467–490, 1968.

[41] A Lelong, L Sommervogel, N Ravot, and M.O Carrion. Distributed reflectometry method for wire fault location using selective average. *Sensors Journal, IEEE*, 10(2):300–310, 2010.

[42] B. M. Levitan. *Inverse Sturm-Lioville Problems.* VNU Science press, 1987.

[43] Harmer M. Inverse scattering for the matrix Schrödinger operator and Schrödinger operator on graphs with general self-adjoint boundary conditions. *ANZIAM J.*, 43:1–8, 2002.

[44] Harmer M. Inverse scattering on matrices with boundary conditions. *J. Phys. A:Math. Gen.*, 38:4875–4885, 2005.

[45] P. J. Medelius and H. J. Simson. Non-intrusive impedance-based cable tester. *U.S. Patent 5 977 773*, Nov 1999.

[46] G. Miano and A. Massucci. *Transmission Lines and Lumped circuits.* Academic Press, 2001.

[47] R. Pike and P. Sabatier, editors. *Scattering: Scattering and Inverse Scattering in Pure and Applied Science.* New York: Academic Press, 2002.

[48] V. Pivovarchik. Inverse problem for the sturm-liouville equation on a simple graph. *SIAM J. Math. Anal.*, 32:801–819, 2000.

[49] V. Pivovarchik. Ambartsumyan's theorem for the Sturm-Liouville boundary value problem on a star-shaped graph. *Funct. Anal. Topology*, 14:159–167, 2005.

[50] V. Pivovarchik. Inverse problem for the sturm-liouville equation on a star-shaped graph. *Math. Nachr.*, 280:1595–1619, 2007.

[51] D. M. Pozar. *Microwave engineering*. Wiley, New York, 3rd ed. edition, 2005.

[52] J. Rahola. Power waves and conjugate matching. *Circuits and Systems II: Express Briefs, IEEE Transactions on*, 55(1):92–96, 2008.

[53] R. Redheffer and P Volkmann. Matrix differential equations. *Bull. Amer. Math. Soc.*, 81(81):485–488, 1975.

[54] R. Redheffer and P Volkmann. Differential equations in operator algebras. *Mathematische Annalen*, 239(2):97–110, 1979.

[55] M. Reed and B. Simon. *Methods of Modern Mathematical Physics, Vol III: Scattering Theory*. Academic Press, 1978.

[56] K.F. Roth. Rational approximations to algebraic numbers. *Mathematika*, 2:1–20, 1955.

[57] M Smail, T Hacib, and L Pichon.... Detection and location of defects in wiring networks using time domain reflectometry and neural networks. ... *Field Computation (CEFC)*, 5:1502–1505, 2011.

[58] M.K Smail, L Pichon, M Olivas, F Auzanneau, and M Lambert. Detection of defects in wiring networks using time domain reflectometry. *Magnetics, IEEE Transactions on*, 46(8):2998–3001, 2010.

[59] D. R. Smith. Decoupling and order reduction via the riccati transformation. *SIAM*, 29(1):91–113, March 1987. disponible sur http://www-ccrma.standford.edu/jos/.

[60] P Smith, C Furse, and J Gunther. Analysis of spread spectrum time domain reflectometry for wire fault location. *Sensors Journal, IEEE*, 5(6):1469–1478, 2005.

[61] M. Sorine and P. Winternitz. Superposition Laws for solutions of Differential Matrix Riccati Equations Arising in Control Theory. *IEEE Trans. Automat. Control*, 40:266–272, 1985.

[62] H. Tang and Q. Zhang. Inverse scattering for lossy electric transmission line soft fault diagnosis. *Antennas and Propagation Society International Symposium (APSURSI)*, Accepted, 2010.

[63] F. Visco-Comandini, M. Mirrahimi, and M. Sorine. Some inverse scattering problem on star-shaped graphs. *J. of Mathematical Analysis and Application*, 378:343–358, 2011.

[64] J. von Below. Can one hear the shape of a network? *Partial Differential Eqs on multidimensional structures in Lect. Notes in Math.*, 219:19–36, 2001.

[65] R. J. Woodward. *Using Frequency Domain Reflectometry for Water Level Measurement*. PhD thesis, Utah State Univ., 2000.

[66] D Youla, L Castriota, and H Carlin. Bounded real scattering matrices and the foundations of linear passive network theory. *Circuit Theory, IRE Transactions on*, 6(1):102–124, 1959.

[67] V. Yurko. Inverse spectral problems for sturm-liouville operators on graphs. *Inverse problems*, 21(3):1075–1086, 2005.

[68] V. Yurko. An inverse problem for higher order differential operators on star-type graphs. *Inverse problems*, 23(3):893–903, 2007.

[69] V. Yurko. Inverse problems for Sturm-Liouville operators on graphs with a cycle. *Oper. Matrices 2*, 4:543–553, 2008.

[70] V.E. Zakharov and A.B. Shabat. Exact theroy of two-dimensional self-focusing and one-dimensional self-modulation of waves in nonlinear media. *Soviet Physics Jetp*, 34(1):62–69, 1972.

[71] Q. Zhang, M. Sorine, and M. Admane. Inverse Scattering for Soft Fault Diagnosis in Electric Transmission Lines. In *48th IEEE Conference on decision and Control, Shanghai, Cina*, 2009.

[72] E. Zuazua and R. Dager. *Wave propagation, Observation and Control in 1-D flexible multi-structures.* Springer-Verlag, New York, 2006.

Abstract

In this thesis, having in mind applications to the fault-detection/diagnosis of electrical networks, we consider some inverse scattering problems for the Zakharov-Shabat equations and time-independent Schrödinger operators over star-shaped graphs.
The first chapter is devoted to describe reflectometry methods applied to electrical networks as an inverse scattering problems on the star-shaped network. Reflectometry methods are presented and modeled by the telegrapher's equations. Reflectometry experiments can be written as inverse scattering problems for Schrödinger operator in the lossless case and for Zakharov-Shabat system for the lossy transmission network.
In chapter 2 we introduce some elements of the inverse scattering theory for $1-d$ Schrödinger equations and the Zakharov-Shabat system. We recall the basic results for these two systems and we present the state of art of scattering theory on network.
The third chapter deals with some inverse scattering for the Schrödinger operators. We prove the identifiability of the geometry of the star-shaped graph: the number of the edges and their lengths. Next, we study the potential identification problem by inverse scattering.
In the last chapter we focus on the inverse scattering problems for lossy transmission star-shaped network. We prove the identifiability of some geometric informations by inverse scattering and we present a result toward the identification of the heterogeneities, showing the identifiability of the loss line factor.

Keywords: Transmission Line Network, Reflectometry, Inverse scattering, Schrödinger operators, Zakharov-Shabat equations.